

NATIONAL AERONAUTICS AND SPACE ADMINISTRATION

*Technical Memorandum 33-698*

*Mariner Venus/Mercury 1973 Solar Radiation  
Force and Torques*

*R. M. Georgevic*

(NASA-CR-142092) MARINER VENUS/MERCURY 1973  
SOLAR RADIATION FORCE AND TORQUES (Jet  
Propulsion Lab.) 162 p HC \$6.25 CSCL 03B

N75-17276

Unclassified  
G3/92 09627



JET PROPULSION LABORATORY  
CALIFORNIA INSTITUTE OF TECHNOLOGY  
PASADENA, CALIFORNIA

December 1, 1974

**Prepared Under Contract No. NAS 7-100**  
**National Aeronautics and Space Administration**

## PREFACE

The work described in this report was performed by the Mission Analysis Division of the Jet Propulsion Laboratory.

## ACKNOWLEDGMENT

The author wishes to express his gratitude to Mr. Harold M. Yamamoto for his excellent work in preparing this report for publication.

## CONTENTS

I.	Introduction . . . . .	1
II.	Basic Principles of the Solar Radiation Pressure Model . . . . .	1
III.	The Ratio of Front and Back Temperatures . . . . .	9
IV.	Approximate Analytic Expression for $\tau(r, \theta)$ . . . . .	12
V.	Expression for the Solar Radiation Force . . . . .	18
VI.	Moment of the Solar Radiation Force . . . . .	20
VII.	The Directional Distribution Law of the Diffuse Reflection . . . . .	21
VIII.	The Diffuse Reflection Coefficient $B(f)$ . . . . .	23
IX.	Spacecraft-Fixed Systems of Reference Axes . . . . .	29
X.	The General Synopsis of the Illuminated Surfaces on the Spacecraft . . . . .	33
XI.	The Solar Radiation Force and Torque on the High-Gain Antenna Reflector . . . . .	33
XII.	The Solar Radiation Force and Torque on Two Solar Panels . . . . .	46
XIII.	The Solar Radiation Force and Torque on the Main Sunshade of the Spacecraft and the Circular TV Camera Heat Shield . . . . .	49
XIV.	The Solar Radiation Force and Torque on the Magnetometer Boom and Shades . . . . .	51
XV.	The Solar Radiation Force and Torque on the Three IRR Instrument Sunshades . . . . .	58
XVI.	The Solar Radiation Force and Torque on PSE Instrument Surfaces . . . . .	61
XVII.	The Solar Radiation Force and Torque on the Surface of the UVS Sunshade . . . . .	63
XVIII.	The Solar Radiation Force and Torque on All Adiabatic Surfaces . . . . .	64
XIX.	Total Solar Radiation Force and Torque on the Mariner Venus/Mercury Spacecraft . . . . .	65

References . . . . .	66
Bibliography . . . . .	67
Definition of Symbols and Abbreviations . . . . .	68
APPENDIX: Program for Computation of the Components of the Solar Radiation Force and the Moment of the Solar Radiation Force . . . . .	130

## TABLES

1. Values of $\tau(r, \theta)$ for the high-gain antenna reflector . . . . .	81
2. Values of $\tau(r, \theta)$ for solar panels . . . . .	82
3. Values of $K(r, \theta)$ for the high-gain antenna reflector . . . . .	83
4. Values of $K(r, \theta)$ for solar panels . . . . .	84
5. Approximate values of $K(r, \theta)$ for the high-gain antenna reflector . . . . .	85
6. Approximate values of $K(r, \theta)$ for solar panels . . . . .	86
7. Approximate values of $K(r, \theta)$ for the high-gain antenna obtained by series expansion . . . . .	87
8. Approximate values of $K(r, \theta)$ for solar panels obtained by series expansion . . . . .	88
9. Scaled values of $D(\theta)$ for chromium . . . . .	89
10. Scaled values of $D(\theta)$ for wood . . . . .	89
11. Survey of irradiated surfaces on Mariner Venus/Mercury spacecraft . . . . .	90
12. Optical properties of reflecting materials . . . . .	91
13. Components of the solar radiation force on the high-gain antenna . . . . .	92
14. Values of the component $F_{yA}$ . . . . .	93
15. Values of the component $F_{zA}$ . . . . .	94
16. Values of the magnitude of the force $\bar{F}_A$ . . . . .	95
17. Values of the acceleration $a_A$ . . . . .	96

18.	Components of the solar pressure force on the high-gain antenna reflector of the Mariner Venus/Mercury spacecraft along the axes of the antenna-fixed reference system . . . . .	97
19.	Solar torque on the high-gain antenna of the Mariner Venus/Mercury spacecraft . . . . .	100
20.	Components of the solar pressure force in the spacecraft-fixed reference frame . . . . .	101
21.	Solar panel tilts . . . . .	104
22.	Components of the solar pressure force on the solar panels of the Mariner Venus/Mercury spacecraft along the axes of the spacecraft-fixed reference system . . . . .	105
23.	Coordinates of centers of mass of magnetometer sunshades . . . . .	109
24.	Coordinates of centers of mass of IRR sunshades . . . . .	109
25.	Components of the solar radiation force and torque on adiabatic surfaces . . . . .	110
26.	Total force and torque on Mariner Venus/Mercury spacecraft . . . . .	111

## FIGURES

1.	Radiation reflected from an elementary surface area . . . . .	116
2.	Orientation of unit vectors along the tangent and normal to the reflecting surface . . . . .	116
3.	Force diagram . . . . .	117
4.	Function $K(r, \theta)$ versus the angle of incidence for the Mariner Venus/Mercury spacecraft solar panels . . . . .	117
5.	Function $K(r, \theta)$ versus the heliocentric distance for the Mariner Venus/Mercury spacecraft solar panels . . . . .	118
6.	Directional emissivity of solid materials . . . . .	119
7.	Emissivity of materials in different directions . . . . .	119
8.	Mariner Venus/Mercury 1973 spacecraft (Sun side) . . . . .	120
9.	Mariner Venus/Mercury 1973 spacecraft (shaded side) . . . . .	121

10.	High-gain antenna geometry . . . . .	122
11.	Sun-Earth-spacecraft geometry . . . . .	122
12.	Solar radiation on the convex side of the reflector . . . . .	123
13.	Relationship between the antenna system and the geometric spacecraft system . . . . .	124
14.	Projection of heliocentric trajectory in ecliptic plane . . . . .	125
15.	Projection of the illuminated outside area of the reflector on the xy-plane of reference . . . . .	126
16.	Relative positions of the two reference frames . . . . .	126
17.	Octagonal sunshade . . . . .	127
18.	Cross section of the octagonal sunshade and force diagram . . . . .	127
19.	Solar radiation on the cylindrical surface of the magnetometer boom . . . . .	128
20.	Solar radiation force on the cylindrical surface of the magnetometer boom in the boom-fixed reference frame . . . . .	128
21.	Position of two IRR sunshades . . . . .	129

## ABSTRACT

The need for an improvement of the mathematical model of the solar radiation force and torques for the Mariner Venus/Mercury spacecraft arises from the fact that this spacecraft will be steering toward the inner planets (Venus and Mercury), where, due to the proximity of the Sun, the effect of the solar radiation pressure is much larger than it was on the antecedent Mariner spacecraft, steering in the opposite direction. Therefore, although the model yielded excellent results in the case of the Mariner 9 Mars Orbiter, additional effects of negligible magnitudes for the previous missions of the Mariner spacecraft should now be included in the model. The purpose of this study is to examine all such effects and to incorporate them into the already existing model, as well as to use the improved model for calculation of the solar radiation force and torques acting on the Mariner Venus/Mercury spacecraft.

## I. INTRODUCTION

The distinction between the Mariner Venus/Mercury spacecraft mission and the missions of its predecessors in the family of Mariner spacecraft is that, unlike the previous ones, this spacecraft will be heading toward the inner planets, Venus and Mercury, or, in other words, heading toward the Sun. The force produced by the solar radiation pressure is increasing proportionally to the square of the ratio of the heliocentric distances of the Earth and the spacecraft. Hence, the solar pressure exerted on the spacecraft moving in the vicinity of the planet Mercury, for instance, would be approximately fifteen times larger than the solar pressure exerted on the same spacecraft moving in the vicinity of the planet Mars. For that reason, although the mathematical model of the solar radiation force and torques (Refs. 1 and 2) yielded excellent results in the case of the Mariner 9 Mars Orbiter (Ref. 3), in agreement with the observational data obtained during the cruise phase of the spacecraft within 0.1%, the same model should now be enhanced and expanded by the inclusion of certain effects which, in the case of all previous spacecraft, could have been neglected as insignificant. Those effects are:

- (1) The deviation of the directional distribution of the diffuse reflection from Lambert's law of cosines (Refs. 4 and 5).
- (2) The difference between the temperatures of front and back surfaces of every illuminated component of the spacecraft which has a considerable non-negligible thickness.

## II. BASIC PRINCIPLES OF THE SOLAR RADIATION PRESSURE MODEL

Let us assume that  $J$  is the total radiant energy per unit area and per unit time of the radiant flux impinging on an intercepting area  $S$  of a component of the spacecraft. One portion of that energy,  $\gamma J$ , where  $\gamma \leq 1$ , will be reflected from the surface according to a certain reflection law, while the rest of the energy,  $(\gamma - 1) J$ , will be absorbed by the material and re-radiated, presumably isotropically, as thermal radiation into the surrounding space. The re-radiation, due to the conductivity of the material, occurs not only on the front surface of the spacecraft's

component which receives the radiation but also on all other enclosing surfaces.

Let  $\theta$  be the angle of incidence of the incoming radiation, i.e., the angle between the direction of the radiation and the local normal to the surface  $S$ . The angular distribution law of the reflected radiation is then a function of the angle of incidence, which we shall denote by  $f(\theta)$ . It is obvious that, for specularly reflecting surfaces (mirror-like surfaces),  $f(\theta)$  is the two-dimensional Dirac delta function, since the angle of incidence is equal to the angle of reflection. For diffusely reflecting surfaces it is usually assumed that they obey Lambert's cosine law  
 $f(\theta) = \cos \theta$ .

The total reflected radiation is the combination of both specular and diffuse reflections for most materials. We shall denote by  $\beta\gamma J$  the portion of the radiant energy reflected specularly ( $\beta \leq 1$ ), and by  $\beta(1 - \gamma) J$  the portion reflected diffusely. In the interior of any infinitesimally small solid angle (Fig. 1)

$$d\omega = \sin \theta \, d\theta \, d\varphi$$

the total reflected radiation is

$$\gamma J = \int_{\sigma} I \, d\omega$$

where  $I$  is the radiant flux per unit solid angle on the hemisphere  $\sigma$ . Since

$$I = I_0 f(\theta)$$

where  $I_0$  is a constant, integrating over the surface of the hemisphere  $\sigma$ , we obtain

$$\gamma J = I_0 \int_0^{2\pi} d\varphi \int_0^{\pi/2} f(\theta) \sin \theta \, d\theta = I_0 A(f) \quad (1)$$

with

$$A(f) = \int_0^{2\pi} d\varphi \int_0^{\pi/2} f(\theta) \sin \theta \, d\theta \quad (2)$$

For specular reflection,  $f(\theta)$  is a two-dimensional Dirac delta function. Hence

$$A(f) = 1$$

The momentum of radiation is  $J/c$ , where  $c$  is the speed of light. The momentum exchange due to the reflected radiation in the direction of the local normal to the surface area  $S$  is

$$\int_{\sigma} \frac{I}{c} \cos \theta \, d\omega = \frac{I_0}{c} \int_{\sigma} f(\theta) \sin \theta \cos \theta \, d\varphi \, d\theta$$

while the momentum exchange in the local tangential plane to the surface  $S$  is zero. Integrating over the surface area of the hemisphere  $\sigma$ , we obtain

$$\frac{\gamma J}{c} B(f) = \frac{\gamma J}{c A(f)} \int_0^{2\pi} d\varphi \int_0^{\pi/2} f(\theta) \sin \theta \cos \theta \, d\theta \quad (3)$$

where

$$B(f) = \frac{1}{A(f)} \int_0^{2\pi} d\varphi \int_0^{\pi/2} f(\theta) \sin \theta \cos \theta \, d\theta \quad (4)$$

For specular reflection,  $f(\theta)$  is the two-dimensional Dirac delta function. Hence, for specular reflection,

$$B(f) = 1$$

For diffuse reflection, however, one can assume that the angular distribution of the reflected radiation obeys Lambert's cosine law  $f(\theta) = \cos \theta$ . Introducing this function into integrals given by Eqs. (2) and (4), and performing the integration, we find

$$\left. \begin{array}{l} A_L(f) = \pi \\ B_L(f) = \frac{2}{3} \end{array} \right\} \quad (5)$$

where the subscript L denotes the values obtained using Lambert's law.

The total radiation force along the local normal to the irradiated surface S is the sum of momentum exchanges due to the incident and reflected radiations. The radiant energy J is inversely proportional to the square of the distance from the source of radiation or, in other words, inversely proportional to the heliocentric distance r:

$$J = \frac{J_0}{r^2}$$

or, in the scaled form,

$$J = J_0 \left( \frac{A_U}{r} \right)^2 \quad (6)$$

where AU is the astronomical unit and  $J_0$  is the radiant energy of the Sun received at the Earth (one astronomical unit).  $J_0$  is also called the solar constant. Its value is

$$J_0 = 1.353 \times 10^3 \text{ W/m}^2 \text{ (Refs. 1 and 6)}$$

or

$$J_0 = 1.353 \times 10^3 \text{ kg/s}^3$$

From all that has been previously said, we can now write the expression for the elementary solar radiation force acting on an elementary surface area

$$d\bar{S} = \bar{N}dS$$

where  $\bar{N}$  is the unit vector along the local normal to the elementary surface area  $dS$ . The force acting along the local normal is

$$d\bar{F}_N = - \frac{J_0}{c} \left( \frac{AU}{r} \right)^2 \bar{N}dS$$

or

$$d\bar{F}_N = - \lambda_S \left( \frac{AU}{r} \right)^2 \bar{N}dS \quad (7)$$

If the area is expressed in  $m^2$ , the value of the constant  $\lambda_S$  is

$$\lambda_S = 4.513 \times 10^{-6} \text{ N/m}^2$$

Finally, if we express the heliocentric distance  $r$  in meters, we obtain, instead of Eq. (7),

$$d\bar{F}_N = - K_S \frac{\bar{N}}{r^2} dS$$

where (Ref. 1)

$$K_S = 1.010 \times 10^{17} \text{ N}$$

Henceforth, we shall call  $\lambda_S$  the solar pressure constant.

When the direction of the incident radiation is inclined to the direction of the local normal to the surface by an angle  $\theta$  (angle of incidence), the solar radiation force will have two components: one along the local normal

to the surface, defined by the unit vector  $\bar{N}$ , and one along the interception line of the local tangential plane to the surface with the plane perpendicular to the tangential plane, which contains the direction of the incident radiation and the unit vector  $\bar{N}$  (Fig. 2). We shall denote by  $\bar{U}$  the unit vector along the direction opposite that of the incoming radiation so that, if  $\bar{T}$  is the unit tangent vector,

$$\bar{U} \cdot (\bar{N} \times \bar{T}) = 0$$

and choose the direction of the unit vector  $\bar{T}$  in such a manner that

$$\bar{U} \cdot \bar{T} > 0$$

(Fig. 2). If  $F(x, y, z) = 0$  is the equation of the irradiated surface in a certain coordinate system (so far arbitrarily chosen), the unit vector along the local normal at a point  $(x, y, z)$  on the surface is defined by

$$\bar{N} = \frac{\text{grad } F(x, y, z)}{|\text{grad } F(x, y, z)|}$$

or, in shorter form,

$$\bar{N} = \frac{\nabla F}{|\nabla F|} \quad (8)$$

From Fig. 2, we see that

$$\bar{U} = \bar{N} \cos \theta + \bar{T} \sin \theta$$

and, hence,

$$\bar{T} = \frac{\bar{U}}{\sin \theta} - \bar{N} \cot \theta \quad (9)$$

Figure 3 shows the diagram of all forces produced by the solar radiation. Expressed in terms of the magnitude of the normal force  $\bar{F}_N$ , those forces are:

- (1) The force caused by the incident radiation  $F_I$ . From Fig. 3, we find

$$F_I = F_N \cos \theta$$

This force has two components: one along the local normal (pressure),  $P_I$ , and one along the tangent unit vector,  $T_I$ . They are, respectively,

$$\left. \begin{aligned} P_I &= F_I \cos \theta = F_N \cos^2 \theta \\ T_I &= F_I \sin \theta = F_N \sin \theta \cos \theta \end{aligned} \right\} \quad (10)$$

- (2) The force produced by the specularly reflected radiation  $F_R$ . Since the portion of the specularly reflected radiation is  $\beta\gamma$ , the magnitude of this force is

$$F_R = \beta\gamma F_I$$

The normal and tangential components of this force are, respectively,

$$\left. \begin{aligned} P_R &= F_R \cos \theta = \beta\gamma F_N \cos^2 \theta \\ T_R &= F_R \sin \theta = \beta\gamma F_N \sin \theta \cos \theta \end{aligned} \right\} \quad (11)$$

- (3) The force caused by the diffuse reflection  $F_D$ . Due to a presumably symmetric angular distribution law, this force has only the normal component which is the resultant of all diffuse reflection forces produced by the diffusely scattered photons. This force is

$$F_D = \gamma B(f) (1 - \beta) F_I$$

or

$$F_D = \gamma(1 - \beta) B(f) F_N \cos \theta \quad (12)$$

- (4) Force produced by the re-radiation  $F_{RR}$ . The portion  $1 - \gamma$  of photons impinging upon the reflecting surface is absorbed by the material and re-radiated, presumably isotropically, into the neighboring space as thermal energy. The re-radiation occurs on both front and back surfaces of a particular spacecraft's component, thus producing another small force. In this case, too, as before, due to a presumably symmetric angular distribution law, this force has the normal component only.

The radiant heat flow emitted by a surface is given by

$$q = \sigma \epsilon T^4 \quad (13)$$

(Stefan's law). Here  $\sigma$  is the Stefan-Boltzmann's constant:

$$\sigma = 5.6697 \times 10^{-8} \text{ kg/s}^3 \cdot \text{K}^4$$

$T$  is the temperature of the surface in kelvins (K), and  $\epsilon$  is the emissivity of the surface (Ref. 5). Hence, the emissive powers of front and back surfaces are, respectively,

$$\left. \begin{aligned} q_F &= \sigma \epsilon_F T_F^4 \\ q_B &= \sigma \epsilon_B T_B^4 \end{aligned} \right\} \quad (14)$$

The re-radiation from the front surface contributes a small force of magnitude

$$(F_{RR})_{FRONT} = B(f)(1 - \gamma) \frac{q_F}{q_F + q_B} F_I$$

and the re-radiation from the back surface contributes a force of magnitude

$$(F_{RR})_{\text{BACK}} = - B(f)(1 - \gamma) \frac{q_B}{q_F + q_B} F_I$$

These two forces have opposite directions.

The total amount of force created by the re-radiation is

$$F_{RR} = B(f) K(r, \theta) (1 - \gamma) F_N \cos \theta \quad (15)$$

where

$$K(r, \theta) = \frac{\epsilon_F T_F^4 - \epsilon_B T_B^4}{\epsilon_F T_F^4 + \epsilon_B T_B^4} \quad (16)$$

For  $T_F = T_B$ , function  $K(r, \theta)$  is a constant (Ref. 4),

$$K = \frac{\epsilon_F - \epsilon_B}{\epsilon_F + \epsilon_B}$$

and, for adiabatic surfaces,  $K = 1$ .

The diagram of all forces is shown in Fig. 3.

### III. THE RATIO OF FRONT AND BACK TEMPERATURES

The K-function (Eq. 16) can be written in the form

$$K(r, \theta) = \frac{\epsilon_F T^4 - \epsilon_B}{\epsilon_F T^4 + \epsilon_B} \quad (17)$$

where  $\tau$  is the ratio of temperatures:

$$\tau = \tau(r, \theta) = \frac{T_F}{T_B} \quad (18)$$

To find this ratio we shall consider an infinitesimally small slab of thickness  $\ell$  made of a certain material which has a thermal conductivity  $k$ . The energy balance between the radiant energy received on the front side of the slab and the re-radiated energy from both front and back sides is given by the equation (Ref. 7)

$$\sigma A_F \epsilon_F T_F^4 + \sigma A_B \epsilon_B T_B^4 = J_0 \left( \frac{AU}{r} \right)^2 (1 - \gamma) A_F \cos \theta$$

or

$$\epsilon_F T_F^4 + \epsilon_B \left( \frac{A_B}{A_F} \right) T_B^4 = J_0 \left( \frac{AU}{r} \right)^2 \frac{1 - \gamma}{\sigma} \cos \theta$$

where  $A_F$  and  $A_B$  are areas of the front and back surfaces, respectively. We shall assume that the front and back surface areas are the same, i.e.,

$$\frac{A_B}{A_F} = 1$$

so that the equation of the energy balance is

$$\epsilon_F T_F^4 + \epsilon_B T_B^4 = J_0 \left( \frac{AU}{r} \right)^2 \frac{1 - \gamma}{\sigma} \cos \theta \quad (19)$$

The quasisteady-state heat flow equation, which reduces to Laplace's equation, yields a linear propagation of heat in the slab along the normal to the surface. From the boundary conditions (Refs. 7 and 8), we obtain

$$T_F = T_B + \frac{\sigma \ell \epsilon_B}{k} T_B^4 \quad (20)$$

Equations (19) and (20) theoretically solve the problem of finding  $\tau(r, \theta)$ . In reality, however, we cannot obtain an analytic solution for  $\tau$  because, by eliminating  $T_B$  from the two equations

$$\epsilon_B + \epsilon_F \tau^4 = \frac{J_0}{T_B^4} \left( \frac{AU}{r} \right)^2 \frac{1 - \gamma}{\sigma} \cos \theta$$

$$\tau = 1 + \frac{\sigma \ell \epsilon_B}{k} T_B^3$$

we ultimately obtain an algebraic equation of the twelfth order.

On the Mariner Venus/Mercury spacecraft only two components have significant thicknesses: the high-gain antenna and the two solar panels. From Ref. 8 we find the following information:

(1) For the high-gain antenna reflector<sup>1</sup>:

$$\ell_A = 0.0191 \text{ m}$$

$$(\epsilon_F)_A = 0.89$$

$$(\epsilon_B)_A = 0.90$$

$$k_A = 1.2921 \text{ kg} \cdot \text{m/s}^3 \cdot \text{K}$$

$$\gamma_A = 0.10$$

(2) For solar panels:

$$\ell_{SP} = 0.0127 \text{ m}$$

$$(\epsilon_F)_{SP} = 0.79$$

$$(\epsilon_B)_{SP} = 0.85$$

---

<sup>1</sup>The high-gain antenna is illuminated from the back.

$$k_{SP} = 1.2921 \text{ kg} \cdot \text{m/s}^3 \cdot \text{K}$$

$$\gamma_{SP} = 0.22$$

A simple computer program, based on Newton's method for approximate solutions, yields the values of the function  $\tau(r, \theta)$ , shown in Tables 1 and 2.

Once the values of  $\tau(r, \theta)$  are known, the values of the function  $K(r, \theta)$  are obtained from Eq. (17). Tables 3 and 4 give the values of the function  $K(r, \theta)$  for the high-gain antenna reflector and solar panels, respectively. Finally, in Figs. 4 and 5, the graphs of the function  $K(r, \theta)$  are shown. Wherever the value of  $K(r, \theta)$  is negative, the resultant re-radiation force is acting in the direction of the local normal, i.e., it acts against the normal component of the solar pressure.

#### IV. APPROXIMATE ANALYTIC EXPRESSION FOR $\tau(r, \theta)$

An extremely good analytic estimate of the function  $\tau(r, \theta)$  can be derived, due to the fact that the ratio

$$\frac{T_F - T_B}{T_B} \leq \begin{cases} 0.1322 & \text{for the high-gain antenna reflector} \\ 0.0863 & \text{for solar panels} \end{cases}$$

Assuming that, in the first approximation,

$$T_F \approx T_B \approx T_0(r, \theta)$$

we obtain, from Eq. (19),

$$T_0 = T_0(r, \theta) = \sqrt[4]{J_0 \left( \frac{AU}{r} \right)^2 \frac{(1 - \gamma) \cos \theta}{\sigma(\epsilon_F + \epsilon_B)}} \quad (21)$$

The next approximation is obtained by substituting  $T_0$  for  $T_B$  in Eq. (20). It yields

$$\frac{T_F}{T_B} = 1 + \frac{\sigma \ell \epsilon_B}{k} T_0^3 \quad (22)$$

Equation (19) can be rewritten in the form

$$T_B^4 \left[ \epsilon_B + \epsilon_F \left( \frac{T_F}{T_B} \right)^4 \right] = (\epsilon_F + \epsilon_B) T_0^4$$

By substituting the value of the ratio  $T_F/T_B$  from Eq. (22), the last equation yields

$$T_B = \left[ \frac{\epsilon_F + \epsilon_B}{\epsilon_B + \epsilon_F \left( 1 + \frac{\sigma \ell \epsilon_B}{k} T_0^3 \right)^4} \right]^{1/4} T_0 \quad (23)$$

which is a further approximation. A better approximation of  $T_F/T_B$  is obtained by substituting the value of  $T_B$ , given by Eq. (23), into Eq. (20):

$$\frac{T_F}{T_B} = 1 + \frac{\sigma \ell \epsilon_B}{k} T_0^3 \left[ \frac{\epsilon_F + \epsilon_B}{\epsilon_B + \epsilon_F \left( 1 + \frac{\sigma \ell \epsilon_B}{k} T_0^3 \right)^4} \right]^{3/4} \quad (24)$$

The last expression can be simplified considerably by expanding the denominator on the right-hand side of Eq. (24). We find that

$$\left[ \frac{\epsilon_F + \epsilon_B}{\epsilon_B + \epsilon_F \left( 1 + \frac{\sigma \ell \epsilon_B}{k} T_0^3 \right)^4} \right]^{3/4} \approx \frac{\epsilon_F + \epsilon_B}{\epsilon_F + \epsilon_B + 3 \frac{\sigma \ell}{k} \epsilon_F \epsilon_B T_0^3}$$

and, without loss of accuracy,

$$\frac{T_F}{T_B} = 1 + \frac{\epsilon_B(\epsilon_F + \epsilon_B) \frac{\sigma\ell}{k} T_0^3}{\epsilon_F + \epsilon_B + 3 \frac{\sigma\ell}{k} \epsilon_F \epsilon_B T_0^3} = \tau(r, \theta) \quad (25)$$

Denoting  $\rho$  as the heliocentric distance of the spacecraft expressed in astronomical units (AU), i.e.,

$$\rho = \frac{r}{AU} \quad (26)$$

we can write Eq. (21) in the form

$$T_0(r, \theta) = T^* \frac{\sqrt[4]{\cos \theta}}{\sqrt{\rho}} \quad (27)$$

where  $T^*$  is the constant

$$T^* = \sqrt[4]{\frac{J_0(1 - \gamma)}{\sigma(\epsilon_F + \epsilon_B)}} \quad (28)$$

The values of the constant  $T^*$  for the high-gain antenna reflector and solar panels are, respectively,

$$\left. \begin{aligned} T_A^* &= 330.96 \text{ kelvins} \\ T_{SP}^* &= 326.40 \text{ kelvins} \end{aligned} \right\} \quad (29)$$

Equation (25) can be written in the form

$$\tau(r, \theta) = 1 + \frac{\frac{\sigma\ell\epsilon_B}{k} T_0^3}{1 + 3 \frac{\epsilon_F}{\epsilon_F + \epsilon_B} \frac{\sigma\ell\epsilon_B}{k} T_0^3}$$

Setting

$$\frac{\sigma \ell \epsilon_B}{k} T_0^3 = A \frac{(\cos \theta)^{3/4}}{f^{3/2}} = AR(r, \theta) \quad (30)$$

where

$$A = \frac{\sigma \ell \epsilon_B}{k} (T^*)^3 \quad (31)$$

$$B = \frac{3A\epsilon_F}{\epsilon_F + \epsilon_B} \quad (32)$$

we can rewrite the last equation in the form

$$\tau(r, \theta) = 1 + \frac{AR(r, \theta)}{1 + BR(r, \theta)} \quad (33)$$

The values of constants A and B for the high-gain antenna reflector and the solar panels are, respectively,

$$\left. \begin{array}{l} A_A = 0.02734 \\ A_{SP} = 0.01647 \\ B_A = 0.04079 \\ B_{SP} = 0.02380 \end{array} \right\} \quad (34)$$

The function

$$R(r, \theta) = \left( \frac{\cos \theta}{\rho^2} \right)^{3/4} \quad (35)$$

as well as the function  $\tau(r, \theta)$  and the constants A and B are dimensionless. For the Mariner Venus/Mercury spacecraft mission,

$$R(r, \theta) \leq 5.864$$

Substituting the expression for  $\tau(r, \theta)$  from Eq. (33) into Eq. (17), we obtain

$$K(r, \theta) = \frac{\epsilon_F [1 + (A + B) R(r, \theta)]^4 - \epsilon_B [1 + BR(r, \theta)]^4}{\epsilon_F [1 + (A + B) R(r, \theta)]^4 + \epsilon_B [1 + BR(r, \theta)]^4}$$

The values of the function  $K(r, \theta)$  obtained from the last expression for the high-gain antenna reflector and solar panels are given in Tables 5 and 6, respectively. It is easy to see that the largest value of the error of the approximate solution of the above equation is 0.002 for the high-gain antenna reflector (0.8%) and 0.001 for solar panels (0.8%); this is an excellent agreement, since the maximum error is just a little above the truncation error.

Sacrificing a little accuracy we can derive another, less accurate, expression for  $K(r, \theta)$  by expanding the last expression into a power series of  $(A + B) R(r, \theta)$  and  $BR(r, \theta)$ . This expression, although less accurate, is more suitable for the purpose of deriving the final form of the solar pressure force. The expansion yields

$$K(r, \theta) = K + \frac{8\epsilon_F \epsilon_B}{(\epsilon_F + \epsilon_B)^2} AR(r, \theta) - 4\epsilon_F \epsilon_B \frac{11\epsilon_F - 3\epsilon_B}{(\epsilon_F + \epsilon_B)^3} [AR(r, \theta)]^2 \quad (36)$$

where K is the constant value of  $K(r, \theta)$  for  $T_F = T_B$ ,

$$K = \frac{\epsilon_F - \epsilon_B}{\epsilon_F + \epsilon_B} \quad (37)$$

The values of  $K(r, \theta)$  obtained from Eq. (36) are given in Tables 7 and 8. The maximum relative error for the high-gain antenna is about 9.7% and for the solar panels about 3.6%.

In order to express the function on the right-hand side of Eq. (36) in a more concise form, we shall introduce the following parameters:

$$\left. \begin{aligned} P &= \frac{8 \epsilon_F \epsilon_B}{(\epsilon_F + \epsilon_B)^2} \quad A = 8 J_0^{3/4} (1 - \gamma)^{3/4} \frac{\epsilon_F \epsilon_B^2 \ell \sigma^{1/4}}{k(\epsilon_F + \epsilon_B)^{11/4}} \\ Q &= -4 \epsilon_F \epsilon_B \frac{11 \epsilon_F - 3 \epsilon_B}{(\epsilon_F + \epsilon_B)^3} \quad A^2 \\ &= -4 J_0^{3/2} (1 - \gamma)^{3/2} \frac{\epsilon_F \epsilon_B^3 (11 \epsilon_F - 3 \epsilon_B) \sigma^{1/2} \ell^2}{k^2 (\epsilon_F + \epsilon_B)^{9/2}} \end{aligned} \right\} \quad (38)$$

The function  $K(r, \theta)$  can now be written in the form

$$K(r, \theta) = K + PR(r, \theta) + Q [R(r, \theta)]^2$$

or, explicitly,

$$K(r, \theta) = K + P \left( \frac{\cos \theta}{\rho^2} \right)^{3/4} + Q \left( \frac{\cos \theta}{\rho^2} \right)^{3/2} \quad (39)$$

The values of constants  $P$  and  $Q$  for the high-gain antenna reflector and solar panels are, respectively,

$$\left. \begin{aligned} P_A &= 0.05468 \\ Q_A &= -0.00296 \\ P_{SP} &= 0.03290 \\ Q_{SP} &= -0.00101 \end{aligned} \right\} \quad (40)$$

## V. EXPRESSION FOR THE SOLAR RADIATION FORCE

We shall now express the total solar radiation pressure force in the vectorial form, adding all the components of the force along the local normal and tangent directions. From Eq. (7), the elementary normal force is

$$d\bar{F}_N = - \frac{\lambda S}{\rho^2} \bar{N} dS$$

The elementary force, generated by the incident radiation, is

$$\begin{aligned} d\bar{F}_I &= - (\bar{N} \cos \theta + \bar{T} \sin \theta) \cos \theta dF_N \\ &= - \bar{U} d\bar{F}_N \cos \theta \end{aligned}$$

The elementary force, created by the specularly reflected photons, is

$$d\bar{F}_R = \beta \gamma (\bar{U} - 2\bar{N} \cos \theta) dF_N \cos \theta$$

The elementary force, due to the diffusely reflected radiation, is

$$d\bar{F}_D = - \gamma B(f)(1 - \beta) \bar{N} dF_N \cos \theta$$

Finally, the elementary force, caused by the thermal re-radiation, is

$$d\bar{F}_{RR} = - B(f)(1 - \gamma) K(r, \theta) \bar{N} dS \cos \theta$$

The vector sum of all these component forces gives the total elementary force

$$d\bar{F} = d\bar{F}_I + d\bar{F}_R + d\bar{F}_D + d\bar{F}_{RR}$$

or, explicitly,

$$d\bar{F} = - \frac{\lambda S \cos \theta}{\rho^2} \left\{ \left[ 2\beta \gamma \cos \theta + B(f) (\gamma(1 - \beta) + (1 - \gamma) K(r, \theta)) \right] \bar{N} + (1 - \beta \gamma) \bar{U} \right\} dS$$

The total force over the entire illuminated surface  $S$  is then

$$\begin{aligned} \bar{F} = - \frac{\lambda S}{\rho^2} & \iint_S \left\{ \left[ 2\beta \gamma \cos \theta + B(f) (\gamma(1 - \beta) + (1 - \gamma) K(r, \theta)) \right] \bar{N} \right. \\ & \left. + (1 - \beta \gamma) \bar{U} \right\} \cos \theta dS \end{aligned} \quad (41)$$

where  $K(r, \theta)$  is a constant for all components of the Mariner Venus/Mercury spacecraft except the high-gain antenna reflector and solar panels.

The unit vector  $\bar{U}$  is a constant insofar as the integration is concerned. Also,

$$\cos \theta = \bar{U} \cdot \bar{N}, \quad d\bar{S} = \bar{N} dS$$

Hence,

$$\begin{aligned} \iint_S \bar{U} \cos \theta dS &= \bar{U} \iint_S \bar{U} \cdot \bar{N} dS \\ &= \bar{U} \left( \bar{U} \cdot \iint_S d\bar{S} \right) = (\bar{U} \cdot \bar{S}) \bar{U} \end{aligned}$$

and Eq. (41) becomes

$$\bar{F} = - \frac{\lambda S}{\rho^2} \iint_S [v(\theta) \bar{N} + (1 - \beta\gamma) \bar{U} \cos \theta] dS \quad (42)$$

or

$$\bar{F} = - \frac{\lambda S}{\rho^2} \left[ \iint_S v(\theta) d\bar{S} + (1 - \beta\gamma)(\bar{U} \cdot \bar{S}) \bar{U} \right] \quad (43)$$

where

$$v(\theta) = 2\beta\gamma \cos^2 \theta + B(f)[\gamma(1 - \beta) + (1 - \gamma) K(r, \theta)] \cos \theta \quad (44)$$

## VI. MOMENT OF THE SOLAR RADIATION FORCE

Let  $x, y, z$  be the coordinates of a point on the spacecraft relative to a certain spacecraft-fixed reference frame with the origin at a certain point O. Let  $\bar{e}_1, \bar{e}_2, \bar{e}_3$  be the unit vectors along the coordinate axes x, y, and z, respectively. The position of a point of the spacecraft ( $x, y, z$ ) is defined by the position vector

$$\bar{X} = x\bar{e}_1 + y\bar{e}_2 + z\bar{e}_3$$

The moment of the elementary force  $d\bar{F}$  at the point  $(x, y, z)$ , with respect to the point of reference O is then

$$d\bar{M}^{(O)} = \bar{X} \times d\bar{F}$$

Thus, the total moment of the solar radiation force about the point O is obtained by an integration over the illuminated surface S:

$$\bar{M}^{(O)} = \iint_S \bar{X} \times d\bar{F}$$

Using the expression for the elementary force  $d\bar{F}$ , we obtain, explicitly,

$$\begin{aligned} \bar{M}^{(O)} = & - \frac{\lambda_S}{\rho^2} \iint_S [v(\theta)(\bar{X} \times \bar{N}) \\ & + (1 - \beta\gamma)(\bar{X} \times \bar{U}) \cos \theta] dS \end{aligned} \quad (45)$$

## VII. THE DIRECTIONAL DISTRIBUTION LAW OF THE DIFFUSE REFLECTION

We have already shown that, using Lambert's directional distribution law of diffuse reflection  $f(\theta) = \cos \theta$ , we obtain for the value of the constant  $B(f)$ :

$$B_L(f) = \frac{2}{3}$$

In reality, however, the directional distribution of the diffuse reflection does not obey Lambert's cosine law (Refs. 4 and 5). Moreover, different materials have different directional reflection distribution; metallic surfaces behave differently from nonmetallic surfaces. We shall introduce a function, for the time being unknown, of the angle of incidence  $\theta$ ,  $D(\theta)$ , and write the reflection law in the form

$$f(\theta) = D(\theta) \cos \theta \quad (46)$$

where, for Lambert's cosine law,  $D(\theta) = 1$ . The graphs of the function  $D(\theta)$  for different metallic surfaces are shown in Fig. 6; the graphs of the function  $D(\theta)$  for nonmetallic surfaces are shown in Fig. 7. We see that for metallic surfaces  $D(\theta) \rightarrow \infty$  when  $\theta \rightarrow 90^\circ$  and that for nonmetallic surfaces  $D(\theta) = 0$  when  $\theta = 90^\circ$ . It is also clear that for small values of the angle of incidence  $\theta$ , the directional distribution agrees well with Lambert's law. The deviation from Lambert's law begins when the angle of incidence is between  $35^\circ$  and  $45^\circ$  for metallic and between  $55^\circ$  and  $70^\circ$  for nonmetallic surfaces. We shall denote by  $\alpha$  the value of the angle of incidence  $\theta$  of the point of  $D(\theta)$  at which the function  $D(\theta)$  begins to deviate from Lambert's law (circle  $D(\theta) = 1$ ). We shall call this angle "the separation angle." Hence, in order to find a unified law of directional reflectivity distribution, we have to find such a function  $D(\theta)$  which satisfies the following constraints:

$$D(\theta) = 1, \text{ for } 0 \leq \theta \leq \alpha$$

$$D(\theta) \rightarrow \infty, \text{ for } \theta \rightarrow \pi/2 \text{ for metallic surfaces}$$

$$D(\pi/2) = 0, \text{ for nonmetallic surfaces}$$

Also, in order to have a smooth continuous transition from Lambert's circle  $D(\theta) = 1$  to  $D(\theta)$  at  $\theta = \alpha$ , the curve  $D(\theta)$  and the circle  $D(\theta) = 1$  ought to have the same tangent at  $\theta = \alpha$ . Hence, the additional condition which the function  $D(\theta)$  must satisfy is

$$\left[ \frac{dD(\theta)}{d\theta} \right]_{\theta=\alpha} = D'(\alpha) = 0$$

The function

$$D(\theta) = \mu(\theta - \alpha) \tan \alpha + \left( \frac{\cos \theta}{\cos \alpha} \right)^\mu \quad (47)$$

where  $\mu < 0$  is a parameter depending on the specific material, satisfies the above-mentioned requirements for metallic materials, while the function

$$D(\theta) = [1 + \mu(\theta - \alpha) \tan \alpha] \left( \frac{\cos \theta}{\cos \alpha} \right)^{\mu} \quad (48)$$

where  $\mu > 0$ , satisfies the requirements listed above for the nonmetallic materials. In both cases we assume that

$$|\mu| < 1$$

We shall now examine two examples: one when  $\mu < 0$ , and one when  $\mu > 0$ . For the first example ( $\mu < 0$ ), we shall take a chromium surface; for the second example ( $\mu > 0$ ), a wooden surface. In the first example we can read from the graph the value of the angle  $\alpha \approx 35^\circ$ ; in the second example we read  $\alpha \approx 64^\circ$ . In both examples we have to scale the values of  $D(\theta)$  obtained from the graphs (Ref. 5) by dividing each value of  $D(\theta)$  by  $D(\alpha)$ , so that we have  $D(\alpha) = 1$ . The scaled values of the function  $D(\theta)$  for both examples are given, respectively, in Tables 9 and 10.

Using a least squares fit in both cases (Ref. 9), we obtain the following values for  $\mu$ . For the chromium (metallic) surface,

$$\mu = -0.673$$

and the sum of squares of residuals is 0.011. For the wooden (nonmetallic) surface, the value is

$$\mu = 0.653$$

and the sum of squares of residuals is 0.002.

### VIII. THE DIFFUSE REFLECTION COEFFICIENT $B(f)$

The directional distribution law of diffuse reflection is (Eq. 46)

$$f(\theta) = D(\theta) \cos \theta$$

Substituting this value of  $f(\theta)$  into Eq. (2), we first obtain the coefficient  $A(f)$  and, then, from Eq. (4), we ultimately obtain the value of  $B(f)$ . Hence, for both metallic and nonmetallic surfaces,

$$A(f) = 2\pi \left[ \int_0^\alpha \sin \theta \cos \theta d\theta + \int_\alpha^{\pi/2} D(\theta) \sin \theta \cos \theta d\theta \right] \quad (49)$$

$$B(f) = \frac{2\pi}{A(f)} \left[ \int_0^\alpha \sin \theta \cos^2 \theta d\theta + \int_\alpha^{\pi/2} D(\theta) \sin \theta \cos^2 \theta d\theta \right] \quad (50)$$

The first two integrals on the right-hand sides of Eqs. (49) and (50) do not depend on the form of the function  $D(\theta)$ . Their values are

$$\left. \begin{aligned} \int_0^\alpha \sin \theta \cos \theta d\theta &= \frac{1}{2} \sin^2 \alpha \\ \int_0^\alpha \sin \theta \cos^2 \theta d\theta &= \frac{1}{3} (1 - \cos^3 \alpha) \end{aligned} \right\} \quad (51)$$

The second two integrals depend on the form of  $D(\theta)$ , and thus have different values for different materials. For metallic materials, substituting  $D(\theta)$  by its value given in Eq. (47), we obtain by integration

$$\begin{aligned} \int_\alpha^{\pi/2} D(\theta) \sin \theta \cos \theta d\theta &= \frac{\mu}{4} \left[ \left( \frac{\pi}{2} - \alpha \right) \tan \alpha - 1 \right. \\ &\quad \left. + \frac{\mu^2 + 2\mu + 4}{\mu(\mu + 2)} \cos^2 \alpha \right] \end{aligned} \quad (52a)$$

$$\int_{\alpha}^{\pi/2} D(\theta) \sin \theta \cos^2 \theta d\theta = \frac{\mu}{9} \cos \alpha \left[ \frac{\mu^2 + 3\mu + 9}{\mu(\mu + 3)} \cos^2 \alpha - \frac{1 - \sin \alpha}{1 + \sin \alpha} \right] \quad (52b)$$

Hence, for metallic materials,

$$A(f) = \frac{\mu\pi}{2} \left[ \left( \frac{\pi}{2} - \alpha \right) \tan \alpha + \frac{2 - \mu}{\mu} + \frac{\mu}{\mu + 2} \cos^2 \alpha \right] \quad (53)$$

$$A(f) B(f) = \frac{2\mu\pi}{9} \left( \frac{3}{\mu} - \frac{1 - \sin \alpha}{1 + \sin \alpha} \cos \alpha + \frac{\mu}{\mu + 3} \cos^3 \alpha \right) \quad (54)$$

Finally, from Eqs. (53) and (54), we obtain

$$B(f) = \frac{4}{9} \frac{\frac{3}{\mu} - \frac{1 - \sin \alpha}{1 + \sin \alpha} \cos \alpha + \frac{\mu}{\mu + 3} \cos^3 \alpha}{\frac{2 - \mu}{\mu} + \left( \frac{\pi}{2} - \alpha \right) \tan \alpha + \frac{\mu}{\mu + 2} \cos^2 \alpha} \quad (55)$$

For a chromium surface, with  $\mu = -0.673$  and  $\alpha \approx 35^\circ$ , we obtain

$$B(f) = 0.5908$$

which differs by 0.0759, or 11.4%, from Lambert's nominal value  $B_L(f) = 2/3$ .

For nonmetallic surfaces we shall substitute the function  $D(\theta)$  from Eq. (48) into integrals in Eqs. (49) and (50). We obtain

$$\int_{\alpha}^{\pi/2} D(\theta) \sin \theta \cos \theta d\theta = \frac{1}{\mu + 2} \left[ \cos^2 \alpha + \mu \frac{\tan \alpha}{(\cos \alpha)^\mu} I_2(\alpha) \right] \quad (56)$$

where<sup>2</sup>

$$\left. \begin{aligned} I_2(\alpha) &= \int_{\alpha}^{\pi/2} (\cos \theta)^{\mu+2} d\theta \\ I_3(\alpha) &= \int_{\alpha}^{\pi/2} (\cos \theta)^{\mu+3} d\theta \end{aligned} \right\} \quad (58)$$

<sup>2</sup> Integrals  $I_2(\alpha)$  and  $I_3(\alpha)$ , given by Eq. (58), have the form

$$I_Y(\alpha) = \int_{\alpha}^{\pi/2} (\cos \theta)^{\mu+\gamma} d\theta$$

Introducing the new variable  $t = \cos^2 \theta$ , we obtain

$$I_Y(\alpha) = \frac{1}{2} \int_0^{\cos^2 \alpha} t^{[(\mu+\gamma+1)/2]-1} (1-t)^{-1/2} dt$$

This integral is of the form (Ref. 10)

$$I_Y(\alpha) = \frac{1}{2} \int_0^{\xi} t^{p-1} (1-t)^{q-1} dt = \frac{1}{2} B_{\xi}(p, q)$$

where  $B_{\xi}(p, q)$  is the incomplete Beta-function,  $p = (\mu + \gamma + 1)/2$ ,  $q = 1/2$ ,  $\xi = \cos^2 \alpha$ .

Hence,

$$I_Y(\alpha) = \frac{\xi^p}{2^p} {}_2F_1(p, 1-q; p+1; \xi)$$

where  ${}_2F_1$  is the hypergeometric function; thus

$$I_2(\alpha) = \frac{(\cos \alpha)^{(\mu+3)/2}}{\mu+3} {}_2F_1\left(\frac{\mu+3}{2}, \frac{1}{2}; \frac{\mu+5}{2}; \cos^2 \alpha\right)$$

$$I_3(\alpha) = \frac{(\cos \alpha)^{(\mu+4)/2}}{\mu+4} {}_2F_1\left(\frac{\mu+4}{2}, \frac{1}{2}; \frac{\mu+6}{2}; \cos^2 \alpha\right)$$

Hence, substituting integrals given by Eqs. (51), (56), and (57) into expressions (53) and (54), we obtain

$$A(f) = \frac{\mu\pi}{\mu+2} \left[ \frac{\mu+2}{\mu} - \cos^2 \alpha + 2 \frac{\tan \alpha}{(\cos \alpha)^\mu} I_2(\alpha) \right] \quad (59)$$

$$A(f)B(f) = \frac{2\pi\mu}{3(\mu+3)} \left[ \frac{\mu+3}{\mu} - \cos^3 \alpha + 3 \frac{\tan \alpha}{(\cos \alpha)^\mu} I_3(\alpha) \right] \quad (60)$$

$$B(f) = \frac{2}{3} \frac{\mu+2}{\mu+3} \frac{\frac{\mu+3}{\mu} - \cos^3 \alpha + 3 \frac{\tan \alpha}{(\cos \alpha)^\mu} I_3(\alpha)}{\frac{\mu+2}{\mu} - \cos^2 \alpha + 2 \frac{\tan \alpha}{(\cos \alpha)^\mu} I_2(\alpha)} \quad (61)$$

For a wooden surface, with  $\mu = 0.653$  and  $\alpha \cong 64^\circ$ , we obtain

$$B(f) = 0.6781$$

a value which differs by  $-0.0114$  or  $1.7\%$  from Lambert's value.

Integrals, given by Eq. (58), can be expressed in terms of a power series of  $\cos \alpha$ . Writing both integrals in the form

$$I_\gamma(\alpha) = \int_{\alpha}^{\pi/2} (\cos \theta)^{\mu+\gamma} d\theta, \quad \gamma = 2, 3$$

and introducing a new variable<sup>3</sup>

$$t = (\cos \theta)^{\mu+\gamma}$$

<sup>3</sup>Suggested by H. Lass.

we obtain the integral  $I_Y(\alpha)$  in the form

$$I_Y(\alpha) = \frac{1}{\mu + \gamma} \int_0^\lambda t^{1/(\mu+\gamma)} \left(1 - t^{2/(\mu+\gamma)}\right)^{-1/2} dt$$

where  $\lambda = (\cos \alpha)^{\mu+\gamma}$ . Since

$$(1 - \xi)^{-1/2} = 1 + \sum_{n=1}^{\infty} \frac{(2n-1)!!}{2^n n!} \xi^n$$

we arrive at the expression

$$I_Y(\alpha) = \frac{1}{\mu + \gamma} \int_0^\lambda t^{1/(\mu+\gamma)} \left[ 1 + \sum_{n=1}^{\infty} \frac{(2n-1)!!}{2^n n!} t^{2n/(\mu+\gamma)} \right] dt$$

which, after the performed integration, becomes

$$I_Y(\alpha) = \frac{(\cos \alpha)^{\mu+\gamma+1}}{\mu + \gamma + 1} \left[ 1 + \sum_{n=1}^{\infty} \frac{(2n-1)!!}{2^n n!} \frac{(\cos \alpha)^{2n}}{1 + \frac{2n}{\mu + \gamma + 1}} \right] \quad (62)$$

It is easy to show that, due to the fast convergence of series (62), for all practical purposes, it is sufficient to take only the first two terms of the series. Thus we have

$$I_3(\alpha) = \frac{(\cos \alpha)^{\mu+4}}{\mu + 4} \left[ 1 + \frac{\mu + 4}{2(\mu + 6)} \cos^2 \alpha \right]$$

$$I_2(\alpha) = \frac{(\cos \alpha)^{\mu+3}}{\mu + 3} \left[ 1 + \frac{\mu + 3}{2(\mu + 5)} \cos^2 \alpha \right]$$

Introducing these two expressions into Eqs. (59), (60), and (61), we finally obtain

$$A(f) = \frac{\mu \pi}{\mu + 2} \left[ \frac{\mu + 2}{\mu} - \cos^2 \alpha + 2 \frac{\sin \alpha \cos^2 \alpha}{\mu + 3} \left( 1 + \frac{1}{2} \frac{\mu + 3}{\mu + 5} \cos^2 \alpha \right) \right]$$

$$A(f)B(f) = \frac{2}{3} \frac{\mu \pi}{\mu + 3} \left[ \frac{\mu + 3}{\mu} - \cos^3 \alpha + 3 \frac{\sin \alpha \cos^3 \alpha}{\mu + 4} \left( 1 + \frac{1}{2} \frac{\mu + 4}{\mu + 6} \cos^2 \alpha \right) \right]$$

from which, by dividing the second expression by the first, the value of  $B(f)$  is obtained.

## IX. SPACECRAFT-FIXED SYSTEMS OF REFERENCE AXES

So far we have not yet specified the spacial orientation and the origin of the spacecraft-fixed reference frame xyz. Due to the fact that the center of gravity of the Mariner Venus/Mercury spacecraft does not coincide with the geometric center of the spacecraft and the fact that the distribution of masses on the spacecraft is such that the axes of the extremum quadratic moments of inertia (principal axes) do not coincide with the geometric reference axes, we have to define two systems of reference. The first system is the geometric system with respect to which the positions of various parts and components of the spacecraft are related. We shall denote by  $\bar{e}_1$ ,  $\bar{e}_2$ ,  $\bar{e}_3$  the unit vectors along the axes of this system, x, y, and z, respectively. The orientation of this system is established with respect to a basic, natural frame of reference, which we shall call the Sun-Canopus basic system (Ref. 11)  $x_S$ ,  $y_S$ ,  $z_S$ . The orientation of unit vectors  $\bar{e}_1'$ ,  $\bar{e}_2'$ ,  $\bar{e}_3'$  along the axes  $x_S$ ,  $y_S$ , and  $z_S$ , respectively, of this system is derived from the spacecraft-Sun and the spacecraft-star Canopus directions. The system is obviously non-inertial and rotates in space following the orbital motion of the spacecraft and the motion of the spacecraft-Sun line relative to the inertial space. If, as previously denoted,  $\bar{U}$  is the unit vector along the spacecraft-Sun direction,

$$\bar{U} = - \frac{\bar{r}}{r}$$

and  $\bar{U}_C$  is the unit vector along the spacecraft-Canopus direction,<sup>4</sup> the unit vectors  $\bar{e}'_1$ ,  $\bar{e}'_2$ ,  $\bar{e}'_3$  are given by (Ref. 11)

$$\left. \begin{aligned} \bar{e}'_1 &= \frac{\bar{U}_C \times \bar{U}}{|\bar{U}_C \times \bar{U}|} \\ \bar{e}'_2 &= \frac{\bar{U} \times (\bar{U}_C \times \bar{U})}{|\bar{U}_C \times \bar{U}|} \\ \bar{e}'_3 &= \bar{U} = -\frac{\bar{r}}{r} \end{aligned} \right\} \quad (63)$$

The geometric spacecraft-fixed system is obtained by a positive rotation of this system (counterclockwise) about the  $z_B$ -axis by an angle of  $30^\circ$ . Hence

$$\begin{pmatrix} \bar{e}_1 \\ \bar{e}_2 \\ \bar{e}_3 \end{pmatrix} = [B] \begin{pmatrix} \bar{e}'_1 \\ \bar{e}'_2 \\ \bar{e}'_3 \end{pmatrix} \quad (64)$$

where  $[B]$  is the transformation matrix

$$[B] = \begin{pmatrix} \cos 30^\circ & \sin 30^\circ & 0 \\ -\sin 30^\circ & \cos 30^\circ & 0 \\ 0 & 0 & 1 \end{pmatrix} \quad (65)$$

---

<sup>4</sup>Due to the fact that, for all practical purposes of flight missions within the solar system, the star Canopus can be considered to be infinitely distant from the solar system; the spacecraft-Canopus direction may be considered the same as the geocentric (or heliocentric) direction of the star.

Equations (64) and (65) yield

$$\begin{aligned}\bar{\mathbf{e}}_1 &= \frac{\sqrt{3}}{2} \bar{\mathbf{e}}'_1 + \frac{1}{2} \bar{\mathbf{e}}'_2 \\ \bar{\mathbf{e}}_2 &= -\frac{1}{2} \bar{\mathbf{e}}'_1 + \frac{\sqrt{3}}{2} \bar{\mathbf{e}}'_2 \\ \bar{\mathbf{e}}_3 &= \bar{\mathbf{e}}'_3\end{aligned}$$

or

$$\left. \begin{aligned}\bar{\mathbf{e}}_1 &= \frac{1}{2 |\bar{\mathbf{U}}_C \times \bar{\mathbf{U}}|} \left[ (\bar{\mathbf{U}}_C \times \bar{\mathbf{U}}) \sqrt{3} + \bar{\mathbf{U}}_C - (\bar{\mathbf{U}}_C \cdot \bar{\mathbf{U}}) \bar{\mathbf{U}} \right] \\ \bar{\mathbf{e}}_2 &= \frac{\sqrt{3}}{2 |\bar{\mathbf{U}}_C \times \bar{\mathbf{U}}|} \left[ \bar{\mathbf{U}}_C - (\bar{\mathbf{U}}_C \cdot \bar{\mathbf{U}}) \bar{\mathbf{U}} - \frac{\bar{\mathbf{U}}_C \times \bar{\mathbf{U}}}{\sqrt{3}} \right] \\ \bar{\mathbf{e}}_3 &= \bar{\mathbf{U}}\end{aligned}\right\} (66)$$

The orientation of axes  $x$ ,  $y$ ,  $z$  of the geometric reference system on the spacecraft is shown in Figs. 8 and 9.

Now let  $x_C$ ,  $y_C$ ,  $z_C$  be the coordinates of the center of mass of the spacecraft relative to the above-defined reference frame. Also let  $a_i$ ,  $b_i$ ,  $c_i$ ,  $i = 1, 2, 3$ , be the direction cosines of the principal axes of inertia relative to the axes of the reference system xyz. If  $\xi$ ,  $\eta$ , and  $\zeta$  are the principal axes of inertia of the spacecraft and  $\bar{i}$ ,  $\bar{j}$ , and  $\bar{k}$  the unit vectors along these axes, respectively, the transformation between the unit vectors of the geometric reference system,  $\bar{\mathbf{e}}_1$ ,  $\bar{\mathbf{e}}_2$ ,  $\bar{\mathbf{e}}_3$  and the unit vectors along the principal axes of inertia (we shall call this system the dynamic reference system) is given by

$$\begin{pmatrix} \bar{\mathbf{e}}_1 \\ \bar{\mathbf{e}}_2 \\ \bar{\mathbf{e}}_3 \end{pmatrix} = [A] \begin{pmatrix} \bar{i} \\ \bar{j} \\ \bar{k} \end{pmatrix} \quad (67)$$

where  $[A]$  is the transformation matrix

$$[A] = \begin{pmatrix} a_1 & a_2 & a_3 \\ b_1 & b_2 & b_3 \\ c_1 & c_2 & c_3 \end{pmatrix} \quad (68)$$

or (Ref. 12)

$$[A] = \begin{pmatrix} 0.948 & -0.315 & 0.037 \\ 0.316 & 0.947 & -0.048 \\ -0.020 & 0.057 & 0.998 \end{pmatrix} \quad (69)$$

The transformation between the coordinates of the two systems is given by

$$\begin{pmatrix} x \\ y \\ z \end{pmatrix} = \begin{pmatrix} x_C \\ y_C \\ z_C \end{pmatrix} + [A] \begin{pmatrix} \xi \\ \eta \\ \zeta \end{pmatrix} \quad (70)$$

and, inversely,

$$\begin{pmatrix} \xi \\ \eta \\ \zeta \end{pmatrix} = [A]^T \begin{pmatrix} x - x_C \\ y - y_C \\ z - z_C \end{pmatrix} \quad (71)$$

The coordinates of the center of mass of the spacecraft in the reference system xyz are (Ref. 12)

$$\left. \begin{array}{l} x_C = 1.22 \text{ cm} \\ y_C = -5.36 \text{ cm} \\ z_C = -32.16 \text{ cm} \end{array} \right\} \quad (72)$$

## X. THE GENERAL SYNOPSIS OF THE ILLUMINATED SURFACES ON THE SPACECRAFT

The configuration of spacecraft components, main parts, instruments, etc., which are illuminated by the Sun, and their positions relative to the xyz system are shown in Figs. 8 and 9. For the sake of simplicity, we shall divide the whole multitude of paraphernalia into two groups. The first group consists of those elements that have a considerable thickness for which the thermal analysis has to be performed, i. e., those elements for which there is an unbalance of the thermal re-radiation on their front and back surfaces. Without any considerable loss of accuracy we can say that the only components of the spacecraft which belong to this group are the high-gain antenna reflector and the two solar panels.

The second group of spacecraft elements can be subdivided into two subgroups. The first subgroup contains all components whose illuminated surfaces are either flat (planar) or very close to being flat. The second subgroup contains the elements whose surfaces are curved. The complete survey of all illuminated surfaces is given in Table 11 (Ref. 8). The survey of materials and their optical properties are given in Table 12.

## XI. THE SOLAR RADIATION FORCE AND TORQUE ON THE HIGH-GAIN ANTENNA REFLECTOR

The high-gain antenna is designed in such a manner that it is free to move at the end of a boom, which can rotate about a point in the xy-plane with coordinates  $x = -21.0$  cm,  $y = 104.6$  cm. The angle between the direction of the boom in the stowed position and its direction in the completely deployed position is  $155.2^\circ$ . In the fully deployed position of the antenna, the lowest point of the antenna dish lies on the y-axis; the coordinates of this point are  $x_{AC} = 0$ ,  $y_{AC} = 207.3$  cm,  $z_{AC} = -56.2$  cm. The axis of symmetry of the antenna is pointed toward the Earth, which requires a constant updating of the antenna position during the mission (Fig. 10).

In order to derive the expressions for the solar pressure force and its moment on the high-gain antenna reflector, we have to establish an

antenna-fixed system of reference axes  $x_A$ ,  $y_A$ ,  $z_A$  (Fig. 10). The  $z_A$ -axis of this system lies along the geocentric position vector of the spacecraft. Since, from Fig. 11, the geocentric position vector of the spacecraft is  $\bar{r} - \bar{r}_E$ , where  $\bar{r}_E$  is the heliocentric position vector of the Earth, the unit vector along the  $z_A$ -axis will be defined by

$$\vec{z}_A^* = - \frac{\bar{r} - \bar{r}_E}{|\bar{r} - \bar{r}_E|} \quad (73)$$

The other two axes,  $x_A$  and  $y_A$ , lie in the plane passing through the bottom point of the antenna dish, perpendicular to the spacecraft-Earth direction.<sup>5</sup> Since the directions of the  $x_A$ - and  $y_A$ -axes are arbitrary in the  $x_A y_A$ -plane, we shall follow the convention used in Ref. 1. In other words, we choose the  $y_A$ -axis to lie in the  $yz$ -plane of the spacecraft-fixed geometric system of reference,  $xyz$  (Fig. 10). The view of the antenna geometry from the positive direction of the  $x_A$ -axis is shown in Fig. 12. The antenna is always illuminated from the back side,<sup>6</sup> and the angle  $\psi$  is the supplementary angle of the Sun-spacecraft-Earth angle  $\alpha'$  (Fig. 12). Thus, from Fig. 11,

$$\alpha' = \arccos \left( \frac{\bar{r} \cdot (\bar{r} - \bar{r}_E)}{r |\bar{r} - \bar{r}_E|} \right) \quad (74)$$

$$\psi = 180^\circ - \alpha' \quad (75)$$

---

<sup>5</sup> Due to the large distance between the spacecraft and Earth, the distance between the lowest point of the antenna dish and the geometric center of the spacecraft (origin of the system  $xyz$ ) can be neglected.

<sup>6</sup> See Fig. 14 (Ref. 13).

The relative positions of the  $x_A^*y_A^*z_A^*$  and xyz systems are shown in Fig. 13, where both systems have the same origin. The transformation equations between the two systems are

$$\left. \begin{aligned} \bar{x}_A^* &= -\bar{e}_1 \\ \bar{y}_A^* &= \bar{e}_2 \cos \psi + \bar{e}_3 \sin \psi \\ \bar{z}_A^* &= \bar{e}_2 \sin \psi - \bar{e}_3 \cos \psi \end{aligned} \right\} \quad (76)$$

where  $\bar{x}_A^*$ ,  $\bar{y}_A^*$ ,  $\bar{z}_A^*$  are the unit vectors along the axes of the system  $x_A^*y_A^*z_A^*$ , respectively. The coordinate transformation is then given by

$$\begin{pmatrix} x_A \\ y_A \\ z_A \end{pmatrix} = \begin{pmatrix} -1 & 0 & 0 \\ 0 & \cos \psi & \sin \psi \\ 0 & \sin \psi & -\cos \psi \end{pmatrix} \begin{pmatrix} x - x_{AC} \\ y - y_{AC} \\ z - z_{AC} \end{pmatrix} \quad (77)$$

or, inversely,

$$\begin{pmatrix} x \\ y \\ z \end{pmatrix} = \begin{pmatrix} x_{AC} \\ y_{AC} \\ z_{AC} \end{pmatrix} + \begin{pmatrix} -1 & 0 & 0 \\ 0 & \cos \psi & \sin \psi \\ 0 & \sin \psi & -\cos \psi \end{pmatrix} \begin{pmatrix} x_A \\ y_A \\ z_A \end{pmatrix} \quad (78)$$

We shall later use Eq. (78) to obtain the components of the solar pressure force and of the moment of that force (torque) along the axes of the system xyz by means of the components of the force and of the moment along the axes of the antenna-fixed system  $x_A^*y_A^*z_A^*$ .

The dish of the high-gain antenna reflector is a paraboloid of revolution. The depth of the reflector is

$$h = 21.6 \text{ cm} \quad (79)$$

and the aperture radius is

$$\delta = 68.6 \text{ cm} \quad (80)$$

The equation of the reflecting surface is

$$\phi(x_A, y_A, z_A) \equiv \lambda \left( x_A^2 + y_A^2 \right) - z = 0 \quad (81)$$

where

$$\lambda = \frac{h}{\delta^2} \quad (82)$$

The local normal to the convex surface of the antenna reflector is given by

$$\bar{N} = \frac{\nabla \phi}{|\nabla \phi|} = \frac{2\lambda x_A \bar{x}_A^* + 2\lambda y_A \bar{y}_A^* - \bar{z}_A^*}{\sqrt{1 + 4\lambda z_A}} \quad (83)$$

and the unit vector along the spacecraft-Sun direction in the system  $x_A y_A z_A$  is

$$\bar{U} = \bar{y}_A^* \sin \psi - \bar{z}_A^* \cos \psi \quad (84)$$

Hence, from Eqs. (83) and (84),

$$\cos \theta = \bar{N} \cdot \bar{U} = \frac{2\lambda y_A \sin \psi + \cos \psi}{\sqrt{1 + 4\lambda z_A}} \quad (85)$$

From Fig. 12 we see that, when the angle  $\psi$  is

$$0 \leq \psi \leq \psi_F$$

where  $\psi_F$  is the critical value of the angle  $\psi$  at which the shadowing of the convex (back) surface of the antenna begins, the projection of the illuminated surface on the  $x_A y_A$ -plane is a circle of radius  $\delta$  (the aperture radius of the antenna), as shown in Fig. 15. If the shadowing occurs, i.e., if the angle  $\psi$  is larger than a certain critical value  $\psi_F$ ,

$$\psi_F < \psi$$

the projection of the illuminated surface is a segment of the circle with a central angle  $2\Phi$  (Fig. 15). The value of the angle  $\psi_F$  can be obtained from the geometric condition that, when  $\psi = \psi_F$ , the incident solar ray, shown in Fig. 15 as passing through the point P, passes through the point C on the brim of the dish of the antenna reflector, and is tangent to the outside surface of the antenna. From the geometric conditions, it follows that

$$\tan \psi_F = \frac{\delta}{2h} \quad (86)$$

so that, for the antenna of the Mariner Venus/Mercury spacecraft,

$$\psi_F = 57.8^\circ$$

We shall now introduce a set of polar coordinates in the  $x_A y_A$ -plane. Since the projection of the illuminated surface is symmetric with respect to the  $y_A$ -axis, we should introduce these polar coordinates, R and  $\varphi$ , in such a manner that the polar angle  $\varphi$  is measured from the  $y_A$ -axis in the positive direction (Fig. 15). This will enable us to evaluate the integrals which appear in the expressions for the solar pressure force (Eq. 41) and the moment of the solar pressure force (Eq. 45) over one-half of the surface and double the result.

In the case when the antenna is partially in the shade, the line which separates the illuminated part of the surface from the part in the shade projects in the  $x_A y_A$ -plane as part of a straight line  $SS_1$  (Fig. 15), at a distance

$$Y_S = - \frac{\cot \psi}{2\lambda} \quad (87)$$

from the  $x_A$ -axis. Hence, the central angle  $\Phi$  is given by

$$\cos \Phi = \frac{Y_S}{\delta} = - \frac{\cot \psi}{2\lambda \delta} \quad (88)$$

The polar coordinates are defined by

$$\left. \begin{array}{l} x_A = - R \sin \varphi \\ y_A = R \cos \varphi \end{array} \right\} \quad (89)$$

Hence,

$$z_A = \lambda R^2 \quad (90)$$

$$\cos \theta = \frac{2\lambda R \cos \varphi \sin \psi + \cos \psi}{\sqrt{1 + 4\lambda^2 R^2}} \quad (91)$$

The surface element,  $dS$ , is

$$dS = \frac{dx_A dy_A}{|\vec{N} \cdot \vec{z}_A^*|} = R dR d\varphi \sqrt{1 + 4\lambda^2 R^2} \quad (92)$$

Since, for the high-gain antenna,  $\beta = 0$  (no specular reflection), the solar radiation force, given by Eq. (41), becomes

$$\bar{F}_A = - \frac{\lambda S}{\rho^2} \iint_S \left\{ B(f)[\gamma + (1 - \gamma) K(r, \theta)] \vec{N} + \vec{U} \right\} dS \cos \theta \quad (93)$$

The back side of the antenna surface is painted black; very little percentage of the incident radiation (10%) is reflected and the major portion (90%) is absorbed and re-radiated isotropically into space as thermal radiation from both surfaces of the antenna. Hence, Eq. (86) can be written in the form

$$\bar{F}_A = -\frac{\lambda_S}{\rho^2} \iint_S \left\{ [B(f) \gamma \bar{N} + \bar{U}] dS \cos \theta + B(f) (1 - \gamma) \iint_S K(r, \theta) \bar{N} dS \cos \theta \right\} \quad (94)$$

From Eqs. (83) and (84) we find the components of vectors  $\bar{N}$  and  $\bar{U}$  along the axes of the antenna-fixed reference system  $x_A y_A z_A$ . They are

$$\left. \begin{aligned} N_{xA} &= \bar{N} \cdot \bar{x}_A^* = \frac{2\lambda x_A}{\sqrt{1 + 4\lambda^2 z_A}} = \frac{-2\lambda R \sin \varphi}{\sqrt{1 + 4\lambda^2 R^2}} \\ N_{yA} &= \bar{N} \cdot \bar{y}_A^* = \frac{2\lambda y_A}{\sqrt{1 + 4\lambda^2 z_A}} = \frac{2\lambda R \cos \varphi}{\sqrt{1 + 4\lambda^2 R^2}} \\ N_{zA} &= \bar{N} \cdot \bar{z}_A^* = -\frac{1}{\sqrt{1 + 4\lambda^2 z_A}} = -\frac{1}{\sqrt{1 + 4\lambda^2 R^2}} \\ U_{xA} &= \bar{U} \cdot \bar{x}_A^* = 0 \\ U_{yA} &= \bar{U} \cdot \bar{y}_A^* = \sin \psi \\ U_{zA} &= \bar{U} \cdot \bar{z}_A^* = -\cos \psi \end{aligned} \right\} \quad (95)$$

Substituting the expression for the function  $K(r, \theta)$  from Eq. (39), by setting  $B(f) = 2/3$ , we obtain, instead of Eq. (94),

$$\begin{aligned}
 \bar{F}_A &= -\frac{\lambda S}{\rho^2} \iint_S B(f)[\gamma + (1 - \gamma) K] \begin{pmatrix} N_{xA} \\ N_{yA} \\ N_{zA} \end{pmatrix} + \begin{pmatrix} U_{xA} \\ U_{yA} \\ U_{zA} \end{pmatrix} dS \cos \theta \\
 &\quad - \frac{2\lambda S^P(1 - \gamma)}{3\rho^{7/2}} \iint_S (\cos \theta)^{7/4} \begin{pmatrix} N_{xA} \\ N_{yA} \\ N_{zA} \end{pmatrix} dS \\
 &\quad - \frac{2\lambda S^Q(1 - \gamma)}{3\rho^5} \iint_S (\cos \theta)^{5/2} \begin{pmatrix} N_{xA} \\ N_{yA} \\ N_{zA} \end{pmatrix} dS \tag{97}
 \end{aligned}$$

or

$$\bar{F}_A \approx \frac{1}{\rho^2} \begin{pmatrix} I_x \\ I_y \\ I_z \end{pmatrix} + \frac{1}{\rho^{7/2}} \begin{pmatrix} J_x \\ J_y \\ J_z \end{pmatrix} + \frac{1}{\rho^5} \begin{pmatrix} K_x \\ K_y \\ K_z \end{pmatrix} \tag{98}$$

The values of components  $I_x, I_y, I_z, J_x, J_y, J_z, K_x, K_y, K_z$  for different values of the angle  $\psi$  are obtained by numerical integrations (see Appendix). They are shown in Table 13.

The components of the force  $\bar{F}_A$ , obtained from Eq. (98) for different values of  $\xi$ , are shown in Tables 14 and 15. The component along the  $x_A$ -axis of the antenna-fixed system is always

$$F_{xA} = 0$$

and the values of  $F_{yA}$  and  $F_{zA}$  are given in  $10^6$  newtons. The values of the magnitude of the force  $\bar{F}_A$  are given in Table 16. The values of the acceleration

$$a_A = \frac{|\bar{F}_A|}{m}$$

where  $m$  is the mass of the spacecraft ( $m = 498.534$  kg), are given in  $10^{11}$   $\text{km/s}^2$  and shown in Table 17.

It is obvious, however, that the angle  $\psi$  cannot take all values between  $0^\circ$  and  $90^\circ$  for every value of the ratio  $\zeta$ . Hence, to find the values of the angle  $\psi$  during the mission of the spacecraft, two unperturbed (elliptical) trajectories have been generated. The first one covers the Earth-Venus cruising period, while the second covers the Venus-Mercury cruise phase. The osculating orbital elements used are:

$a$  = semimajor axis of the ellipse

$e$  = eccentricity of the ellipse

$i$  = inclination of the spacecraft's orbit to the ecliptic plane  
of 1950.0

$\Omega$  = longitude of the ascending node of the spacecraft's orbit

$\omega$  = argument of perihelion of the spacecraft's orbit

$M_0$  = mean anomaly of the spacecraft at the time of the trajectory initialization

All orbital parameters are osculating parameters for a certain date, and the last four, the angles  $i$ ,  $\Omega$ ,  $\omega$ , and  $M_0$ , are taken relative to the inertial Earth's ecliptic reference plane of 1950.0. For the first cruise phase, from Earth to the neighborhood of Venus, the orbital parameters are:

$$a = 1.197432 \times 10^8 \text{ km}$$

$$e = 0.239245$$

$$i = 3^\circ 2591$$

$$\Omega = 40^\circ 1884$$

$$\omega = 181^\circ 4284$$

$$M_0 = 186^\circ 2239$$

Epoch = 1973, Nov. 9.81

For the cruise phase between Venus and Mercury, the osculating orbital elements are taken to be

$$a = 0.931175 \times 10^8 \text{ km}$$

$$e = 0.258303$$

$$i = 4^\circ 3516$$

$$\Omega = 10^\circ 1687$$

$$\omega = 271^\circ 4563$$

$$M_0 = 252^\circ 6186$$

Epoch = 1974, Feb. 8.71

A simple program (see Appendix) was used to obtain the values of the angle  $\psi$  and the components of the solar radiation force in the high-gain antenna reference frame  $x_A y_A z_A$ , and the magnitude of the acceleration  $a_A$ . The results are shown in Table 18. Time is given in days, counted since the beginning of the Earth-Venus cruise phase (1973, Nov. 3.81).

The moment of the solar pressure force about the origin of the antenna-fixed reference system is given by Eq. (45):

$$\overline{M}_A^{(O)} = -\frac{\lambda S}{\rho^2} \iint_S [v(\theta)(\bar{X} \times \bar{N}) + (1 - \beta\gamma)(\bar{X} \times \bar{U}) \cos \theta] dS$$

where the function  $v(\theta)$  is given by Eq. (44). Because of the fact that the specular reflection coefficient  $\beta = 0$ , we find that

$$v(\theta) = B(f)[\gamma + (1 - \gamma) K(r, \theta)] \cos \theta$$

where  $K(r, \theta)$  is given by Eq. (39). Also,

$$\bar{\mathbf{X}} = \begin{pmatrix} x_A \\ y_A \\ z_A \end{pmatrix} = \begin{pmatrix} -R \sin \varphi \\ R \cos \varphi \\ \lambda R^2 \end{pmatrix}$$

Due to the fact that the  $x_A$ -component of the force  $\bar{\mathbf{F}}_A$  vanishes, the  $y_A$ - and  $z_A$ -components of the moment  $\bar{\mathbf{M}}_A^{(O)}$  vanish, i.e.,

$$M_{yA}^{(O)} = 0$$

$$M_{zA}^{(O)} = 0$$

and the only component (and also the total moment vector) of  $\bar{\mathbf{M}}_A^{(O)}$  is the one along the  $x_A$ -axis,  $M_{xA}^{(O)}$ . The time variations of the magnitude of the moment  $|\bar{\mathbf{M}}_A^{(O)}|$  are shown in Table 19.

To obtain the components of the force  $\bar{\mathbf{F}}_A$  in the spacecraft-fixed reference system xyz, we shall use the transformation equation (78).

Denoting these components by  $F_{Ax}$ ,  $F_{Ay}$ ,  $F_{Az}$ , we find

$$\bar{\mathbf{F}}_A = \begin{pmatrix} F_{Ax} \\ F_{Ay} \\ F_{Az} \end{pmatrix} = \begin{pmatrix} -1 & 0 & 0 \\ 0 & \cos \psi & \sin \psi \\ 0 & \sin \psi & -\cos \psi \end{pmatrix} \begin{pmatrix} F_{yA} \\ F_{zA} \end{pmatrix} \quad (99)$$

The values of components  $F_{Ax}$ ,  $F_{Ay}$ , and  $F_{Az}$  are shown in Table 20.

The components of the moment vector of the solar radiation force in the spacecraft-fixed reference frame xyz (the unit vectors along these axes have previously been denoted by  $\bar{\mathbf{e}}_1$ ,  $\bar{\mathbf{e}}_2$ ,  $\bar{\mathbf{e}}_3$  and defined in expressions 66) can be derived in the following manner.

The elementary moment vector of the radiation force about the origin O of the antenna-fixed system of reference is

$$d\bar{M}_A^{(O)} = \bar{x} \times d\bar{F}_A$$

where  $d\bar{F}_A$  is the elementary force vector. From Fig. 16, which shows the spacial relationship between the antenna-fixed and the spacecraft-fixed reference system, we see that, for any point P of the antenna,

$$\bar{x} = \bar{x}_A - \bar{x}_0$$

Hence,

$$d\bar{M}_A^{(O)} = \bar{x}_A \times d\bar{F}_A - \bar{x}_0 \times d\bar{F}_A$$

where

$$\bar{x}_A \times d\bar{F}_A = d\bar{M}_A^{(C)}$$

$$d\bar{M}_A^{(O)} = d\bar{M}_A^{(C)} - \bar{x}_0 \times d\bar{F}_A$$

Integrating over the illuminated surface area of the high-gain antenna reflector, we obtain the moment vector of the solar radiation force about the origin of the spacecraft-fixed system:

$$\bar{M}_A^{(C)} = \bar{M}_A^{(O)} + \bar{x}_0 \times \bar{F}_A \quad (100)$$

Because of the fact that the moment vector  $\bar{M}_A^{(O)}$  has only one component,  $M_{xA}^{(O)}$ , and since the axis  $x_A$  and  $x$  are antiparallel, we have

$$\bar{M}_A^{(O)} = \begin{pmatrix} M_{Ax}^{(O)} \\ 0 \\ 0 \end{pmatrix} = \begin{pmatrix} -M_{xA}^{(O)} \\ 0 \\ 0 \end{pmatrix}$$

$$M_{Ax}^{(O)} = -M_{xA}^{(O)}$$

Hence,

$$\bar{M}_A^{(C)} = \begin{pmatrix} -M_{xA}^{(O)} \\ 0 \\ 0 \end{pmatrix} + \begin{pmatrix} \bar{e}_1 & \bar{e}_2 & \bar{e}_3 \\ x_{AC} & y_{AC} & z_{AC} \\ 0 & F_{Ay} & F_{Az} \end{pmatrix} \quad (101)$$

where  $x_{AC}$ ,  $y_{AC}$ ,  $z_{AC}$  (Eq. 78) are the coordinates of the origin of the antenna-fixed reference frame in the spacecraft-fixed system,  $\bar{e}_1$ ,  $\bar{e}_2$ ,  $\bar{e}_3$  are the unit vectors along the axes of the spacecraft-fixed system, and, from Eq. (99),

$$\left. \begin{aligned} F_{Ay} &= F_{yA} \cos \psi + F_{zA} \sin \psi \\ F_{Az} &= F_{yA} \sin \psi - F_{zA} \cos \psi \end{aligned} \right\} \quad (102)$$

At this point it should be mentioned that all of the derived expressions for the solar radiation force and its moment are valid through the Earth-Venus and Venus-Mercury phases. After the encounter with Mercury, the Earth-spacecraft-antisolar point angle  $\psi$  becomes greater than  $90^\circ$ , and the Sun rays reach the front (concave) side of the antenna reflector. For

$$90^\circ < \psi < 180^\circ - \psi_F \cong 122.2^\circ$$

both front and back surfaces of the antenna reflector are partially irradiated, while for

$$180^\circ - \psi_F \leq \psi \leq 180^\circ$$

the back side of the antenna is in the shade and only the front (concave) side of the antenna is irradiated. At the point of the superior conjunction (when

the spacecraft, Sun, and the Earth are on a line, the Sun being between the Earth and the spacecraft),  $\psi = 180^\circ$

The expressions for the solar pressure and its moment for the concave side of the high-gain antenna reflector are given in Refs. 1 and 2. The solar radiation force on the antenna during the extended mission of the Mariner Venus/Mercury spacecraft (beyond Mercury encounter) will be treated elsewhere.

## XII. THE SOLAR RADIATION FORCE AND TORQUE ON TWO SOLAR PANELS

The two solar panels of the Mariner Venus/Mercury spacecraft are flat surfaces covered with solar cells which supply the spacecraft with electric energy. The x-axis of the spacecraft-fixed frame of reference is the axis of symmetry of solar panels. The total area of both panels is  $5.8312 \text{ m}^2$  (Table 11).

At the beginning of the mission, both solar panels are perpendicular to the Sun-spacecraft line. Later, when the spacecraft approaches the Sun, the temperature of the solar panels would rise considerably and the voltage of the electric power system would suffer considerable changes. For that reason, in order to counteract and neutralize these effects, the solar panels are tilted during the mission about the x-axis of the spacecraft-fixed reference frame in such a manner that the angle of tilt

$$\theta = \arccos (\bar{U} \cdot \bar{N})$$

increases as the distance of the spacecraft from the Sun decreases. The process is not continuous, and the position of the solar panels is updated at certain times, as shown in Table 21 (Ref. 14). Both panels are tilted (rotated) in the same direction in order to avoid additional torques, which would require an extra amount of fuel to counteract, and by the same angle.

The Sun-side (front side) of the panels is covered with solar cells. About 22% of the radiant energy is reflected, 75% of it specularly (Table 12). The remaining 78% of the energy is absorbed and re-radiated from both surfaces of the panels. Since the emissivity of the antisolar point side is

higher than the emissivity of the Sun side, that portion of the solar radiation force due to the thermal re-radiation will, therefore, be directed toward the Sun. The thickness of the material of which the solar panels are made is 1.27 cm, and the thermal conductivity of the material is the same as that of the antenna reflector.

Since the area of the solar panels is flat and the angle  $\theta$  is a step-function of time, the function  $K(r, \theta)$ , given by Eq. (16), depends on  $r$  only. Hence, because

$$\bar{N} = \begin{pmatrix} 0 \\ \sin \theta \\ \cos \theta \end{pmatrix}$$

$$\bar{U} = \begin{pmatrix} 0 \\ 0 \\ 1 \end{pmatrix}$$

the solar radiation force, given by Eq. (41), becomes, after integration

$$\begin{aligned} \bar{F}_{SP} = - \frac{\lambda S_{SP}^A}{r^2} & \left\{ \left[ 2\beta_{SP} \gamma_{SP} \cos \theta + B(f) (\gamma_{SP}(1 - \beta_{SP}) \right. \right. \\ & \left. \left. + (1 - \gamma_{SP}) K(r, \theta) \right] \begin{pmatrix} 0 \\ \sin \theta \\ \cos \theta \end{pmatrix} \right. \\ & \left. + (1 - \beta_{SP} \gamma_{SP}) \begin{pmatrix} 0 \\ 0 \\ 1 \end{pmatrix} \right\} \cos \theta \quad (103) \end{aligned}$$

It is easy to see from the spacecraft geometry that the component of this force along the x-axis of the spacecraft-fixed system is zero, i.e.,

$$F_{SPx} = 0$$

By the same token, the moment of the solar radiation force about the origin of the spacecraft-fixed reference frame xyz vanishes, i. e.,

$$\overline{M}_{SP}^{(C)} = 0$$

This fact can also be derived from Eq. (45), which gives the moment vector of the solar radiation force. The only two integrals which appear in Eq. (45) are

$$\iint_S (\bar{X} \times \bar{N}) dS$$

and

$$\iint_S (\bar{X} \times \bar{U}) dS$$

The unit vectors  $\bar{N}$  and  $\bar{U}$  are constant insofar as the integration over the surface area of solar panels is concerned. Hence,

$$\iint_S (\bar{X} \times \bar{N}) dS = - \bar{N} \times \iint_S \bar{X} dS$$

$$\iint_S (\bar{X} \times \bar{U}) dS = - \bar{U} \times \iint_S \bar{X} dS$$

where the integral

$$\iint_S \bar{X} dS$$

represents the static (linear) moment vector of inertia. The origin of the spacecraft-fixed reference system is located at the center of mass of the solar panels; therefore,

$$\iint_S \bar{X} dS = \bar{X}_C S \equiv 0$$

and the total moment of the solar radiation force vanishes.

The values of the components of the solar radiation force,  $F_{SPx}$ ,  $F_{SPy}$ ,  $F_{SPz}$ , acting on two solar panels during the Earth-Venus and Venus-Mercury phases are computed using the program shown in the Appendix and in Table 22. The acceleration due to this force is

$$a_{SP} = \frac{|\bar{F}_{SP}|}{m}$$

Its values are also listed in Table 22.

### XIII. THE SOLAR RADIATION FORCE AND TORQUE ON THE MAIN SUNSHADE OF THE SPACECRAFT AND THE CIRCULAR TV CAMERA HEAT SHIELD

The main sunshade of the Mariner Venus/Mercury spacecraft consists of eight flat trapezoidal surfaces and one circular heat shield of radius 45.7 cm in the middle (Fig. 17). All surfaces are adiabatic and, therefore,

$$K(r, \theta) = 1$$

In Table 11, the shades are defined by the coordinates of their endpoints, in the spacecraft-fixed system of reference. Let

$$\bar{F}_{SS} = \begin{pmatrix} F_{SSx} \\ F_{SSy} \\ F_{SSz} \end{pmatrix}$$

be the total force on the spacecraft's sunshade. The angle of incidence of all eight trapezoids are approximately the same. The average value of the angle is  $\theta = 15.86^\circ$ , and the average surface area of one particular trapezoid is  $0.3500 \text{ m}^2$ .

The cross-section of the sunshade and the force diagram are shown in Fig. 18. It is obvious that, assuming the same surface areas and the same angle of incidence, the lateral force components, parallel to the xy-plane of the spacecraft-fixed system, cancel; therefore, the sum of all lateral forces will vanish. In other words,

$$F_{SSx} = F_{SSy} = 0$$

and, by the same token, the total moment of the solar radiation force

$$\bar{M}_{SS}^{(C)} = 0$$

To obtain the value of the z-component of the solar radiation force  $\bar{F}_{SS}$  on eight trapezoids of the main sunshade and the circular heat shield in the middle, we can use Eq. (103). For the octagon sunshade (Table 12)

$$\gamma_{SS} = 0.48 \text{ (after exposure)}$$

$$\beta_{SS} = 0.21 \text{ (after exposure)}$$

and, for the circular heat shield,<sup>7</sup>

$$\gamma_{HS} = 0.72 \text{ (after exposure)}$$

$$\beta_{HS} = 1.0$$

---

<sup>7</sup>Including the jet nozzle on the +z-axis, which is small.

Hence, the total force on all shading surfaces along the z-axis is

$$F_{SSz} = - \frac{\lambda_s A_{SS}}{\rho^2} [ 2\beta_{SS} \gamma_{SS} \cos^2 \theta + B(f) \gamma_{SS} (1 - \beta_{SS}) \cos \theta \\ + (1 - \beta_{SS} \gamma_{SS}) + B(f) (1 - \gamma_{SS}) \cos \theta ] \cos \theta \\ - \frac{\lambda_s A_{HS}}{\rho^2} [ \gamma_{HS} + B(f) (1 - \gamma_{HS}) + 1 ]$$

where

$A_{SS} = 2.3106 \text{ m}^2$  = total surface area of the illuminated part of the octagon

$A_{HS} = 0.6563 \text{ m}^2$  = area of the circular TV camera heat shield

Thus,

$$F_{SSz} = - 4.94624 \frac{\lambda_s}{\rho^2} (\text{newtons}) \quad (104)$$

#### XIV. THE SOLAR RADIATION FORCE AND TORQUE ON THE MAGNETOMETER BOOM AND SHADES

The magnetometer boom is a circular cylinder of radius  $r_B = 3.2 \text{ cm}$ , made of silvered Teflon. The position of the axis of symmetry of the boom relative to the spacecraft-fixed reference frame is defined by two points on the axis (Table 11), which is parallel to the y-axis of the spacecraft. The length of the boom is

$$L_B = 6.012 \text{ m}$$

and the surface of the cylinder is adiabatic, which implies that  $K(r, \theta) = 1$ . The position of the boom is shown in Fig. 19;  $x_{B0}$ ,  $y_{B0}$ ,  $z_{B0}$  are coordinates of the footpoint of the magnetometer boom, which is taken as the origin of a local, boom-fixed system of reference axes  $x_B y_B z_B$ .

From Table 12, we find

$$\gamma_B = 0.85 \text{ (after exposure)}$$

$$\beta_B = 1.0$$

and, from Table 11,

$$x_{B0} = -25.4 \text{ cm}$$

$$y_{B0} = -120.7 \text{ cm}$$

$$z_{B0} = 31.8 \text{ cm}$$

From Fig. 19 we see that

$$\left. \begin{aligned} x &= x_B + x_{B0} \\ y &= -y_B + y_{B0} \\ z &= -z_B + z_{B0} \end{aligned} \right\} \quad (105)$$

Since the cylinder is symmetric about the plane parallel to the direction of the solar rays ( $y_B z_B$ -plane), it is easy to conclude that

$$F_{Bx} = 0$$

$$F_{By} = 0$$

and the only component of the solar radiation force on the magnetometer boom,  $\bar{F}_B$ , is the one along the  $z$ -axis,  $F_{Bz}$ .

The unit vector along the local normal to the cylindrical surface of the boom is given by (Fig. 20)

$$\bar{N} = \begin{pmatrix} \sin \varphi \\ 0 \\ \cos \varphi \end{pmatrix}$$

and the unit vector along the spacecraft-Sun line is given by

$$\bar{U} \approx \begin{pmatrix} 0 \\ 0 \\ -1 \end{pmatrix}$$

where the angle  $\varphi$  is measured in the positive direction from the  $z_B$ -axis.

As we have previously mentioned, the surface of the boom is assumed to be adiabatic; hence  $K(r, \theta) = 1$ . Also,  $\beta_B = 1.0$ ;  $1 - \beta_B = 0$ . The expression for the solar radiation force along the  $z$ -axis, which we take from Eq. (41) again, is

$$F_{Bz} = \frac{\lambda S}{\rho^2} \iint_S [2\gamma_B \cos \varphi \cos \theta - (1 - \gamma_B) + B(f)(1 - \gamma_B) \cos \varphi] \cos \theta \, dS$$

Here

$$\cos \theta = \bar{U} \cdot \bar{N} = -\cos \varphi$$

and

$$dS = \frac{dx_B dy_B}{\cos \varphi} = r_B dy_B d\varphi$$

Hence,

$$F_{Bz} = \frac{\lambda S r_B}{\rho^2} \int_{y_B=0}^{L_B} dy_B \int_{\varphi=\pi/2}^{3\pi/2} [2\gamma_B \cos^3 \varphi + (1 - \gamma_B) \cos \varphi + B(f)(1 - \gamma_B) \cos^2 \varphi] \, d\varphi$$

or

$$F_{Bz} = - \frac{6 + \pi - (\pi - 2) \gamma_B}{3} r_B L_B \frac{\lambda_S}{\rho^2} \quad (106)$$

or

$$F_{Bz} = - 0.52401 \frac{\lambda_S}{\rho^2} \text{ (newtons)} \quad (107)$$

With  $K(r, \theta) = 1$  and  $\beta_B = 1.0$ , the expression for the solar radiation torque, given by Eq. (45), about the origin of the spacecraft-fixed system of reference axes, because of

$$\bar{x} = \begin{pmatrix} x_B + x_{B0} \\ -y_B + y_{B0} \\ -z_B + z_{B0} \end{pmatrix}$$

becomes

$$\bar{M}_B^{(C)} = \begin{vmatrix} \bar{e}_1 & \bar{e}_2 & \bar{e}_3 \\ x_{B0} & y_{B0} & z_{B0} \\ 0 & 0 & F_{Bz} \end{vmatrix} + \int \int \int_S \begin{pmatrix} x_B \\ -y_B \\ -z_B \end{pmatrix} \times d\bar{F}_B$$

or

$$\overline{M}_B^{(C)} = \begin{pmatrix} y_{B0} \\ -x_{B0} \\ 0 \end{pmatrix} F_{Bz} - \frac{\lambda_S r_B}{2\rho} \int_{y_B=0}^{L_B} \int_{\varphi=\pi/2}^{3\pi/2} \left[ 2\gamma_B \begin{pmatrix} y_B \cos^3 \varphi \\ 2r_B \sin \varphi \cos^3 \varphi \\ -y_B \sin \varphi \cos^2 \varphi \end{pmatrix} \right.$$

$$- B(f)(1 - \gamma_B) \begin{pmatrix} y_B \cos^2 \varphi \\ 2r_B \sin \varphi \cos \varphi \\ -y_B \sin \varphi \end{pmatrix}$$

$$+ (1 - \gamma_B) \left[ \begin{pmatrix} y_B \cos \varphi \\ r_B \sin \varphi \cos \varphi \\ 0 \end{pmatrix} \right] dy_B d\varphi$$

After the performed integration, we obtain

$$M_{Bx}^{(C)} = y_{B0} F_{Bz} + \frac{\lambda_S r_B L_B^2}{6\rho} [6 + \pi - (\pi - 2)\gamma_B] = \left( y_{B0} - \frac{L_B}{2} \right) F_{Bz}$$

$$M_{By}^{(C)} = -x_{B0} F_{Bz}$$

$$M_{Bz}^{(C)} = 0$$

or

$$\left. \begin{aligned} M_{Bx}^{(C)} &= \left( y_{B0} - \frac{L_B}{2} \right) F_{Bz} \\ M_{By}^{(C)} &= -x_{B0} F_{Bz} \\ M_{Bz}^{(C)} &= 0 \end{aligned} \right\} \quad (108)$$

Finally, substituting the numerical values of  $\gamma_B$ ,  $x_{B0}$ ,  $y_{B0}$ ,  $r_B$ , and  $L_B$ , we obtain

$$\left. \begin{aligned} M_{Bx}^{(C)} &= 2.20763 \frac{\lambda_S}{\rho^2} \\ M_{By}^{(C)} &= -0.13310 \frac{\lambda_S}{\rho^2} \\ M_{Bz}^{(C)} &= 0 \end{aligned} \right\} \quad (109)$$

The three magnetometer shades are flat surfaces made of the same material from which the magnetometer boom is made. The total area, perpendicular to the Sun-spacecraft line, of all three sunshades is  $0.2566 \text{ m}^2$ . Since all three surfaces face the Sun, the angle of incidence  $\theta = 0$ , and the total force is along the z-axis of the spacecraft-fixed system of reference. For  $K = 1$  (surfaces are adiabatic) and  $\beta_B = 1$ , the total force on all three surfaces may be obtained directly from Eq. (103):

$$F_{MSz} = - \frac{0.2566 \lambda_S}{3\rho^2} (5 + \gamma_B) \quad (110)$$

or

$$F_{MSz} = -0.50037 \frac{\lambda_S}{\rho^2} (\text{newtons}) \quad (111)$$

To obtain the total moment of the solar radiation forces on all three rectangular sunshades, we shall calculate the coordinates of their respective centers of mass, using end-point coordinates from Table 11. The results are shown in Table 23.

If  $F_{MSz}^{(i)}$ ,  $i = 1, 2, 3$ , are the forces on the three sunshades and  $x_{Ci}$ ,  $y_{Ci}$ ,  $z_{Ci}$  are the coordinates of their respective centers of mass, the moment vectors about the origin of the spacecraft-fixed system of reference, C, are

$$\overline{M}_{MS(i)}^{(C)} = \begin{vmatrix} \bar{e}_1 & \bar{e}_2 & \bar{e}_3 \\ x_{Ci} & y_{Ci} & z_{Ci} \\ 0 & 0 & F_{MSz}^{(i)} \end{vmatrix}, \quad i = 1, 2, 3$$

or

$$\overline{M}_{MS(i)}^{(C)} = \begin{pmatrix} y_{Ci} \\ -x_{Ci} \\ 0 \end{pmatrix} F_{MSz}^{(i)} \quad (112)$$

Because

$$\left. \begin{aligned} F_{MSz}^{(1)} &= -\frac{0.0605 \lambda_S}{3\rho^2} (5 + \gamma_B) = -0.11797 \frac{\lambda_S}{\rho^2} \\ F_{MSz}^{(2)} &= -\frac{0.0877 \lambda_S}{3\rho^2} (5 + \gamma_B) = -0.17101 \frac{\lambda_S}{\rho^2} \\ F_{MSz}^{(3)} &= -\frac{0.1084 \lambda_S}{3\rho^2} (5 + \gamma_B) = -0.21138 \frac{\lambda_S}{\rho^2} \end{aligned} \right\}$$

we obtain, using Eq. (112),

$$\overline{M}_{MS(1)}^{(C)} = \frac{\lambda_S}{\rho^2} \begin{pmatrix} 0.53956 \\ -0.03014 \\ 0 \end{pmatrix}$$

$$\overline{M}_{MS(2)}^{(C)} = \frac{\lambda_S}{\rho^2} \begin{pmatrix} 1.16974 \\ -0.04361 \\ 0 \end{pmatrix}$$

$$\overline{M}_{MS(3)}^{(C)} = \frac{\lambda_S}{\rho^2} \begin{pmatrix} 0.89076 \\ -0.05929 \\ 0 \end{pmatrix}$$

Hence, the components of the total moment vectors are

$$\left. \begin{aligned} M_{MSx}^{(C)} &= 2.60006 \frac{\lambda_S}{\rho^2} \\ M_{MSy}^{(C)} &= -0.13304 \frac{\lambda_S}{\rho^2} \\ M_{MSz}^{(C)} &= 0 \end{aligned} \right\} \quad (113)$$

in newton-meters.

## XV. THE SOLAR RADIATION FORCE AND TORQUE ON THE THREE IRR INSTRUMENT SUNSHADES

The infrared radiometer (IRR) is protected from the direct solar radiation by means of two flat, rectangular plates, one perpendicular to the direction of solar radiation, the other inclined by an angle  $\theta_{RS} = 43.10^\circ$  to the z-axis of the spacecraft-fixed system. The position of the two sunshades relative to the reference axes of the spacecraft's reference system is shown in Fig. 21. Both surfaces are coated with Teflon Beta cloth and are adiabatic ( $K(r, \theta) = 1$ ). The two reflectivity parameters of the surface are

$$\beta_{RS} = 0.21 \text{ (after exposure)}$$

$$\gamma_{RS} = 0.48 \text{ (after exposure)}$$

The surface area of the first sunshade is  $0.0406 \text{ m}^2$ , and the area of the second (tilted) sunshade is  $0.0299 \text{ m}^2$ . Denoting by  $\bar{F}_{RS}^{(i)}$ ,  $i = 1, 2$ , the solar radiation forces of two sunshades, we find, using Eq. (103),

$$\bar{F}_{RS}^{(1)} = \begin{pmatrix} 0 \\ 0 \\ -0.06903 \end{pmatrix} \frac{\lambda S}{\rho^2} \text{ (newtons)} \quad (114)$$

For the second (tilted) sunshade, the cone angle of the normal to the surface is

$$\theta_{RS} = 43.10^\circ$$

and its clock angle is (Fig. 21)

$$\varphi_{RS} = 218.55^\circ$$

Hence,

$$\bar{N} = \begin{pmatrix} \cos \varphi_{RS} \sin \theta_{RS} \\ \sin \varphi_{RS} \sin \theta_{RS} \\ \cos \theta_{RS} \end{pmatrix} = \begin{pmatrix} -0.53436 \\ -0.42581 \\ 0.73016 \end{pmatrix}$$

and the expression for the solar radiation force, taken from Eq. (103), yields

$$\bar{F}_{RS}^{(2)} = -0.0299 \frac{\lambda_S}{\rho^2} \left[ \begin{aligned} & \left[ 2\beta_{RS} \gamma_{RS} \cos \theta_{RS} + B(f)(1 - \beta_{RS} \gamma_{RS}) \right] \begin{pmatrix} \cos \varphi_{RS} & \sin \theta_{RS} \\ \sin \varphi_{RS} & \sin \theta_{RS} \\ \cos \theta_{RS} \end{pmatrix} \\ & + (1 - \beta_{RS} \gamma_{RS}) \begin{pmatrix} 0 \\ 0 \\ 1 \end{pmatrix} \cos \theta_{RS} \end{aligned} \right]$$

and, finally,

$$\bar{F}_{RS}^{(2)} = \begin{pmatrix} 0.008711 \\ 0.006941 \\ -0.031534 \end{pmatrix} \frac{\lambda_S}{\rho^2} \text{ (newtons)} \quad (115)$$

If  $x_{RC}^{(i)}$ ,  $y_{RC}^{(i)}$ ,  $z_{RC}^{(i)}$ ,  $i = 1, 2$ , are coordinates of the centers of mass of the two sunshades, the moments of the solar radiation forces acting on their respective surfaces, about the origin of the spacecraft-fixed system C, are

$$\bar{M}_{RS(i)}^{(C)} = \bar{r}_{RC}^{(i)} \times \bar{F}_{RS}^{(i)}, \quad i = 1, 2$$

where

$$\bar{r}_{RC}^{(i)} = x_{RC}^{(i)} \bar{e}_1 + y_{RC}^{(i)} \bar{e}_2 + z_{RC}^{(i)} \bar{e}_3, \quad i = 1, 2$$

are position vectors of centers of mass of the IRR shades. The coordinates of the centers of mass of the two IRR sunshades are given in Table 24. The moment vectors  $\bar{M}_{RS(i)}^{(C)}$ ,  $i = 1, 2$ , are

$$\bar{M}_{RS(1)}^{(C)} = \begin{pmatrix} 0.06063 \\ -0.03262 \\ 0 \end{pmatrix} \frac{\lambda_S}{\rho^2} \quad (116)$$

$$\overline{M}_{RS(2)}^{(C)} = \begin{pmatrix} 0.02581 \\ -0.01251 \\ 0.00438 \end{pmatrix} \frac{\lambda S}{\rho^2} \quad (117)$$

The total solar radiation force on both sunshades is then

$$\overline{F}_{RS} = \overline{F}_{RS}^{(1)} + \overline{F}_{RS}^{(2)} = \begin{pmatrix} 0.008711 \\ 0.006941 \\ -0.100564 \end{pmatrix} \frac{\lambda S}{\rho^2} \text{ (newtons)} \quad (118)$$

and the total moment vector is

$$\overline{M}_{RS}^{(C)} = \begin{pmatrix} 0.08644 \\ -0.04513 \\ 0.00438 \end{pmatrix} \frac{\lambda S}{\rho^2} \text{ (newton-meters)} \quad (119)$$

## XVI. THE SOLAR RADIATION FORCE AND TORQUE ON PSE INSTRUMENT SURFACES

The plasma science experiment instrument has three flat adiabatic surfaces covered with silvered Teflon. The instrument is rotating about an axis parallel to the  $xy$ -axis of the spacecraft-fixed system of reference, the position of which is defined by two points (Table 11). The areas of the three rectangular surfaces are  $0.0705$ ,  $0.0830$ , and  $0.0830 \text{ m}^2$ , respectively, with one of the surfaces always facing the Sun. The lateral components of the solar radiation force, parallel to the  $xy$ -plane, which are periodically generated by the rotation of the instrument, are very small due to the fact that they always appear in antiparallel pairs. Therefore, without any loss of accuracy, we shall compute the solar radiation force and its moment on one of the rectangles when its surface area is facing the Sun. The reflectivity coefficients of the coating material are

$$\gamma_p = 0.85 \text{ (after exposure)}$$

$$\beta_p = 1.0$$

Also,  $K(r, \theta) = 1$ . Equation (103) yields, for the solar radiation force,

$$\bar{F}_P = -0.0830 \frac{\lambda_S}{\rho^2} \frac{5 + \gamma_P}{\rho^3} \begin{pmatrix} 0 \\ 0 \\ 1 \end{pmatrix}$$

or

$$\bar{F}_P = \begin{pmatrix} 0 \\ 0 \\ -0.16185 \end{pmatrix} \frac{\lambda_S}{\rho^2} \quad (120)$$

The position of the center of mass of the rectangle is defined by the vector

$$\bar{r}_{PC} = \begin{pmatrix} -0.6445 \\ -1.314 \\ 0.610 \end{pmatrix}$$

and the moment of the solar radiation force on this surface, about the origin of the spacecraft-fixed system of reference, is given by

$$\bar{M}_P^{(C)} = \bar{r}_{PC} \times \bar{F}_P$$

or

$$\bar{M}_P^{(C)} = \begin{pmatrix} 0.21267 \\ -0.10431 \\ 0 \end{pmatrix} \frac{\lambda_S}{\rho^2} \text{ (newton-meters)} \quad (121)$$

## XVII. THE SOLAR RADIATION FORCE AND TORQUE ON THE SURFACE OF THE UVS SUNSHADE

The adiabatic surface of the ultraviolet spectrometer (UVS) sunshade is a rectangle, perpendicular to the z-axis of the spacecraft-fixed reference system, coated with the alzak anodized aluminum. The reflectivity parameters of the coating material are

$$\gamma_U = 0.72 \text{ (after exposure)}$$

$$\beta_U = 1.0$$

and the surface area is  $0.0546 \text{ m}^2$ . Also,  $K(r, \theta) = 1$ . The expression for the solar radiation force can be obtained again from Eq. (103), or from the equation preceding Eq. (120):

$$\bar{F}_U = -0.0546 \frac{\lambda S}{\rho^2} \frac{5 + \gamma_U}{3} \begin{pmatrix} 0 \\ 0 \\ 1 \end{pmatrix}$$

or

$$\bar{F}_U = \begin{pmatrix} 0 \\ 0 \\ -0.104104 \end{pmatrix} \frac{\lambda S}{\rho^2} \text{ (newtons)} \quad (122)$$

The center of mass of the rectangle is defined by the vector (Table 11)

$$\bar{r}_{UC} = \begin{pmatrix} 0.2055 \\ -1.2025 \\ 0.4040 \end{pmatrix}$$

and the moment of the solar radiation force about the origin of the spacecraft-fixed reference system is

$$\bar{M}_U^{(C)} = \bar{r}_{UC} \times \bar{F}_U$$

or

$$\bar{M}_U^{(C)} = \begin{pmatrix} 0.12519 \\ 0.02139 \\ 0 \end{pmatrix} \frac{\lambda_S}{\rho^2} \text{ (newton-meters)} \quad (123)$$

### XVIII. THE SOLAR RADIATION FORCE AND TORQUE ON ALL ADIABATIC SURFACES

To obtain the total solar radiation force on all adiabatic surfaces, we have to add algebraically the expressions for the constituent parts of the force given by Eqs. (104), (107), (111), (118), (120), and (122). The resultant force is then given by

$$\bar{F}_{AD} = \begin{pmatrix} 0.008711 \\ 0.006941 \\ -6.337135 \end{pmatrix} \frac{\lambda_S}{\rho^2} \text{ (newtons)} \quad (124)$$

In exactly the same manner we shall obtain the total moment of the solar radiation force on all adiabatic surfaces. By adding algebraically the corresponding components of moment vectors given by Eqs. (109), (113), (119), (121), and (123), we obtain

$$\bar{M}_{AD}^{(C)} = \begin{pmatrix} 5.23199 \\ -0.39419 \\ 0.00438 \end{pmatrix} \frac{\lambda_S}{\rho^2} \text{ (newton-meters)} \quad (125)$$

The total acceleration is given by

$$a_{AD} = \frac{|\bar{F}_{AD}|}{m}$$

where  $m$  is the mass of the spacecraft.

The results, obtained from the numerical program shown in the Appendix, are given in Table 25.

#### XIX. TOTAL SOLAR RADIATION FORCE AND TORQUE ON THE MARINER VENUS/MERCURY SPACECRAFT

The total solar radiation force on the Mariner Venus/Mercury spacecraft and the moment of the force are obtained by the vectorial addition of vector force and vector moments on all parts of the spacecraft. They are, respectively,

$$\bar{F}_R = \begin{pmatrix} F_{Rx} \\ F_{Ry} \\ F_{Rz} \end{pmatrix} = \bar{F}_A + \bar{F}_{SP} + \bar{F}_{AD}$$

$$\bar{M}_R^{(C)} = \begin{pmatrix} M_{Rx}^{(C)} \\ M_{Ry}^{(C)} \\ M_{Rz}^{(C)} \end{pmatrix} = \bar{M}_A^{(C)} + \bar{M}_{AD}^{(C)}$$

Table 26 gives the values of the components of the total solar radiation force and the total torque along the axes of the spacecraft-fixed system of reference. To obtain the moment of the solar radiation force on the high-gain antenna reflector, the lowest point of the reflector (the origin of the antenna-fixed reference system  $x_A y_A z_A$ ) is taken to be in its extreme position on the  $+y$ -axis of the spacecraft-fixed system of reference.

The magnitude of the total acceleration is

$$a_R = \frac{|\bar{F}_R|}{m}$$

## REFERENCES

1. Georgevic, R. M., Mathematical Model of the Solar Radiation Force and Torques Acting on the Components of a Spacecraft, Technical Memorandum 33-494, Jet Propulsion Laboratory, Pasadena, Calif., Oct. 1, 1971.
2. Georgevic, R. M., "The Solar Radiation Pressure Force and Torques Model," J. Astronaut. Sci., Vol. XX, No. 5, pp. 257-274, Mar.-Apr. 1973.
3. Georgevic, R. M., "The Solar Radiation Pressure on the Mariner 9 Mars Orbiter," Astronaut. Acta, Vol. 18, pp. 109-115, Pergamon Press, 1973.
4. Jaworski, W., IOM 351:71:M273, Mar. 31, 1971 (JPL internal document).
5. Eckert, E. R. G., Introduction to Heat and Mass Transfer, McGraw-Hill Book Co., Inc., New York, 1963.
6. Thekaekara, M. P., and Drummond, A. J., "Standard Values for the Solar Constant and Its Spectral Components," Nature, Phys. Sci., Vol. 229, No. 1, Jan. 4, 1971.
7. O'Reilly, B. D., private communication.
8. Becker, R. A., Spacecraft Surface Data for Solar Force/Torque Calculations, IOM 3533 MVM'73-036, Oct. 24, 1973 (JPL internal document).
9. Georgevic, R. M., Program FITMU, Dec. 1973 (JPL internal document).
10. Gradstein, I. S., and Rizhik, I. M., Tables of Integrals, Sums, Series, and Products, 4th Edition, Fizmatgiz, Moscow, 1962.
11. Georgevic, R. M., Motion of the Sun-Canopus Oriented Attitude Control Reference Frame of the Mariner Venus/Mercury Spacecraft, Technical Memorandum 391-429, Mar. 30, 1973 (JPL internal document).

12. Georgevic, R. M., Program TORQUE, Sept. 1973 (JPL internal document).
13. Mashburn, J. H., Mariner Venus/Mercury 1973 Preliminary Trajectory Characteristics, Project Document 615-36, Feb. 15, 1972 (JPL internal document).
14. Pease, G. E., Mariner 10 Solar Panel Tilts, IOM 391.8-138, Dec. 20, 1973 (JPL internal document).

#### BIBLIOGRAPHY

- Allen, L. H., Astrophysics, The Ronald Press Co., New York, 1953.
- Condon, E. U., and Odishaw, H., editors, Handbook of Physics, McGraw-Hill Book Co., Inc., New York, 1958.
- Doornink, D. G., and Hering, R. G., "Simultaneous Radiative and Conductive Heat Transfer in Non-Gray Media," J. Quant. Spectros. Radiative Transfer, Vol. 13, No. 4, pp. 323-332, Apr. 1973, Pergamon Press, 1973.
- Georgevic, R. M., Solar Radiation Pressure Force and Torques for Pioneer F/G High Gain Antenna Reflector, Technical Memorandum 391-134, Nov. 23, 1970 (JPL internal document).
- Georgevic, R. M., Solar Radiation Pressure Force and Torques on the Back Side of the Pioneer F/G High Gain Antenna Reflector, Technical Memorandum 391-155, Jan. 22, 1971 (JPL internal document).
- Georgevic, R. M., Solar Radiation Pressure Force on the Surface of a Circular Cylinder, Technical Memorandum 391-156, Jan. 29, 1971 (JPL internal document).
- Hausmann, E. and Slask, E. P., Physics, D. Van Nostrand Co., Inc., New York, 1939.
- Joos, G., Theoretical Physics, Third Edition, Blackie and Son, Ltd., London.
- Koshlyakov, N. S., et al., Differential Equations of Mathematical Physics, North-Holland Publishing Co., Amsterdam, 1964.
- Mariner Venus/Mercury 1973 Study, Technical Memorandum 33-434, Jet Propulsion Laboratory, Pasadena, Calif., Aug. 1, 1969.

Melbourne, W. G., Radiation Pressure Perturbations of Interplanetary Trajectories, Technical Memorandum 391-151, Dec. 11, 1961 (JPL internal document).

Melbourne, W. G., et al., Constants and Related Information for Astrodynamical Calculations, 1968, Technical Report 32-1306, Jet Propulsion Laboratory, Pasadena, Calif., July 15, 1968.

Mendenhall, C. E., et al., College Physics, D. C. Heath and Co., Boston, 1944.

Poynting, J. H., and Thomson, J. J., A Textbook of Physics: Vol. III. Heat, C. Griffin and Co., Ltd, London, 1928.

Suslov, G. K., Theoretical Mechanics, OGIZ, Moscow, 1946.

Westphal, W. H., Physik, Ein Lehrbuch, Fifth and Sixth Editions, Springer-Verlag, Berlin, 1939.

#### DEFINITION OF SYMBOLS AND ABBREVIATIONS

A	a constant
[A]	transformation matrix
$A_A$	value of the constant A for the high-gain antenna reflector
$A_B$	surface area of the back (not irradiated) surface
$A_F$	surface area of the front (irradiated) surface
$A(f)$	reflectivity function
$A_L(f)$	value of the reflectivity function $A(f)$ obtained from Lambert's directional distribution law
$A_{HS}$	surface area of the TV camera heat shield
$A_{SP}$	value of the constant A for solar panels; also surface area of solar panels
$A_{SS}$	total surface area of the main octagonal sunshade
AU	astronomical unit
a	semimajor axis of the spacecraft's orbit

$a_A$	magnitude of the acceleration of the solar radiation force on the high-gain antenna reflector
$a_{AD}$	magnitude of the total acceleration of the solar radiation force on all adiabatic surfaces
$a_i, b_i, c_i$	direction cosines of the principal axes of inertia of the spacecraft relative to the axes of the spacecraft-fixed system xyz ( $i = 1, 2, 3$ )
$a_R$	magnitude of the total acceleration of the solar radiation force on the Mariner Venus/Mercury spacecraft
$a_{SP}$	magnitude of the acceleration of the solar radiation force on two solar panels
B	a constant
[B]	transformation matrix
$B_A$	value of the constant B for the high-gain antenna reflector
$B(f)$	reflectivity function
$B_L(f)$	value of $B(f)$ obtained from Lambert's directional distribution law
$B_{SP}$	value of the constant B for solar panels
C	origin of the spacecraft-fixed reference system
c	speed of light
$D(\theta)$	directional distribution law of diffuse reflection
e	eccentricity of the spacecraft's orbit
$\bar{e}_1, \bar{e}_2, \bar{e}_3$	unit vectors along the axes of the spacecraft-fixed reference frame
$\bar{e}'_1, \bar{e}'_2, \bar{e}'_3$	unit vectors along the axes of the Sun-Canopus reference system
$\bar{F}$	total solar radiation force

$\bar{F}_A$	solar radiation force on the high-gain antenna reflector
$\bar{F}_{AD}$	total solar radiation force on all adiabatic surfaces of the Mariner Venus/Mercury spacecraft
$F_{ADx}, F_{ADy}, F_{ADz}$	components of force $\bar{F}_{AD}$ along the axes of the spacecraft-fixed reference system
$F_{Ax}, F_{Ay}, F_{Az}$	components of force $\bar{F}_A$ along the axes of the spacecraft-fixed reference system
$\bar{F}_B$	solar radiation force on the cylindrical surface of the magnetometer boom
$F_{Bx}, F_{By}, F_{Bz}$	components of force $\bar{F}_B$ along the axes of the spacecraft-fixed reference system
$F_D$	component of the solar radiation force due to diffuse reflection
$F_I$	force generated by the incident radiation
$F_{MSz}$	total solar radiation force on the three magnetometer sunshades
$F_{MSz}^{(i)}$	solar radiation forces on magnetometer sunshades ( $i = 1, 2, 3$ )
$F_N$	magnitude of force $\bar{F}_N$
$\bar{F}_N$	normal component of the solar radiation force
$\bar{F}_P$	solar radiation force on the surface of the PSE instrument
$F_R$	component of the solar radiation force due to specular reflection
$F_R$	total solar radiation force on the Mariner Venus/Mercury spacecraft
$F_{RR}$	component of the solar radiation force due to the thermal re-radiation
$\bar{F}_{RS}$	total solar radiation force on two IRR sunshades

$\bar{F}_{RS}^{(i)}$	solar radiation force on two IRR sunshades (i = 1, 2)
$F_{Rx}, F_{Ry}, F_{Rz}$	components of force $\bar{F}_R$ along the axes of the spacecraft-fixed reference system
$\bar{F}_{SP}$	solar radiation force on two solar panels
$F_{SPx}, F_{SPy}, F_{SPz}$	components of force $\bar{F}_{SP}$ along the axes of the spacecraft-fixed reference system
$\bar{F}_{SS}$	solar radiation force on the surface of the main octagonal sunshade of the spacecraft
$F_{SSx}, F_{SSy}, F_{SSz}$	components of force $\bar{F}_{SS}$ along the axes of the spacecraft-fixed reference system
$\bar{F}_U$	solar radiation force on the surface of the UVS sunshade
$F_{xA}, F_{yA}, F_{zA}$	components of force $\bar{F}_A$ along the axes of the antenna-fixed reference system
$F(x, y, z)$	equation of the reflecting surface
$f(\theta)$	angular distribution law of the diffuse reflection
$h$	depth of the high-gain antenna reflector
$I$	radiant flux per unit solid angle
$I_0$	a constant
$I_x, I_y, I_z$	components of the solar radiation force on the high-gain antenna reflector
IRR	infrared radiometer
$i$	inclination of the spacecraft's orbit plane to the ecliptic plane of 1950.0
$\vec{i}$	unit vector along the first principal axis of inertia of the spacecraft
$J$	radiant energy per unit area per unit time
$J_0$	solar constant

$J_x, J_y, J_z$	components of the solar radiation force on the high-gain antenna reflector
$\hat{j}$	unit vector along the second principal axis of inertia of the spacecraft
K	thermal re-radiation constant
$K(r, \theta)$	thermal re-radiation function
$K_S$	solar radiation constant
$K_x, K_y, K_z$	components of the solar radiation force on the high-gain antenna reflector
k	thermal conductivity of material
$\hat{k}$	unit vector along the third principal axis of inertia of the spacecraft
$k_A$	thermal conductivity of the high-gain antenna reflector
$k_{SP}$	thermal conductivity of solar panels
$L_B$	length of the magnetometer boom
$\ell$	thickness of the conducting material
$\ell_A$	thickness of the high-gain antenna reflector
$\ell_{SP}$	thickness of solar panels
$M_0$	mean anomaly of the spacecraft at the time of the trajectory initialization
$\bar{M}^{(O)}$	total moment of the solar radiation force about a point O
$\bar{M}_A^{(O)}$	moment of the solar radiation force on the high-gain antenna reflector about the origin of the antenna-fixed reference frame
$\bar{M}_A^{(C)}$	moment of the solar radiation force on the high-gain antenna reflector about the origin of the spacecraft-fixed reference system

$\overline{M}_{AD}^{(C)}$	total moment of the solar radiation force on all adiabatic surfaces of the spacecraft about the origin of the spacecraft-fixed reference system
$M_{ADx}^{(C)}, M_{ADy}^{(C)}, M_{ADz}^{(C)}$	components of the moment vector $\overline{M}_{AD}^{(C)}$ along the axes of the spacecraft-fixed reference system
$M_{Ax}^{(O)}$	component of the moment vector $\overline{M}_A^{(O)}$ along the x-axis of the spacecraft-fixed reference system about the origin of the antenna-fixed reference system
$M_{Ax}^{(C)}$	component of the moment vector $\overline{M}_A^{(C)}$ along the x-axis of the spacecraft-fixed reference system
$\overline{M}_B^{(C)}$	moment of the solar radiation force on the cylindrical surface of the magnetometer boom about the origin of the spacecraft-fixed reference system
$M_{Bx}^{(C)}, M_{By}^{(C)}, M_{Bz}^{(C)}$	components of the moment vector $\overline{M}_B^{(C)}$ along the axes of the spacecraft-fixed reference frame
$\overline{M}_{MS}^{(C)}$	total moment of the solar radiation force on all three magnetometer sunshades about the origin of the spacecraft-fixed reference frame
$\overline{M}_{MS(i)}^{(C)}$	moments of the solar radiation forces on magnetometer sunshades ( $i = 1, 2, 3$ ) about the origin of the spacecraft-fixed reference system
$M_{MSx}^{(C)}, M_{MSy}^{(C)}, M_{MSz}^{(C)}$	components of the moment vector $\overline{M}_{MS}^{(C)}$ along the axes of the spacecraft-fixed reference system
$\overline{M}_P^{(C)}$	moment of the solar radiation force on the surface of the PSE instrument about the origin of the spacecraft-fixed reference system

$\overline{M}_R^{(C)}$	total moment of the solar radiation force on the Mariner Venus/Mercury spacecraft about the origin of the spacecraft-fixed frame reference
$\overline{M}_{RS}^{(C)}$	total moment of the solar radiation force on two IRR sunshades about the origin of the spacecraft-fixed reference system
$\overline{M}_{RS(i)}^{(C)}$	moments of the solar radiation forces on two IRR sunshades ( $i = 1, 2$ ) about the origin of the spacecraft-fixed reference system
$M_{Rx}^{(C)}, M_{Ry}^{(C)}, M_{Rz}^{(C)}$	components of the moment vector $\overline{M}_R^{(C)}$ along the axes of the spacecraft-fixed reference system
$\overline{M}_{SP}^{(C)}$	moment of the solar radiation force on two solar panels about the origin of the spacecraft-fixed reference frame
$\overline{M}_{SS}^{(C)}$	moment of the solar radiation force on the surface of the main octagonal sunshade about the origin of the spacecraft-fixed reference system
$\overline{M}_U^{(C)}$	moment of the solar radiation force on the surface of the UVS sunshade about the origin of the spacecraft-fixed reference frame
$M_{xA}^{(O)}, M_{yA}^{(O)}, M_{zA}^{(O)}$	components of the moment $\overline{M}_A^{(O)}$ along the axes of the antenna-fixed reference system
m	mass of the spacecraft
$\vec{N}$	unit vector along the local normal to the reflecting surface
$N_{xA}, N_{yA}, N_{zA}$	components of the unit vector of the local normal to the surface of the high-gain antenna reflector along the axes of the antenna-fixed reference system
O	origin of the antenna-fixed reference system
P	auxiliary constant

$P_A$	value of the constant P for the high-gain antenna reflector
$P_I$	normal component of the force $F_I$
$P_R$	normal component of the force $F_R$
$P_{SP}$	value of the constant P for solar panels
PSE	plasma science experiment (instrument)
$Q$	auxiliary constant
$Q_A$	value of the constant Q for the high-gain antenna reflector
$Q_{SP}$	value of the constant Q for solar panels
$q$	emissive power of a surface
$q_B$	emissive power of the back (not irradiated) surface
$q_F$	emissive power of the front (irradiated) surface
R	polar distance in the $x_A y_A$ -plane of the antenna-fixed reference frame
$R(r, \theta)$	function of the heliocentric distance and the angle of incidence in the expression for the thermal re-radiation
r	heliocentric distance of the spacecraft
$\bar{r}$	heliocentric position vector of the spacecraft
$r_B$	radius of the magnetometer boom
$\bar{r}_E$	heliocentric position vector of the Earth
$\bar{r}_{PC}$	position vector of the center of mass of the PSE instrument surface in the spacecraft-fixed reference frame
$\bar{r}_{RC}^{(i)}$	position vectors of centers of mass of IRR sunshades ( $i = 1, 2$ ) in the spacecraft-fixed reference system

$\bar{r}_{UC}$	position vector of the center of mass of the UVS sunshade in the spacecraft-fixed reference system
S	surface area
T	temperature in kelvins (K)
$\bar{T}$	unit vector along the local tangent
$T^*$	a constant
$T_0(r, \theta)$	first approximation of the surface temperature
$T_A^*$	value of constant $T^*$ for the high-gain antenna reflector
$T_B$	temperature of the back (not irradiated) surface
$T_F$	temperature of the front (irradiated) surface
$T_I$	tangential component of force $F_I$
$T_R$	tangential component of force $F_R$
$T_{SP}^*$	value of constant $T^*$ for solar panels
$\bar{U}$	unit vector along the spacecraft-Sun direction
$\bar{U}_C$	unit vector along the spacecraft-star Canopus direction
$U_{xA}, U_{yA}, U_{zA}$	components of the unit vector $\bar{U}$ along the axes of the antenna-fixed reference system
UVS	ultraviolet spectrometer
$\bar{x}$	position vector of a point relative to the spacecraft-fixed reference frame
$\bar{x}_0$	position vector of the origin of the antenna-fixed reference system relative to the origin of the spacecraft-fixed system
$\bar{x}_A$	position vector of a point on the high-gain antenna surface relative to the origin of the antenna-fixed reference system

$x, y, z$	coordinates of a point of the spacecraft in the spacecraft-fixed reference frame
$x_A, y_A, z_A$	coordinate axes of the high-gain antenna-fixed reference system
$\underline{x}_A^*, \underline{y}_A^*, \underline{z}_A^*$	unit vectors along the axes of the antenna-fixed reference frame
$x_{AC}, y_{AC}, z_{AC}$	coordinates of the origin of the antenna-fixed reference system in the spacecraft-fixed system
$x_B, y_B, z_B$	coordinate axes of the magnetometer boom-fixed reference frame
$x_{B0}, y_{B0}, z_{B0}$	coordinates of the footpoint of the magnetometer boom in the spacecraft-fixed reference frame
$x_C, y_C, z_C$	coordinates of the center of mass of the spacecraft in the spacecraft-fixed reference system
$x_{Ci}, y_{Ci}, z_{Ci}$	coordinates of centers of mass of magnetometer sunshades ( $i = 1, 2, 3$ ) in the spacecraft-fixed reference system
$x_{RC}^{(i)}, y_{RC}^{(i)}, z_{RC}^{(i)}$	coordinates of centers of mass of two IRR sunshades ( $i = 1, 2$ ) in the spacecraft-fixed reference frame
$x_S, y_S, z_S$	coordinate axes of the Sun-Canopus system of reference
$y_S$	distance from the line of shadow of the high-gain antenna reflector from the $x_A$ -axis of the antenna-fixed reference system
$\alpha$	value of the angle of incidence ( $\theta$ ) at which the directional distribution law of the diffuse reflection begins to deviate from Lambert's cosine law
$\alpha'$	Sun-spacecraft-Earth angle
$\beta$	portion of specularly reflected radiation
$\beta_B$	value of $\beta$ for the surface of the magnetometer boom

$\beta_{HS}$	value of $\beta$ for the surface of the TV camera heat shield
$\beta_P$	value of $\beta$ for the surface of the PSE instrument
$\beta_{RS}$	value of $\beta$ for the surfaces of IRR sunshades
$\beta_{SP}$	value of $\beta$ for the illuminated surfaces of solar panels
$\beta_{SS}$	value of $\beta$ for the surface of the main octagonal sunshade of the spacecraft
$\beta_U$	value of $\beta$ for the surface of the UVS sunshade
$\gamma$	portion of reflected radiation
$\gamma_A$	value of $\gamma$ for the surface of the high-gain antenna reflector
$\gamma_B$	value of $\gamma$ for the surface of the magnetometer boom
$\gamma_{HS}$	value of $\gamma$ for the surface of the TV camera heat shield
$\gamma_P$	value of $\gamma$ for the surface of the PSE instrument
$\gamma_{RS}$	value of $\gamma$ for the surfaces of IRR sunshades
$\gamma_{SP}$	value of $\gamma$ for the surfaces of solar panels
$\gamma_{SS}$	value of $\gamma$ for the surface of the main octagonal sunshade
$\gamma_U$	value of $\gamma$ for the surface of the UVS sunshade
$\delta$	radius of aperture of the high-gain antenna reflector
$\epsilon$	emissivity of a surface
$\epsilon_B$	emissivity of the back (not irradiated) surface
$\epsilon_F$	emissivity of the front (irradiated) surface
$(\epsilon_B)_A$	value of $\epsilon_B$ for the high-gain antenna reflector
$(\epsilon_B)_{SP}$	value of $\epsilon_B$ for solar panels

$(\epsilon_F)_A$	value of $\epsilon_F$ for the high-gain antenna reflector
$(\epsilon_F)_{SP}$	value of $\epsilon_F$ for solar panels
$\theta$	angle of incidence of the solar radiation
$\theta_{RS}$	tilt angle of the second (tilted) IRR sunshade
$\lambda$	constant of the high-gain antenna reflector
$\lambda_S$	solar pressure constant
$\mu$	parameter in the diffuse reflection directional distribution law
$v(\theta)$	function of the angle of incidence $\theta$
$\xi, \eta, \zeta$	coordinates of a point on the spacecraft relative to the reference system of principal axes of inertia of the spacecraft
$\rho$	heliocentric distance of the spacecraft in astronomical units
$\sigma$	Stefan-Boltzmann's constant
$\tau(r, \theta)$	ratio of front and back temperatures of a surface
$\Phi$	central angle in the $x_A y_A$ -plane of the antenna-fixed reference frame; half of the central angle of the projection of the illuminated surface of the antenna in the $x_A y_A$ -plane
$\phi(x_A, y_A, z_A)$	equation of the convex surface of the high-gain antenna in the antenna-fixed reference system
$\varphi$	polar angle in the $x_A y_A$ -plane of the high-gain antenna-fixed reference system; also, azimuthal angle of the incident radiation
$\varphi_{RS}$	clock angle of the normal to the surface of the second (tilted) IRR sunshade
$\psi$	Earth-spacecraft-antisolar point angle

- $\psi_F$  value of  $\psi$  at which the shadowing of the convex surface of the high-gain antenna begins
- $\Omega$  longitude of the ascending node of the spacecraft's orbit plane
- $\omega$  argument of perihelion of the spacecraft's orbit; also a solid angle

Table 1. Values of  $\tau(r,\theta)$  for the high-gain antenna reflector

$\theta$ , deg	$\tau(r,\theta)$						
	$r = 1.000$	$r = 0.884$	$r = 0.768$	$r = 0.652$	$r = 0.536$	$r = 0.420$	$r = 0.304$
0	1.026	1.031	1.038	1.048	1.063	1.088	1.132
5	1.026	1.031	1.038	1.048	1.063	1.087	1.132
10	1.026	1.031	1.038	1.048	1.062	1.087	1.130
15	1.026	1.031	1.037	1.047	1.062	1.086	1.129
20	1.025	1.030	1.037	1.046	1.061	1.084	1.127
25	1.024	1.029	1.036	1.045	1.059	1.082	1.124
30	1.024	1.028	1.035	1.044	1.057	1.080	1.121
35	1.023	1.027	1.033	1.042	1.055	1.077	1.117
40	1.022	1.026	1.032	1.040	1.053	1.073	1.112
45	1.020	1.024	1.030	1.038	1.050	1.069	1.106
50	1.019	1.023	1.028	1.035	1.047	1.065	1.100
55	1.018	1.021	1.026	1.033	1.043	1.060	1.093
60	1.016	1.019	1.023	1.030	1.039	1.055	1.085
65	1.014	1.017	1.021	1.026	1.035	1.049	1.076
70	1.012	1.014	1.018	1.022	1.030	1.042	1.066
75	1.010	1.012	1.014	1.018	1.024	1.035	1.054
80	1.007	1.009	1.011	1.014	1.018	1.026	1.041
85	1.004	1.005	1.006	1.008	1.011	1.016	1.025
90	1.000	1.000	1.000	1.000	1.000	1.000	1.000

Table 2. Values of  $\tau(r,\theta)$  for solar panels

$\theta$ , deg	$\tau(r,\theta)$							
	r = 1.000	r = 0.884	r = 0.768	r = 0.652	r = 0.536	r = 0.420	r = 0.304	
0	1.016	1.019	1.024	1.030	1.040	1.056	1.086	
5	1.016	1.019	1.024	1.030	1.040	1.056	1.086	
10	1.016	1.019	1.023	1.030	1.039	1.055	1.085	
15	1.016	1.019	1.023	1.029	1.039	1.054	1.084	
20	1.015	1.018	1.023	1.029	1.038	1.053	1.083	
25	1.015	1.018	1.022	1.028	1.037	1.052	1.081	
30	1.015	1.017	1.021	1.027	1.036	1.050	1.078	
35	1.014	1.017	1.021	1.026	1.034	1.049	1.076	
40	1.013	1.016	1.020	1.025	1.033	1.046	1.072	
45	1.013	1.015	1.018	1.023	1.031	1.044	1.068	
50	1.012	1.014	1.017	1.022	1.029	1.041	1.064	
55	1.011	1.013	1.016	1.020	1.027	1.038	1.059	
60	1.010	1.012	1.014	1.018	1.024	1.034	1.054	
65	1.009	1.010	1.013	1.016	1.021	1.030	1.048	
70	1.007	1.009	1.011	1.014	1.018	1.026	1.041	
75	1.006	1.007	1.009	1.011	1.015	1.021	1.034	
80	1.004	1.005	1.007	1.008	1.011	1.016	1.026	
85	1.003	1.003	1.004	1.005	1.007	1.010	1.015	
90	1.000	1.000	1.000	1.000	1.000	1.000	1.000	

Table 3. Values of  $K(r, \theta)$  for the high-gain antenna reflector

$\theta$ , deg	$K(r, \theta)$							
	$r = 1.000$	$r = 0.884$	$r = 0.768$	$r = 0.652$	$r = 0.536$	$r = 0.420$	$r = 0.304$	
0	0.046	0.056	0.069	0.088	0.116	0.161	0.238	
5	0.046	0.056	0.069	0.088	0.116	0.160	0.238	
10	0.046	0.055	0.069	0.087	0.115	0.159	0.236	
15	0.045	0.054	0.068	0.086	0.114	0.157	0.233	
20	0.044	0.053	0.066	0.084	0.111	0.154	0.230	
25	0.043	0.052	0.064	0.082	0.109	0.151	0.225	
30	0.041	0.050	0.062	0.080	0.105	0.146	0.219	
35	0.039	0.048	0.060	0.076	0.101	0.141	0.212	
40	0.037	0.045	0.057	0.073	0.097	0.135	0.204	
45	0.035	0.043	0.053	0.068	0.091	0.128	0.194	
50	0.032	0.039	0.049	0.064	0.085	0.120	0.183	
55	0.029	0.036	0.045	0.058	0.078	0.111	0.170	
60	0.026	0.032	0.040	0.052	0.071	0.101	0.156	
65	0.022	0.028	0.035	0.046	0.062	0.089	0.140	
70	0.018	0.023	0.029	0.039	0.053	0.077	0.121	
75	0.014	0.018	0.023	0.031	0.042	0.062	0.100	
80	0.009	0.012	0.016	0.022	0.031	0.046	0.075	
85	0.003	0.005	0.007	0.011	0.016	0.026	0.044	
90	-0.006	-0.006	-0.006	-0.006	-0.006	-0.006	-0.006	

Table 4. Values of  $K(r,\theta)$  for solar panels

$\theta$ , deg	$K(r,\theta)$							
	$r = 1.000$	$r = 0.884$	$r = 0.768$	$r = 0.652$	$r = 0.536$	$r = 0.420$	$r = 0.304$	
0	-0.005	0.002	0.010	0.022	0.041	0.072	0.128	
5	-0.005	0.002	0.010	0.022	0.041	0.071	0.128	
10	-0.005	0.001	0.010	0.022	0.040	0.071	0.127	
15	-0.006	0.001	0.009	0.021	0.039	0.069	0.125	
20	-0.006	0.000	0.008	0.020	0.038	0.067	0.122	
25	-0.007	-0.001	0.007	0.018	0.036	0.065	0.118	
30	-0.008	-0.002	0.006	0.017	0.034	0.062	0.114	
35	-0.009	-0.004	0.004	0.015	0.031	0.058	0.109	
40	-0.010	-0.005	0.002	0.012	0.028	0.054	0.103	
45	-0.012	-0.007	0.000	0.010	0.024	0.049	0.096	
50	-0.014	-0.009	-0.003	0.006	0.020	0.044	0.088	
55	-0.015	-0.011	-0.005	0.003	0.016	0.037	0.078	
60	-0.017	-0.014	-0.008	-0.001	0.011	0.031	0.068	
65	-0.020	-0.016	-0.012	-0.005	0.006	0.023	0.057	
70	-0.022	-0.019	-0.015	-0.009	0.000	0.015	0.044	
75	-0.025	-0.022	-0.019	-0.014	-0.007	0.006	0.030	
80	-0.028	-0.026	-0.024	-0.020	-0.015	-0.005	0.014	
85	-0.031	-0.030	-0.029	-0.027	-0.023	-0.018	-0.006	
90	-0.037	-0.037	-0.037	-0.037	-0.037	-0.037	-0.037	

Table 5. Approximate values of  $K(r,\theta)$  for the high-gain antenna reflector

$\theta$ , deg	$K(r,\theta)$						
	$r = 1.000$	$r = 0.884$	$r = 0.768$	$r = 0.652$	$r = 0.536$	$r = 0.420$	$r = 0.304$
0	0.046	0.056	0.069	0.088	0.116	0.160	0.236
5	0.046	0.056	0.069	0.088	0.116	0.160	0.236
10	0.046	0.055	0.069	0.087	0.115	0.159	0.234
15	0.045	0.054	0.068	0.086	0.113	0.157	0.231
20	0.044	0.053	0.066	0.084	0.111	0.154	0.228
25	0.043	0.052	0.064	0.082	0.108	0.150	0.223
30	0.041	0.050	0.062	0.079	0.105	0.146	0.217
35	0.039	0.048	0.060	0.076	0.101	0.141	0.211
40	0.037	0.045	0.057	0.073	0.096	0.135	0.202
45	0.035	0.043	0.053	0.068	0.091	0.128	0.193
50	0.032	0.039	0.049	0.064	0.085	0.120	0.182
55	0.029	0.036	0.045	0.058	0.078	0.111	0.170
60	0.026	0.032	0.040	0.052	0.071	0.101	0.156
65	0.022	0.028	0.035	0.046	0.062	0.089	0.139
70	0.018	0.023	0.029	0.039	0.053	0.077	0.121
75	0.014	0.018	0.023	0.031	0.042	0.062	0.100
80	0.009	0.012	0.016	0.022	0.031	0.046	0.075
85	0.003	0.005	0.007	0.011	0.016	0.026	0.044
90	-0.006	-0.006	-0.006	-0.006	-0.006	-0.006	-0.006

Table 6. Approximate values of  $K(r,\theta)$  for solar panels

$\theta$ , deg	$K(r,\theta)$							
	r = 1.000	r = 0.884	r = 0.768	r = 0.652	r = 0.536	r = 0.420	r = 0.304	
0	-0.005	0.002	0.010	0.022	0.041	0.071	0.128	
5	-0.005	0.002	0.010	0.022	0.041	0.071	0.127	
10	-0.005	0.001	0.010	0.022	0.040	0.071	0.126	
15	-0.006	0.001	0.009	0.021	0.039	0.069	0.124	
20	-0.006	0.000	0.008	0.020	0.038	0.067	0.122	
25	-0.007	-0.001	0.007	0.018	0.036	0.065	0.118	
30	-0.008	-0.002	0.006	0.017	0.034	0.062	0.114	
35	-0.009	-0.004	0.004	0.015	0.031	0.058	0.108	
40	-0.010	-0.005	0.002	0.012	0.028	0.054	0.102	
45	-0.012	-0.007	0.000	0.010	0.024	0.049	0.095	
50	-0.014	-0.009	-0.003	0.006	0.020	0.044	0.087	
55	-0.015	-0.011	-0.005	0.003	0.016	0.037	0.078	
60	-0.017	-0.014	-0.008	-0.001	0.011	0.031	0.068	
65	-0.020	-0.016	-0.012	-0.005	0.006	0.023	0.057	
70	-0.022	-0.019	-0.015	-0.009	0.000	0.015	0.044	
75	-0.025	-0.022	-0.019	-0.014	-0.007	0.006	0.030	
80	-0.028	-0.026	-0.024	-0.020	-0.015	-0.005	0.014	
85	-0.031	-0.030	-0.029	-0.027	-0.023	-0.018	-0.006	
90	-0.037	-0.037	-0.037	-0.037	-0.037	-0.037	-0.037	

Table 7. Approximate values of  $K(r,\theta)$  for the high-gain antenna obtained by series expansion

$\theta$ , deg	$K(r,\theta)$						
	$r = 1.000$	$r = 0.884$	$r = 0.768$	$r = 0.652$	$r = 0.536$	$r = 0.420$	$r = 0.304$
0	0.046	0.056	0.069	0.087	0.114	0.155	0.215
5	0.046	0.056	0.069	0.087	0.114	0.155	0.215
10	0.046	0.055	0.068	0.086	0.113	0.154	0.214
15	0.045	0.054	0.067	0.085	0.112	0.152	0.212
20	0.044	0.053	0.066	0.084	0.110	0.149	0.210
25	0.043	0.052	0.064	0.082	0.107	0.146	0.206
30	0.041	0.050	0.062	0.079	0.104	0.142	0.202
35	0.039	0.048	0.059	0.076	0.100	0.138	0.197
40	0.037	0.045	0.056	0.072	0.095	0.132	0.191
45	0.035	0.043	0.053	0.068	0.090	0.125	0.183
50	0.032	0.039	0.049	0.063	0.084	0.118	0.174
55	0.029	0.036	0.045	0.058	0.078	0.109	0.163
60	0.026	0.032	0.040	0.052	0.070	0.100	0.151
65	0.022	0.028	0.035	0.046	0.062	0.089	0.136
70	0.018	0.023	0.029	0.039	0.053	0.076	0.119
75	0.014	0.018	0.023	0.031	0.042	0.062	0.099
80	0.009	0.012	0.016	0.022	0.030	0.045	0.074
85	0.003	0.005	0.007	0.011	0.016	0.026	0.044
90	-0.006	-0.006	-0.006	-0.006	-0.006	-0.006	-0.006

Table 8. Approximate values of  $K(r,\theta)$  for solar panels obtained by series expansion

$\theta$ , deg	$K(r,\theta)$						
	$r = 1.000$	$r = 0.884$	$r = 0.768$	$r = 0.652$	$r = 0.536$	$r = 0.420$	$r = 0.304$
0	-0.005	0.002	0.010	0.022	0.041	0.071	0.124
5	-0.005	0.002	0.010	0.022	0.041	0.070	0.123
10	-0.005	0.001	0.010	0.022	0.040	0.070	0.122
15	-0.006	0.001	0.009	0.021	0.039	0.068	0.120
20	-0.006	0.000	0.008	0.020	0.037	0.066	0.118
25	-0.007	-0.001	0.007	0.018	0.036	0.064	0.115
30	-0.008	-0.002	0.006	0.017	0.033	0.061	0.111
35	-0.009	-0.004	0.004	0.015	0.031	0.057	0.106
40	-0.010	-0.005	0.002	0.012	0.028	0.053	0.100
45	-0.012	-0.007	0.000	0.009	0.024	0.049	0.093
50	-0.014	-0.009	-0.003	0.006	0.020	0.043	0.086
55	-0.015	-0.011	-0.005	0.003	0.016	0.037	0.077
60	-0.017	-0.014	-0.008	-0.001	0.011	0.030	0.067
65	-0.020	-0.016	-0.012	-0.005	0.006	0.023	0.056
70	-0.022	-0.019	-0.015	-0.009	0.000	0.015	0.044
75	-0.025	-0.022	-0.019	-0.014	-0.007	0.006	0.030
80	-0.028	-0.026	-0.024	-0.020	-0.015	-0.005	0.014
85	-0.031	-0.030	-0.029	-0.027	-0.023	-0.018	-0.006
90	-0.037	-0.037	-0.037	-0.037	-0.037	-0.037	-0.037

Table 9. Scaled values of  $D(\theta)$   
for chromium ( $\alpha \cong 34^\circ$ )

$\theta$ , deg	$D(\theta)$
35	1.0000
40	1.0158
45	1.0632
50	1.0947
55	1.1368
60	1.2368
65	1.3474
70	1.5526
75	1.8579
80	2.4368

Table 10. Scaled values of  $D(\theta)$   
for wood ( $\alpha \cong 64^\circ$ )

$\theta$ , deg	$D(\theta)$
64	1.0000
65	0.9844
70	0.9469
75	0.9000
80	0.7781
85	0.5000
90	0.0000

C - 2  
Table 11. Survey of irradiated surfaces on Mariner Venus/Mercury spacecraft  
(all lengths in centimeters)

Element of spacecraft	Coordinates of endpoints in cm and/or description												Area, m <sup>2</sup>	Surface materials (Table 12)	Notes	Angle of incidence, deg				
	Point 1			Point 2			Point 3			Point 4										
	x	y	z	x	y	z	x	y	z	x	y	z								
+x Solar panel	382.5	-53.3	0	382.5	53.3	0	109.2	53.3	0	109.2	-53.3	0	2.9156	③	②	Thickness 1.3 cm	0			
-x Solar panel	-382.5	-53.3	0	-382.5	53.3	0	-109.2	53.3	0	-109.2	-53.3	0	2.9156	③	②		0			
S/C sunshade	Eight trapezoids																			
Shade 1	92.7	40.4	76.7	92.7	-38.1	76.7	23.1	-9.7	96.5	23.1	9.7	96.5	0.3535				15.89			
Shade 2	40.4	96.5	76.7	96.5	40.4	76.7	23.1	9.7	96.5	9.7	23.1	96.5	0.3761				15.06			
Shade 3	-40.4	96.5	76.7	40.4	96.5	76.7	9.7	23.1	96.5	-9.7	23.1	96.5	0.3801				15.10			
Shade 4	-96.5	40.4	76.7	-40.4	96.5	76.7	-9.7	23.1	96.5	-23.1	9.7	96.5	0.3761	⑥			15.06			
Shade 5	-92.7	-38.1	76.7	-92.7	40.4	76.7	-23.1	9.7	96.5	-23.1	-9.7	96.5	0.3535				15.89			
Shade 6	38.1	-88.9	76.7	-88.9	-38.1	76.7	-23.1	-9.7	96.5	-9.7	-23.1	96.5	0.3161				16.56			
Shade 7	38.1	-38.9	76.7	-38.1	-88.9	76.7	-9.7	-23.1	96.5	9.7	-23.1	96.5	0.3278				16.76			
Shade 8	88.9	-38.1	76.7	38.1	-88.9	76.7	9.7	-23.1	96.5	23.1	-9.7	96.5	0.3161				16.56			
Magnetometer boom	Cylinder of radius 3.2 cm points defining the center line are:													①						
				-25.4	-120.7	31.8	-25.4	-721.9	31.8											
Magnetometer	Three rectangles																0			
Shade 1	-35.1	-441.5	34.0	-16.0	-441.5	34.0	-16.0	-473.2	34.0	-35.1	-473.2	34.0	0.0605				0			
Shade 2	-36.3	-663.7	34.0	-14.7	-663.7	34.0	-14.7	-704.3	34.0	-36.3	-704.3	34.0	0.0877	①			0			
Shade 3	-41.4	-401.1	34.0	-14.7	-401.1	34.0	-14.7	-441.7	34.0	-41.4	-441.7	34.0	0.1084				0			
IRR sunshades	Two rectangles																			
Shade 1	-46.2	-73.7	73.4	-61.0	-85.6	73.4	-48.3	-102.1	73.4	-33.5	-89.9	73.4	0.0406	⑥			0			
Shade 2	-61.0	-85.6	73.4	-69.1	-91.9	63.8	-56.1	-108.2	63.8	-48.3	-102.1	73.4	0.0299				43.10			
PSE instrument	Three rectangles, rotating																			
Surface 1	-65.3	-111.8	61.0	-82.0	-140.5	61.0	-63.5	-150.9	61.0	-47.0	-122.4	61.0	0.0705				0			
Surface 2	-47.0	-122.4	61.0	-63.5	-150.9	61.0	-63.5	-150.9	35.8	-47.0	-122.4	35.8	0.0830	①			0			
Surface 3	-82.0	-140.5	61.0	-65.3	-111.8	61.0	-65.3	-111.8	35.8	-82.0	-140.5	35.8	0.0830				0			
Rotation axis	Two points defining the axis:						-56.6	-117.3	53.3	-72.9	-145.5	53.3					0			
UVS sunshade	One rectangle																			
	6.6	-110.5	40.4	34.5	-110.5	40.4	34.5	-130.0	40.4	6.6	-130.0	40.4	0.0546	④						
TVCA heat shield	One annulus perpendicular to and centered on z-axis, at z = 96.5 cm, inner radius = 7.6 cm, outer radius = 45.7 cm												0.1595	④			0			
High-gain antenna	Paraboloid of revolution, aperture radius = 68.6 cm, depth = 21.6 cm												Curved	③	⑦	Thickness 1.9 cm	Variable			

Table 12. Optical properties of reflecting materials

Material Number	Material	Unexposed			After exposure		
		$\gamma$	$\beta$	$\epsilon$	$\gamma$	$\beta$	$\epsilon$
1	Silvered Teflon 127 $\mu\text{m}$ thick	0.93 $\pm 0.02$	1.0	0.80 $\pm 0.03$	0.85 $\pm 0.03$	1.0	0.80 $\pm 0.03$
2	DC92-007 white paint ( $\text{TiO}_2$ )	0.79 $\pm 0.02$	0.51	0.85 $\pm 0.03$	0.50 $\pm 0.05$	0.50	0.85 $\pm 0.03$
3	Z-93 paint ( $\text{ZnO}/\text{K}_2\text{SiO}_3$ )	0.84 $\pm 0.02$	0	0.90 $\pm 0.03$	0.74 $\pm 0.03$	0	0.90 $\pm 0.03$
4	Alzak anodized aluminum	0.86 $\pm 0.02$	1.0	0.74 $\pm 0.03$	0.72 $\pm 0.03$	1.0	0.78 $\pm 0.03$
5	Aluminized Teflon 25.4 $\mu\text{m}$ thick	0.89 $\pm 0.02$	1.0	0.03 $\pm 0.03$	0.85 $\pm 0.04$	1.0	0.03 $\pm 0.03$
6	Beta cloth Teflon	0.79 $\pm 0.02$	0.13	0.842 $\pm 0.03$	0.48 $\pm 0.31$	0.21	0.842 $\pm 0.03$
7	Cat-a-lac black paint	0.10 $\pm 0.02$	0	0.89 $\pm 0.03$	0.10 $\pm 0.03$	0	0.89 $\pm 0.03$
8	Solar cells	0.22 $\pm 0.02$	0.75	0.79 $\pm 0.03$	0.22 $\pm 0.02$	0.75	0.79 $\pm 0.03$

Table 13. Components of the solar radiation force on the high-gain antenna

Component	Solar radiation force, $10^6$ meters									
	$\psi = 0^\circ$	$\psi = 10^\circ$	$\psi = 20^\circ$	$\psi = 30^\circ$	$\psi = 40^\circ$	$\psi = 50^\circ$	$\psi = 60^\circ$	$\psi = 70^\circ$	$\psi = 80^\circ$	$\psi = 90^\circ$
$I_x$	0	0	0	0	0	0	0	0	0	0
$J_x$	0	0	0	0	0	0	0	0	0	0
$K_x$	0	0	0	0	0	0	0	0	0	0
$I_y$	0	-1.1559	-2.1639	-2.9177	-3.3221	-3.3291	-2.9399	-2.2917	-1.5773	-0.9201
$J_y$	0	-0.0053	-0.0101	-0.0139	-0.0163	-0.0169	-0.0157	-0.0125	-0.0084	-0.0046
$K_y$	0	0.0005	0.0007	0.0009	0.0010	0.0009	0.0007	0.0005	0.0003	0.0001
$I_z$	7.4422	4.6954	6.4473	5.5162	4.3683	3.1368	1.9646	1.0273	0.4080	0.0777
$J_z$	0.1883	0.1837	0.1703	0.1494	0.1233	0.0946	0.0666	0.0426	0.0240	0.0112
$K_z$	-0.0096	-0.0093	-0.0084	-0.0071	-0.0055	-0.0039	-0.0026	-0.0015	-0.0007	-0.0003

Table 14. Values of the component  $F_{yA}$ 

$\psi$ , deg	$F_{yA}, 10^6$ newtons						
	$\rho = 1.000$ AU	$\rho = 0.884$ AU	$\rho = 0.768$ AU	$\rho = 0.652$ AU	$\rho = 0.536$ AU	$\rho = 0.420$ AU	$\rho = 0.304$ AU
0	0	0	0	0	0	0	0
10	-1.156	-1.480	-1.963	-2.728	-4.045	-6.607	-12.654
20	-2.173	-2.783	-3.692	-5.130	-7.606	-12.425	-23.804
30	-2.931	-3.753	-4.978	-6.918	-10.259	-16.761	-32.124
40	-3.337	-4.274	-5.670	-7.879	-11.686	-19.098	-36.626
50	-3.345	-4.285	-5.684	-7.899	-11.718	-19.156	-36.769
60	-2.955	-3.785	-5.021	-6.980	-10.356	-16.937	-32.544
70	-2.304	-2.951	-3.915	-5.443	-8.077	-13.214	-25.413
80	-1.586	-2.031	-2.694	-3.746	-5.559	-9.096	-17.504
90	-0.925	-1.184	-1.571	-2.184	-3.241	-5.303	-10.206

Table 15. Values of the component  $F_{zA}$ 

$\psi$ , deg	$F_{zA}, 10^6$ newtons						
	$\rho = 1.000$ AU	$\rho = 0.884$ AU	$\rho = 0.768$ AU	$\rho = 0.652$ AU	$\rho = 0.536$ AU	$\rho = 0.420$ AU	$\rho = 0.304$ AU
0	7.442	9.567	12.753	17.846	26.736	44.365	87.062
10	7.228	9.291	12.386	17.334	25.970	43.101	84.608
20	6.609	8.497	11.328	15.856	23.762	39.454	77.525
30	5.659	7.276	9.702	13.584	20.366	33.842	66.611
40	4.486	5.770	7.696	10.780	16.174	26.909	53.101
50	3.228	4.152	5.542	7.768	11.668	19.450	38.528
60	2.029	2.612	3.489	4.897	7.371	12.328	24.571
70	1.068	1.377	1.843	2.594	3.920	6.597	13.294
80	0.431	0.558	0.750	1.061	1.617	2.758	5.685
90	0.089	0.116	0.159	0.231	0.364	0.653	1.457

Table 16. Values of the magnitude of the force  $\bar{F}_A$ 

$\psi$ , deg	Magnitude of force $\bar{F}_A$ , $10^6$ newtons						
	$\rho = 1.000$ AU	$\rho = 0.884$ AU	$\rho = 0.768$ AU	$\rho = 0.652$ AU	$\rho = 0.536$ AU	$\rho = 0.420$ AU	$\rho = 0.304$ AU
0	7.442	9.567	12.753	17.846	26.736	44.365	87.062
10	7.320	9.409	12.541	17.547	26.283	43.604	85.549
20	6.957	8.941	11.915	16.665	24.950	41.364	81.097
30	6.372	8.187	10.905	15.244	22.804	37.765	73.953
40	5.591	7.180	9.959	13.326	19.954	32.997	64.507
50	4.648	5.967	7.938	11.079	16.536	27.300	53.258
60	3.584	4.599	6.114	8.526	12.711	20.949	40.778
70	2.539	3.257	4.327	6.029	8.977	14.769	28.681
80	1.643	2.106	2.797	3.893	5.789	9.505	18.404
90	0.929	1.190	1.579	2.196	3.261	5.343	10.309

Table 17. Values of the acceleration  $a_A$ 

$\psi$ , deg	Acceleration $a_A$ , $10^{11} \text{ km/s}^2$						
	$\rho = 1.000 \text{ AU}$	$\rho = 0.884 \text{ AU}$	$\rho = 0.768 \text{ AU}$	$\rho = 0.652 \text{ AU}$	$\rho = 0.536 \text{ AU}$	$\rho = 0.420 \text{ AU}$	$\rho = 0.304 \text{ AU}$
0	1.493	1.919	2.558	3.580	5.363	8.899	17.464
10	1.468	1.887	2.516	3.520	5.272	8.747	17.160
20	1.396	1.794	2.390	3.343	5.005	8.297	16.267
30	1.278	1.642	2.187	3.058	4.574	7.575	14.834
40	1.122	1.440	1.917	2.678	4.003	6.619	12.939
50	0.932	1.197	1.592	2.222	3.317	5.476	10.683
60	0.719	0.922	1.227	1.710	2.550	4.202	8.180
70	0.509	0.653	0.868	1.209	1.801	2.963	5.753
80	0.330	0.423	0.561	0.781	1.161	1.907	3.692
90	0.186	0.239	0.317	0.441	0.654	1.072	2.068

Table 18. Components of the solar pressure force on the high-gain antenna reflector of the Mariner Venus/Mercury spacecraft along the axes of the antenna-fixed reference system

Time, days	$\psi$ , deg	$a_A$ , $10^{11} \text{ km/s}^2$	$F_{xA}$ , $10^6 \text{ N}$	$F_{yA}$ , $10^6 \text{ N}$	$F_{zA}$ , $10^6 \text{ N}$	$ F_A $ , $10^6 \text{ N}$
.00	90.00	.1872	.0000	-.9312	.0631	.9333
1.00	90.00	.1873	.0000	-.9319	.0631	.9340
2.00	90.00	.1875	.0000	-.9327	.0632	.9348
3.00	90.00	.1877	.0000	-.9336	.0633	.9358
4.00	90.00	.1879	.0000	-.9347	.0633	.9369
5.00	89.46	.1949	.0000	-.9688	.0747	.9717
6.00	88.69	.2051	.0000	-1.0182	.0922	1.0224
7.00	87.91	.2157	.0000	-1.0694	.1114	1.0752
8.00	87.13	.2267	.0000	-1.1222	.1323	1.1300
9.00	86.33	.2381	.0000	-1.1766	.1551	1.1868
10.00	85.53	.2499	.0000	-1.2328	.1799	1.2458
11.00	84.72	.2622	.0000	-1.2906	.2067	1.3070
12.00	83.91	.2749	.0000	-1.3501	.2358	1.3705
13.00	83.08	.2861	.0000	-1.4114	.2672	1.4364
14.00	82.25	.3018	.0000	-1.4744	.3011	1.5048
15.00	81.41	.3161	.0000	-1.5392	.3376	1.5757
16.00	80.56	.3308	.0000	-1.6058	.3768	1.6494
17.00	79.70	.3462	.0000	-1.6742	.4191	1.7258
18.00	78.83	.3621	.0000	-1.7445	.4644	1.8052
19.00	77.96	.3786	.0000	-1.8166	.5131	1.8877
20.00	77.07	.3958	.0000	-1.8907	.5653	1.9734
21.00	76.17	.4137	.0000	-1.9666	.6213	2.0624
22.00	75.25	.4323	.0000	-2.0445	.6812	2.1550
23.00	74.33	.4516	.0000	-2.1242	.7454	2.2512
24.00	73.39	.4716	.0000	-2.2059	.8140	2.3513
25.00	72.44	.4925	.0000	-2.2894	.8874	2.4554
26.00	71.48	.5142	.0000	-2.3748	.9658	2.5637
27.00	70.50	.5368	.0000	-2.4619	1.0495	2.6763
28.00	69.51	.5603	.0000	-2.5508	1.1389	2.7935
29.00	68.50	.5848	.0000	-2.6413	1.2342	2.9154
30.00	67.48	.6102	.0000	-2.7333	1.3359	3.0423
31.00	66.44	.6367	.0000	-2.8267	1.4441	3.1742
32.00	65.38	.6642	.0000	-2.9213	1.5593	3.3114
33.00	64.31	.6928	.0000	-3.0169	1.6818	3.4540
34.00	63.22	.7226	.0000	-3.1133	1.8122	3.6023
35.00	62.11	.7534	.0000	-3.2101	1.9503	3.7561
36.00	60.99	.7854	.0000	-3.3068	2.0967	3.9155
37.00	59.84	.8185	.0000	-3.4031	2.2516	4.0805
38.00	58.68	.8527	.0000	-3.4984	2.4150	4.2510
39.00	57.50	.8879	.0000	-3.5917	2.5870	4.4264
40.00	56.30	.9238	.0000	-3.6816	2.7671	4.6056
41.00	55.09	.9605	.0000	-3.7677	2.9552	4.7884
42.00	53.85	.9979	.0000	-3.8494	3.1513	4.9748
43.00	52.60	1.0360	.0000	-3.9262	3.3555	5.1647
44.00	51.32	1.0748	.0000	-3.9976	3.5677	5.3581

Table 18 (contd)

Time, days	$\psi$ , deg	$a_A$ , $10^{11} \text{ km/s}^2$	$F_{xA}$ , $10^6 \text{ N}$	$F_{yA}$ , $10^6 \text{ N}$	$F_{zA}$ , $10^6 \text{ N}$	$ F_A $ , $10^6 \text{ N}$
45.00	50.03	1.1142	.0000	-4.0630	3.7879	5.5548
46.00	48.72	1.1543	.0000	-4.1219	4.0159	5.7548
47.00	47.40	1.1951	.0000	-4.1737	4.2515	5.9578
48.00	46.06	1.2363	.0000	-4.2178	4.4942	6.1635
49.00	44.70	1.2782	.0000	-4.2538	4.7443	6.3720
50.00	43.32	1.3205	.0000	-4.2811	5.0009	6.5831
51.00	41.94	1.3633	.0000	-4.2992	5.2637	6.7963
52.00	40.54	1.4064	.0000	-4.3075	5.5322	7.0114
53.00	39.13	1.4499	.0000	-4.3058	5.8056	7.2281
54.00	37.71	1.4936	.0000	-4.2936	6.0834	7.4460
55.00	36.29	1.5374	.0000	-4.2707	6.3646	7.6646
56.00	34.86	1.5814	.0000	-4.2368	6.6488	7.8840
57.00	33.43	1.6254	.0000	-4.1921	6.9344	8.1030
58.00	32.00	1.6693	.0000	-4.1364	7.2211	8.3219
59.00	30.58	1.7130	.0000	-4.0703	7.5073	8.5397
60.00	29.17	1.7564	.0000	-3.9940	7.7921	8.7561
61.00	27.78	1.7994	.0000	-3.9082	8.0745	8.9706
62.00	26.41	1.8419	.0000	-3.8140	8.3532	9.1827
63.00	25.07	1.8839	.0000	-3.7125	8.6270	9.3919
64.00	23.77	1.9251	.0000	-3.6054	8.8945	9.5975
65.00	22.52	1.9656	.0000	-3.4946	9.1549	9.7992
66.00	21.33	2.0052	.0000	-3.3827	9.4066	9.9964
67.00	20.21	2.0437	.0000	-3.2726	9.6486	10.1885
68.00	19.19	2.0811	.0000	-3.1678	9.8795	10.3750
69.00	18.27	2.1173	.0000	-3.0723	10.0984	10.5554
70.00	17.48	2.1522	.0000	-2.9904	10.3042	10.7293
71.00	16.84	2.1857	.0000	-2.9268	10.4958	10.8962
72.00	16.36	2.2176	.0000	-2.8862	10.6722	11.0556
73.00	16.06	2.2480	.0000	-2.8725	10.8327	11.2071
74.00	15.95	2.2767	.0000	-2.8890	10.9765	11.3503
75.00	16.03	2.3037	.0000	-2.9375	11.1027	11.4847
76.00	16.30	2.3288	.0000	-3.0184	11.2109	11.6101
77.00	16.75	2.3521	.0000	-3.1306	11.3004	11.7260
78.00	17.37	2.3734	.0000	-3.2716	11.3709	11.8322
79.00	18.13	2.3927	.0000	-3.4384	11.4220	11.9283
80.00	19.02	2.4099	.0000	-3.6271	11.4533	12.0139
81.00	20.01	2.4249	.0000	-3.8341	11.4648	12.0889
82.00	21.10	2.4377	.0000	-4.0554	11.4564	12.1530
83.00	22.26	2.4483	.0000	-4.2678	11.4279	12.2058
84.00	23.48	2.4566	.0000	-4.5279	11.3794	12.2471
85.00	24.75	2.4626	.0000	-4.7727	11.3109	12.2767
86.00	26.07	2.4661	.0000	-5.0196	11.2228	12.2942
87.00	27.42	2.4671	.0000	-5.2661	11.1151	12.2995
88.00	28.80	2.4657	.0000	-5.5100	10.9881	12.2922
89.00	30.20	2.4617	.0000	-5.7491	10.8422	12.2722
90.00	31.63	2.4550	.0000	-5.9817	10.6778	12.2391
91.00	33.06	2.4457	.0000	-6.2058	10.4954	12.1929
92.00	34.51	2.4337	.0000	-6.4200	10.2953	12.1330

Table 18 (contd)

Time, days	$\psi$ , deg	$a_A$ , $10^{11} \text{ km/s}^2$	$F_{xA}$ , $10^6 \text{ N}$	$F_{yA}$ , $10^6 \text{ N}$	$F_{zA}$ , $10^6 \text{ N}$	$ F_A $ , $10^6 \text{ N}$
92.00	32.35	2.4832	.0000	-6.1765	10.7286	12.3796
93.00	33.25	2.4882	.0000	-6.3442	10.6595	12.4045
94.00	34.16	2.4926	.0000	-6.5130	10.5832	12.4267
95.00	35.10	2.4964	.0000	-6.6828	10.4993	12.4456
96.00	36.05	2.4995	.0000	-6.8528	10.4076	12.4611
97.00	37.02	2.5019	.0000	-7.0226	10.3077	12.4726
98.00	38.01	2.5033	.0000	-7.1915	10.1994	12.4798
99.00	39.02	2.5038	.0000	-7.3591	10.0822	12.4823
100.00	40.04	2.5032	.0000	-7.5246	9.9556	12.4793
101.00	41.08	2.5015	.0000	-7.6872	9.8195	12.4706
102.00	42.15	2.4984	.0000	-7.8463	9.6732	12.4553
103.00	43.22	2.4939	.0000	-8.0010	9.5162	12.4328
104.00	44.32	2.4878	.0000	-8.1504	9.3482	12.4023
105.00	45.44	2.4798	.0000	-8.2934	9.1685	12.3629
106.00	46.58	2.4700	.0000	-8.4289	8.9767	12.3137
107.00	47.73	2.4580	.0000	-8.5557	8.7723	12.2537
108.00	48.91	2.4435	.0000	-8.6724	8.5548	12.1818
109.00	50.11	2.4265	.0000	-8.7775	8.3239	12.0968
110.00	51.33	2.4065	.0000	-8.8693	8.0789	11.9972
111.00	52.58	2.3834	.0000	-8.9462	7.8197	11.8820
112.00	53.84	2.3568	.0000	-9.0059	7.5457	11.7493
113.00	55.14	2.3263	.0000	-9.0465	7.2569	11.5975
114.00	56.45	2.2917	.0000	-9.0656	6.9532	11.4251
115.00	57.80	2.2526	.0000	-9.0607	6.6347	11.2301
116.00	59.17	2.2089	.0000	-9.0303	6.3024	11.0121
117.00	60.57	2.1611	.0000	-8.9754	5.9591	10.7736
118.00	62.00	2.1093	.0000	-8.8959	5.6069	10.5155
119.00	63.46	2.0536	.0000	-8.7911	5.2474	10.2381
120.00	64.95	1.9942	.0000	-8.6603	4.8822	9.9417
121.00	66.47	1.9309	.0000	-8.5028	4.5133	9.6264
122.00	68.02	1.8639	.0000	-8.3180	4.1422	9.2923
123.00	69.61	1.7932	.0000	-8.1052	3.7710	8.9395
124.00	71.24	1.7188	.0000	-7.8643	3.4021	8.5686
125.00	72.89	1.6408	.0000	-7.5951	3.0377	8.1800
126.00	74.58	1.5595	.0000	-7.2979	2.6804	7.7746
127.00	76.31	1.4750	.0000	-6.9735	2.3329	7.3534
128.00	78.07	1.3877	.0000	-6.6231	1.9981	6.9179
129.00	79.87	1.2978	.0000	-6.2482	1.6787	6.4697
130.00	81.71	1.2057	.0000	-5.8510	1.3777	6.0111
131.00	83.57	1.1121	.0000	-5.4346	1.0978	5.5444
132.00	85.48	1.0175	.0000	-5.0024	.8417	5.0727
133.00	87.41	.9226	.0000	-4.5585	.6116	4.5994
134.00	89.37	.8280	.0000	-4.1077	.4095	4.1281
135.00	90.00	.8066	.0000	-4.0056	.3563	4.0214
136.00	90.00	.8180	.0000	-4.0620	.3626	4.0781

Table 19. Solar torque on the high-gain antenna of the  
Mariner Venus/Mercury spacecraft

Time, days	Torque, $10^6 \text{ N} \cdot \text{m}$	Time, days	Torque, $10^6 \text{ N} \cdot \text{m}$	Time, days	Torque, $10^6 \text{ N} \cdot \text{m}$
.00	.1467	45.00	.9358	90.00	1.3746
1.00	.1468	46.00	.9484	91.00	1.4273
2.00	.1470	47.00	.9594	92.00	1.4780
3.00	.1471	48.00	.9687	92.00	1.4204
4.00	.1473	49.00	.9761	93.00	1.4599
5.00	.1553	50.00	.9816	94.00	1.4997
6.00	.1672	51.00	.9850	95.00	1.5399 *
7.00	.1796	52.00	.9863	96.00	1.5803
8.00	.1926	53.00	.9853	97.00	1.6208
9.00	.2061	54.00	.9819	98.00	1.6612
10.00	.2203	55.00	.9761	99.00	1.7014
11.00	.2351	56.00	.9679	100.00	1.7413
12.00	.2505	57.00	.9572	101.00	1.7808
13.00	.2664	58.00	.9441	102.00	1.8196
14.00	.2830	59.00	.9287	103.00	1.8576
15.00	.3002	60.00	.9110	104.00	1.8945
16.00	.3181	61.00	.8911	105.00	1.9302
17.00	.3365	62.00	.8694	106.00	1.9644
18.00	.3555	63.00	.8461	107.00	1.9968
19.00	.3752	64.00	.8216	108.00	2.0272
20.00	.3954	65.00	.7962	109.00	2.0551
21.00	.4163	66.00	.7706	110.00	2.0802
22.00	.4377	67.00	.7455	111.00	2.1022
23.00	.4596	68.00	.7216	112.00	2.1205
24.00	.4821	69.00	.6999	113.00	2.1347
25.00	.5050	70.00	.6812	114.00	2.1442
26.00	.5284	71.00	.6668	115.00	2.1484
27.00	.5522	72.00	.6576	116.00	2.1465
28.00	.5763	73.00	.6546	117.00	2.1368
29.00	.6006	74.00	.6585	118.00	2.1187
30.00	.6251	75.00	.6697	119.00	2.0915
31.00	.6497	76.00	.6883	120.00	2.0547
32.00	.6742	77.00	.7141	121.00	2.0082
33.00	.6986	78.00	.7465	122.00	1.9517
34.00	.7227	79.00	.7849	123.00	1.8854
35.00	.7464	80.00	.8283	124.00	1.8094
36.00	.7694	81.00	.8760	125.00	1.7242
37.00	.7917	82.00	.9270	126.00	1.6302
38.00	.8131	83.00	.9806	127.00	1.5282
39.00	.8336	84.00	1.0361	128.00	1.4193
40.00	.8532	85.00	1.0928	129.00	1.3046
41.00	.8719	86.00	1.1500	130.00	1.1855
42.00	.8897	87.00	1.2073	131.00	1.0635
43.00	.9063	88.00	1.2642	132.00	.9405
44.00	.9218	89.00	1.3201		

Table 20. Components of the solar pressure force in the spacecraft-fixed reference frame

Time, days	$\rho$ , AU	$\psi$ , deg	FAx, $10^6$ N	FAy, $10^6$ N	FAz, $10^6$ N	$ F_A $ , $10^6$ N
.00	.991198	90.000	.000000	.063079	-.931169	.933303
1.00	.990837	90.000	.000000	.063131	-.931850	.933987
2.00	.990404	90.000	.000000	.063193	-.932669	.934807
3.00	.989899	90.000	.000000	.063266	-.933624	.935765
4.00	.989322	90.000	.000000	.063350	-.934716	.936861
5.00	.988674	89.463	.000000	.065630	-.969448	.971667
6.00	.987954	88.692	.000000	.068935	-1.020083	1.022410
7.00	.987162	87.913	.000000	.072354	-1.072728	1.075165
8.00	.986299	87.127	.000000	.075885	-1.127401	1.129952
9.00	.985365	86.333	.000000	.079531	-1.184150	1.186817
10.00	.984359	85.532	.000000	.083291	-1.243037	1.245824
11.00	.983281	84.723	.000000	.087169	-1.304128	1.307038
12.00	.982133	83.907	.000000	.091166	-1.367510	1.370546
13.00	.980913	83.083	.000000	.095285	-1.433270	1.436434
14.00	.979623	82.251	.000000	.099529	-1.501501	1.504796
15.00	.978262	81.411	.000000	.103901	-1.572314	1.575744
16.00	.976830	80.561	.000000	.108404	-1.645817	1.649384
17.00	.975327	79.702	.000000	.113042	-1.722130	1.725837
18.00	.973754	78.834	.000000	.117817	-1.801383	1.805232
19.00	.972111	77.955	.000000	.122734	-1.883705	1.887699
20.00	.970398	77.066	.000000	.127795	-1.969239	1.973381
21.00	.968615	76.165	.000000	.133003	-2.058131	2.062424
22.00	.966762	75.253	.000000	.138363	-2.150536	2.154983
23.00	.964840	74.328	.000000	.143875	-2.246613	2.251215
24.00	.962848	73.391	.000000	.149544	-2.346531	2.351291
25.00	.960788	72.441	.000000	.155372	-2.450459	2.455380
26.00	.958658	71.477	.000000	.161359	-2.558572	2.563655
27.00	.956460	70.499	.000000	.167507	-2.671053	2.676301
28.00	.954194	69.507	.000000	.173817	-2.788082	2.793495
29.00	.951860	68.499	.000000	.180288	-2.909843	2.915423
30.00	.949458	67.476	.000000	.186917	-3.036521	3.042269
31.00	.946989	66.437	.000000	.193703	-3.168289	3.174204
32.00	.944453	65.381	.000000	.200639	-3.305316	3.311400
33.00	.941850	64.309	.000000	.207719	-3.447750	3.454002
34.00	.939181	63.218	.000000	.214941	-3.595909	3.602327
35.00	.936445	62.111	.000000	.222272	-3.749501	3.756083
36.00	.933645	60.986	.000000	.229704	-3.908764	3.915508
37.00	.930779	59.844	.000000	.237210	-4.073647	4.080548
38.00	.927849	58.682	.000000	.244752	-4.243961	4.251013
39.00	.924855	57.502	.000000	.252267	-4.419173	4.426367
40.00	.921796	56.304	.000000	.259658	-4.598249	4.605574
41.00	.918675	55.087	.000000	.266873	-4.780956	4.788399
42.00	.915491	53.851	.000000	.273873	-4.967263	4.974807
43.00	.912245	52.596	.000000	.280616	-5.157108	5.164737
44.00	.908938	51.323	.000000	.287059	-5.350417	5.358112

Table 20 (contd)

Time, days	$\rho$ , AU	$\psi$ , deg	$F_{Ax}$ , $10^6$ N	$F_{Ay}$ , $10^6$ N	$F_{Az}$ , $10^6$ N	$ F_A $ , $10^6$ N
45.00	.905570	50.032	.000000	.293156	-5.547084	5.554825
46.00	.902141	48.723	.000000	.298858	-5.746992	5.754757
47.00	.898654	47.397	.000000	.304115	-5.949985	5.957752
48.00	.895108	46.055	.000000	.308874	-6.155715	6.163459
49.00	.891503	44.697	.000000	.313090	-6.364351	6.372048
50.00	.887341	43.323	.000000	.316708	-6.575462	6.583085
51.00	.884123	41.936	.000000	.319677	-6.788778	6.796300
52.00	.880350	40.537	.000000	.321948	-7.004007	7.011403
53.00	.876522	39.128	.000000	.323476	-7.220830	7.228071
54.00	.872640	37.710	.000000	.324218	-7.438897	7.445959
55.00	.868706	36.286	.000000	.324142	-7.657785	7.664642
56.00	.864721	34.856	.000000	.323210	-7.877327	7.883955
57.00	.860685	33.428	.000000	.321416	-8.096666	8.103043
58.00	.856599	32.000	.000000	.318737	-8.315791	8.321897
59.00	.852466	30.581	.000000	.315189	-8.533874	8.539693
60.00	.848286	29.172	.000000	.310790	-8.750579	8.756096
61.00	.844061	27.780	.000000	.305577	-8.965397	8.970603
62.00	.839791	26.411	.000000	.299613	-9.177807	9.182697
63.00	.835480	25.071	.000000	.292987	-9.387281	9.391852
64.00	.831127	23.772	.000000	.285824	-9.593200	9.597457
65.00	.826735	22.520	.000000	.278260	-9.795238	9.799190
66.00	.822304	21.330	.000000	.270502	-9.992704	9.996364
67.00	.817838	20.214	.000000	.262785	-10.185078	10.188467
68.00	.813338	19.189	.000000	.255393	-10.371847	10.374991
69.00	.808805	18.271	.000000	.248653	-10.552515	10.555444
70.00	.804242	17.481	.000000	.242932	-10.726590	10.729340
71.00	.799651	16.836	.000000	.238622	-10.893602	10.896216
72.00	.795034	16.357	.000000	.236116	-11.053096	11.055618
73.00	.790393	16.057	.000000	.235768	-11.204633	11.207114
74.00	.785730	15.947	.000000	.237864	-11.347796	11.350288
75.00	.781049	16.030	.000000	.242573	-11.482168	11.484730
76.00	.776352	16.303	.000000	.249952	-11.607410	11.610101
77.00	.771640	16.755	.000000	.259920	-11.723153	11.726034
78.00	.766917	17.370	.000000	.272298	-11.829060	11.832194
79.00	.762187	18.131	.000000	.286829	-11.924813	11.928262
80.00	.757451	19.018	.000000	.303212	-12.010110	12.013936
81.00	.752713	20.013	.000000	.321133	-12.084657	12.088923
82.00	.747978	21.098	.000000	.340264	-12.148223	12.152987
83.00	.743246	22.258	.000000	.360328	-12.200472	12.205791
84.00	.738523	23.481	.000000	.381036	-12.241172	12.247101
85.00	.733812	24.755	.000000	.402127	-12.270066	12.276654
86.00	.729116	26.071	.000000	.423365	-12.286903	12.294195
87.00	.724439	27.422	.000000	.444530	-12.291435	12.299470
88.00	.719786	28.801	.000000	.465420	-12.283409	12.292223
89.00	.715161	30.204	.000000	.485850	-12.262580	12.272201
90.00	.710568	31.625	.000000	.505645	-12.228694	12.239144
91.00	.706011	33.061	.000000	.524637	-12.181591	12.192883
92.00	.701495	34.511	.000000	.542689	-12.120868	12.133011

Table 20 (contd)

Time, days	$\rho$ , AU	$\psi$ , deg	$F_{Ax}$ , $10^6$ N	$F_{Ay}$ , $10^6$ N	$F_{Az}$ , $10^6$ N	$ F_A $ , $10^6$ N
92.00	.703688	32.355	.000000	.523933	-12.368468	12.379560
93.00	.699315	33.249	.000000	.538801	-12.392823	12.404530
94.00	.694839	34.163	.000000	.553805	-12.414355	12.426701
95.00	.690262	35.097	.000000	.568913	-12.432625	12.445635
96.00	.685587	36.049	.000000	.584075	-12.447368	12.461064
97.00	.680815	37.020	.000000	.599241	-12.458199	12.472603
98.00	.675949	38.009	.000000	.614361	-12.464696	12.479827
99.00	.670992	39.016	.000000	.629381	-12.466389	12.482266
100.00	.665945	40.042	.000000	.644243	-12.462704	12.479345
101.00	.660814	41.084	.000000	.658877	-12.453189	12.470607
102.00	.655601	42.145	.000000	.673216	-12.437127	12.455334
103.00	.650309	43.225	.000000	.687183	-12.413816	12.432821
104.00	.644942	44.323	.000000	.700692	-12.382501	12.402310
105.00	.639503	45.440	.000000	.713652	-12.342275	12.362890
106.00	.633999	46.577	.000000	.725959	-12.292289	12.313708
107.00	.628432	47.734	.000000	.737503	-12.231514	12.253728
108.00	.622808	48.912	.000000	.748162	-12.158754	12.181750
109.00	.617133	50.111	.000000	.757805	-12.073008	12.096767
110.00	.611411	51.332	.000000	.766288	-11.972730	11.997227
111.00	.605650	52.576	.000000	.773462	-11.856770	11.881971
112.00	.599856	53.844	.000000	.779158	-11.723396	11.749260
113.00	.594034	55.136	.000000	.783207	-11.571061	11.597537
114.00	.588194	56.454	.000000	.785427	-11.398025	11.425054
115.00	.582344	57.798	.000000	.785642	-11.202560	11.230075
116.00	.576491	59.170	.000000	.783767	-10.984163	11.012090
117.00	.570643	60.570	.000000	.779892	-10.745321	10.773586
118.00	.564612	61.999	.000000	.773992	-10.486951	10.515474
119.00	.559007	63.458	.000000	.765996	-10.209419	10.238115
120.00	.553238	64.948	.000000	.755817	-9.912909	9.941682
121.00	.547518	66.470	.000000	.743364	-9.597675	9.626420
122.00	.541857	68.025	.000000	.728534	-9.263663	9.292266
123.00	.536268	69.613	.000000	.711245	-8.911197	8.939535
124.00	.530764	71.235	.000000	.691427	-8.540660	8.568602
125.00	.525359	72.892	.000000	.669031	-8.152620	8.180025
126.00	.520067	74.584	.000000	.644040	-7.747876	7.774598
127.00	.514902	76.312	.000000	.616476	-7.327511	7.353398
128.00	.509880	78.075	.000000	.586414	-6.893031	6.917931
129.00	.505015	79.873	.000000	.553961	-6.445982	6.469742
130.00	.500324	81.706	.000000	.519304	-5.988583	6.011057
131.00	.495823	83.574	.000000	.482690	-5.523357	5.544408
132.00	.491527	85.475	.000000	.444435	-5.053232	5.072739
133.00	.487454	87.409	.000000	.404923	-4.581530	4.599389
134.00	.483618	89.374	.000000	.364605	-4.111951	4.128084
135.00	.480037	90.000	.000000	.356312	-4.005599	4.021416
136.00	.476724	90.000	.000000	.362598	-4.061997	4.078149

Table 21. Solar panel tilts

Date	$\theta$ , deg
Jan. 17, 1974	+45.0
Feb. 9, 1974	+58.0
Mar. 1, 1974	+68.0
Mar. 20, 1974	+71.0

Table 22. Components of the solar pressure force on the solar panels of the Mariner Venus/Mercury spacecraft along the axes of the spacecraft-fixed reference system

Time, days	$\theta$ tilt, deg	$a_{SP}$ , $10^{11} \text{ km/s}^2$	$F_{SPx}$ , $10^6 \text{ N}$	$F_{SPy}$ , $10^6 \text{ N}$	$F_{SPz}$ , $10^6 \text{ N}$	$ F_{SP} $ , $10^6 \text{ N}$
.00	.00	6.4447	.0000	.0000	-32.1289	32.1289
1.00	.00	6.4494	.0000	.0000	-32.1525	32.1525
2.00	.00	6.4551	.0000	.0000	-32.1809	32.1809
3.00	.00	6.4618	.0000	.0000	-32.2141	32.2141
4.00	.00	6.4694	.0000	.0000	-32.2521	32.2521
5.00	.00	6.4780	.0000	.0000	-32.2948	32.2948
6.00	.00	6.4875	.0000	.0000	-32.3424	32.3424
7.00	.00	6.4980	.0000	.0000	-32.3948	32.3948
8.00	.00	6.5095	.0000	.0000	-32.4521	32.4521
9.00	.00	6.5220	.0000	.0000	-32.5144	32.5144
10.00	.00	6.5355	.0000	.0000	-32.5815	32.5815
11.00	.00	6.5499	.0000	.0000	-32.6537	32.6537
12.00	.00	6.5654	.0000	.0000	-32.7309	32.7309
13.00	.00	6.5819	.0000	.0000	-32.8132	32.8132
14.00	.00	6.5995	.0000	.0000	-32.9006	32.9006
15.00	.00	6.6180	.0000	.0000	-32.9932	32.9932
16.00	.00	6.6377	.0000	.0000	-33.0910	33.0910
17.00	.00	6.6583	.0000	.0000	-33.1941	33.1941
18.00	.00	6.6801	.0000	.0000	-33.3025	33.3025
19.00	.00	6.7029	.0000	.0000	-33.4164	33.4164
20.00	.00	6.7269	.0000	.0000	-33.5357	33.5357
21.00	.00	6.7519	.0000	.0000	-33.6606	33.6606
22.00	.00	6.7781	.0000	.0000	-33.7911	33.7911
23.00	.00	6.8054	.0000	.0000	-33.9273	33.9273
24.00	.00	6.8339	.0000	.0000	-34.0693	34.0693
25.00	.00	6.8635	.0000	.0000	-34.2171	34.2171
26.00	.00	6.8944	.0000	.0000	-34.3709	34.3709
27.00	.00	6.9265	.0000	.0000	-34.5308	34.5308
28.00	.00	6.9598	.0000	.0000	-34.6967	34.6967
29.00	.00	6.9943	.0000	.0000	-34.8689	34.8689
30.00	.00	7.0301	.0000	.0000	-35.0475	35.0475
31.00	.00	7.0672	.0000	.0000	-35.2325	35.2325
32.00	.00	7.1056	.0000	.0000	-35.4240	35.4240
33.00	.00	7.1454	.0000	.0000	-35.6222	35.6222
34.00	.00	7.1865	.0000	.0000	-35.8273	35.8273
35.00	.00	7.2290	.0000	.0000	-36.0391	36.0391
36.00	.00	7.2729	.0000	.0000	-36.2581	36.2581
37.00	.00	7.3183	.0000	.0000	-36.4842	36.4842
38.00	.00	7.3651	.0000	.0000	-36.7175	36.7175
39.00	.00	7.4134	.0000	.0000	-36.9584	36.9584
40.00	.00	7.4632	.0000	.0000	-37.2068	37.2068
41.00	.00	7.5146	.0000	.0000	-37.4629	37.4629
42.00	.00	7.5676	.0000	.0000	-37.7269	37.7269
43.00	.00	7.6221	.0000	.0000	-37.9989	37.9989
44.00	.00	7.6783	.0000	.0000	-38.2791	38.2791

Table 22 (contd)

Time, days	$\theta$ tilt, deg	$a_{SP}$ , $10^{11} \text{ km/s}^2$	$F_{SPx}$ , $10^6 \text{ N}$	$F_{SPy}$ , $10^6 \text{ N}$	$F_{SPz}$ , $10^6 \text{ N}$	$ F_{SP} $ , $10^6 \text{ N}$
45.00	.00	7.7362	.0000	.0000	-38.5677	38.5677
46.00	.00	7.7958	.0000	.0000	-38.8648	38.8648
47.00	.00	7.8572	.0000	.0000	-39.1706	39.1706
48.00	.00	7.9203	.0000	.0000	-39.4852	39.4852
49.00	.00	7.9852	.0000	.0000	-39.8089	39.8089
50.00	.00	8.0520	.0000	.0000	-40.1419	40.1419
51.00	.00	8.1207	.0000	.0000	-40.4843	40.4843
52.00	.00	8.1913	.0000	.0000	-40.8362	40.8362
53.00	.00	8.2638	.0000	.0000	-41.1980	41.1980
54.00	.00	8.3384	.0000	.0000	-41.5698	41.5698
55.00	.00	8.4150	.0000	.0000	-41.9518	41.9518
56.00	.00	8.4937	.0000	.0000	-42.3442	42.3442
57.00	.00	8.5746	.0000	.0000	-42.7472	42.7472
58.00	.00	8.6576	.0000	.0000	-43.1610	43.1610
59.00	.00	8.7428	.0000	.0000	-43.5858	43.5858
60.00	.00	8.8303	.0000	.0000	-44.0219	44.0219
61.00	.00	8.9200	.0000	.0000	-44.4693	44.4693
62.00	.00	9.0121	.0000	.0000	-44.9284	44.9284
63.00	.00	9.1066	.0000	.0000	-45.3993	45.3993
64.00	.00	9.2034	.0000	.0000	-45.8822	45.8822
65.00	.00	9.3028	.0000	.0000	-46.3775	46.3775
66.00	.00	9.4046	.0000	.0000	-46.8852	46.8852
67.00	.00	9.5090	.0000	.0000	-47.4055	47.4055
68.00	45.00	5.8809	.0000	-5.3389	-28.8279	29.3181
69.00	45.00	5.9476	.0000	-5.4017	-29.1547	29.6509
70.00	45.00	6.0160	.0000	-5.4661	-29.4894	29.9918
71.00	45.00	6.0860	.0000	-5.5321	-29.8321	30.3407
72.00	45.00	6.1576	.0000	-5.5997	-30.1827	30.6978
73.00	45.00	6.2309	.0000	-5.6689	-30.5415	31.0631
74.00	45.00	6.3058	.0000	-5.7397	-30.9084	31.4368
75.00	45.00	6.3825	.0000	-5.8121	-31.2833	31.8187
76.00	45.00	6.4608	.0000	-5.8862	-31.6666	32.2091
77.00	45.00	6.5407	.0000	-5.9620	-32.0582	32.6078
78.00	45.00	6.6224	.0000	-6.0394	-32.4580	33.0150
79.00	45.00	6.7058	.0000	-6.1185	-32.8660	33.4307
80.00	45.00	6.7908	.0000	-6.1992	-33.2822	33.8546
81.00	45.00	6.8775	.0000	-6.2816	-33.7066	34.2869
82.00	45.00	6.9659	.0000	-6.3655	-34.1389	34.7273
83.00	45.00	7.0559	.0000	-6.4512	-34.5793	35.1759
84.00	45.00	7.1474	.0000	-6.5384	-35.0274	35.6325
85.00	45.00	7.2406	.0000	-6.6271	-35.4832	36.0968
86.00	45.00	7.3352	.0000	-6.7174	-35.9464	36.5687
87.00	45.00	7.4314	.0000	-6.8092	-36.4168	37.0479
88.00	45.00	7.5289	.0000	-6.9024	-36.8940	37.5341
89.00	45.00	7.6276	.0000	-6.9970	-37.3778	38.0270
90.00	45.00	7.7279	.0000	-7.0929	-37.8677	38.5262
91.00	45.00	7.8292	.0000	-7.1899	-38.3632	39.0312
92.00	58.00	5.4736	.0000	-5.0476	-26.8177	27.2886

Table 22 (contd)

Time, days	$\theta$ tilt, deg	$a_{SP}$ , $10^{11} \text{ km/s}^2$	$F_{SPx}$ , $10^6 \text{ N}$	$F_{SPy}$ , $10^6 \text{ N}$	$F_{SPz}$ , $10^6 \text{ N}$	$ F_{SP} $ , $10^6 \text{ N}$
92.00	58.00	5.4394	.0000	-5.0143	-26.6497	27.1173
93.00	58.00	5.5083	.0000	-5.0810	-26.9864	27.4606
94.00	58.00	5.5801	.0000	-5.1507	-27.3377	27.8187
95.00	58.00	5.6550	.0000	-5.2235	-27.7041	28.1922
96.00	58.00	5.7331	.0000	-5.2995	-28.0861	28.5817
97.00	58.00	5.8145	.0000	-5.3787	-28.4841	28.9875
98.00	58.00	5.8994	.0000	-5.4614	-28.8988	29.4103
99.00	58.00	5.9877	.0000	-5.5476	-29.3306	29.8506
100.00	58.00	6.0797	.0000	-5.6375	-29.7802	30.3091
101.00	58.00	6.1754	.0000	-5.7311	-30.2481	30.7862
102.00	58.00	6.2749	.0000	-5.8287	-30.7348	31.2827
103.00	58.00	6.3785	.0000	-5.9303	-31.2411	31.7990
104.00	58.00	6.4862	.0000	-6.0361	-31.7674	32.3358
105.00	58.00	6.5981	.0000	-6.1463	-32.3144	32.8937
106.00	58.00	6.7144	.0000	-6.2608	-32.8826	33.4733
107.00	58.00	6.8351	.0000	-6.3800	-33.4726	34.0752
108.00	58.00	6.9604	.0000	-6.5040	-34.0850	34.7000
109.00	58.00	7.0904	.0000	-6.6327	-34.7201	35.3480
110.00	58.00	7.2252	.0000	-6.7664	-35.3786	36.0199
111.00	68.00	4.8852	.0000	-3.9399	-24.0334	24.3542
112.00	68.00	4.9807	.0000	-4.0225	-24.5024	24.8304
113.00	68.00	5.0795	.0000	-4.1080	-24.9875	25.3230
114.00	68.00	5.1816	.0000	-4.1966	-25.4889	25.8320
115.00	68.00	5.2870	.0000	-4.2883	-26.0064	26.3575
116.00	68.00	5.3957	.0000	-4.3830	-26.5401	26.8996
117.00	68.00	5.5077	.0000	-4.4809	-27.0898	27.4579
118.00	68.00	5.6229	.0000	-4.5818	-27.6552	28.0322
119.00	68.00	5.7413	.0000	-4.6856	-28.2360	28.6221
120.00	68.00	5.8626	.0000	-4.7924	-28.8313	29.2269
121.00	68.00	5.9867	.0000	-4.9019	-29.4405	29.8458
122.00	68.00	6.1135	.0000	-5.0141	-30.0626	30.4778
123.00	68.00	6.2427	.0000	-5.1287	-30.6963	31.1218
124.00	68.00	6.3739	.0000	-5.2454	-31.3401	31.7761
125.00	68.00	6.5069	.0000	-5.3639	-31.9924	32.4390
126.00	68.00	6.6411	.0000	-5.4839	-32.6510	33.1083
127.00	68.00	6.7762	.0000	-5.6050	-33.3136	33.7818
128.00	68.00	6.9116	.0000	-5.7266	-33.9774	34.4566
129.00	68.00	7.0466	.0000	-5.8482	-34.6395	35.1297
130.00	71.00	6.1301	.0000	-4.6975	-30.1974	30.5606
131.00	71.00	6.2428	.0000	-4.7919	-30.7511	31.1223
132.00	71.00	6.3532	.0000	-4.8846	-31.2939	31.6728
133.00	71.00	6.4607	.0000	-4.9751	-31.8221	32.2086
134.00	71.00	6.5644	.0000	-5.0626	-32.3317	32.7256
135.00	71.00	6.6635	.0000	-5.1464	-32.8187	33.2198
136.00	71.00	6.7572	.0000	-5.2258	-33.2790	33.6869

Table 22 (contd)

Time, days	$\theta$ tilt, deg	$a_{SP}$ , $10^{11} \text{ km/s}^2$	$F_{SPx}$ , $10^6 \text{ N}$	$F_{SPy}$ , $10^6 \text{ N}$	$F_{SPz}$ , $10^6 \text{ N}$	$ F_{SP} $ , $10^6 \text{ N}$
137.00	71.00	6.8446	.0000	-5.3000	-33.7085	34.1226
138.00	71.00	6.9249	.0000	-5.3683	-34.1030	34.5229
139.00	71.00	6.9972	.0000	-5.4300	-34.4584	34.8836
140.00	71.00	7.0609	.0000	-5.4843	-34.7710	35.2009
141.00	71.00	7.1151	.0000	-5.5306	-35.0374	35.4713
142.00	71.00	7.1593	.0000	-5.5684	-35.2545	35.6916
143.00	71.00	7.1929	.0000	-5.5972	-35.4197	35.8593
144.00	71.00	7.2156	.0000	-5.6166	-35.5311	35.9723
145.00	71.00	7.2270	.0000	-5.6264	-35.5872	36.0293
146.00	71.00	7.2271	.0000	-5.6264	-35.5874	36.0295
147.00	71.00	7.2157	.0000	-5.6167	-35.5317	35.9729
148.00	71.00	7.1932	.0000	-5.5974	-35.4208	35.8603
149.00	71.00	7.1596	.0000	-5.5687	-35.2559	35.6930
150.00	71.00	7.1155	.0000	-5.5309	-35.0392	35.4731
151.00	71.00	7.0613	.0000	-5.4847	-34.7732	35.2031
152.00	71.00	6.9977	.0000	-5.4304	-34.4609	34.8861
153.00	71.00	6.9254	.0000	-5.3688	-34.1057	34.5257
154.00	71.00	6.8452	.0000	-5.3006	-33.7116	34.1257
155.00	71.00	6.7579	.0000	-5.2264	-33.2823	33.6902
156.00	71.00	6.6642	.0000	-5.1470	-32.8222	33.2233
157.00	71.00	6.5651	.0000	-5.0632	-32.3353	32.7294
158.00	71.00	6.4614	.0000	-4.9758	-31.8259	32.2125
159.00	71.00	6.3540	.0000	-4.8853	-31.2979	31.6769
160.00	71.00	6.2436	.0000	-4.7926	-30.7552	31.1264
161.00	71.00	6.1309	.0000	-4.6982	-30.2015	30.5647
162.00	71.00	6.0167	.0000	-4.6028	-29.6402	29.9955
163.00	71.00	5.9017	.0000	-4.5070	-29.0745	29.4217
164.00	71.00	5.7863	.0000	-4.4111	-28.5073	28.8466
165.00	71.00	5.6711	.0000	-4.3156	-27.9411	28.2724
166.00	71.00	5.5566	.0000	-4.2210	-27.3782	27.7017
167.00	71.00	5.4433	.0000	-4.1276	-26.8208	27.1365
168.00	71.00	5.3313	.0000	-4.0356	-26.2704	26.5786
169.00	71.00	5.2212	.0000	-3.9453	-25.7287	26.0295
170.00	71.00	5.1131	.0000	-3.8569	-25.1970	25.4904
171.00	71.00	5.0072	.0000	-3.7706	-24.6762	24.9626
172.00	71.00	4.9037	.0000	-3.6864	-24.1672	24.4468
173.00	71.00	4.8028	.0000	-3.6045	-23.6707	23.9436

Table 23. Coordinates of centers of mass of magnetometer sunshades

i	$x_{Gi}$ , m	$y_{Gi}$ , m	$z_{Gi}$ , m	Area, $m^2$
1	-0.2555	-4.5735	0.340	0.0605
2	-0.2550	-6.840	0.340	0.0877
3	-0.2805	-4.214	0.340	0.1084

Table 24. Coordinates of centers of mass of IRR sunshades

Shade	$x_{RC}$ , cm	$y_{RC}$ , cm	$z_{RC}$ , cm	Area, $m^2$
1	-47.25	-87.825	73.40	0.0406
2	-58.625	-96.95	68.60	0.0299

Table 25. Components of the solar radiation force and torque on adiabatic surfaces

Time, days	$a_{AD}$ , $10^{11} \text{ km/s}^2$	$F_{ADx}$ , $10^6 \text{ N}$	$F_{ADy}$ , $10^6 \text{ N}$	$F_{ADz}$ , $10^6 \text{ N}$	$M_{ADx}^{(C)}$ , $10^6 \text{ N}\cdot\text{m}$	$M_{ADy}^{(C)}$ , $10^6 \text{ N}\cdot\text{m}$	$M_{ADz}^{(C)}$ , $10^6 \text{ N}\cdot\text{m}$	$ F_{AD} $ , $10^6 \text{ N}$	$ M_{AD}^{(C)} $ , $10^6 \text{ N}\cdot\text{m}$
.00	5.8392	.0400	.0319	-29.1105	24.0338	-1.8108	.0201	29.1105	24.1020
1.00	5.8435	.0400	.0319	-29.1317	24.0513	-1.8121	.0201	29.1317	24.1195
2.00	5.8486	.0401	.0319	-29.1572	24.0724	-1.8137	.0202	29.1572	24.1406
3.00	5.8546	.0401	.0320	-29.1869	24.0969	-1.8155	.0202	29.1870	24.1653
4.00	5.8614	.0402	.0320	-29.2209	24.1250	-1.8176	.0202	29.2210	24.1934
5.00	5.8691	.0402	.0320	-29.2593	24.1567	-1.8200	.0202	29.2593	24.2252
6.00	5.8776	.0403	.0321	-29.3019	24.1919	-1.8227	.0203	29.3020	24.2605
7.00	5.8871	.0403	.0321	-29.3490	24.2307	-1.8256	.0203	29.3490	24.2994
8.00	5.8974	.0404	.0322	-29.4004	24.2732	-1.8288	.0203	29.4004	24.3420
9.00	5.9086	.0405	.0323	-29.4562	24.3192	-1.8323	.0204	29.4562	24.3882
10.00	5.9206	.0406	.0323	-29.5164	24.3690	-1.8360	.0204	29.5164	24.4381
11.00	5.9336	.0407	.0324	-29.5811	24.4224	-1.8400	.0204	29.5812	24.4916
12.00	5.9475	.0408	.0325	-29.6503	24.4796	-1.8443	.0205	29.6504	24.5489
13.00	5.9623	.0409	.0326	-29.7241	24.5405	-1.8489	.0205	29.7241	24.6100
14.00	5.9780	.0410	.0326	-29.8025	24.6052	-1.8538	.0206	29.8025	24.6749
15.00	5.9947	.0411	.0327	-29.8655	24.6737	-1.8590	.0207	29.8855	24.7436
16.00	6.0123	.0412	.0328	-29.9732	24.7461	-1.8644	.0207	29.9732	24.8162
17.00	6.0308	.0413	.0329	-30.0656	24.8224	-1.8702	.0208	30.0656	24.8927
18.00	6.0503	.0415	.0330	-30.1628	24.9026	-1.8762	.0208	30.1628	24.9732
19.00	6.0708	.0416	.0331	-30.2648	24.9869	-1.8826	.0209	30.2649	25.0577
20.00	6.0922	.0417	.0333	-30.3718	25.0752	-1.8892	.0210	30.3718	25.1463
21.00	6.1147	.0419	.0334	-30.4837	25.1676	-1.8962	.0211	30.4838	25.2389
22.00	6.1381	.0421	.0335	-30.6007	25.2642	-1.9035	.0212	30.6007	25.3358
23.00	6.1626	.0422	.0337	-30.7227	25.3649	-1.9111	.0212	30.7228	25.4368
24.00	6.1881	.0424	.0338	-30.8499	25.4700	-1.9190	.0213	30.8500	25.5422
25.00	6.2147	.0426	.0339	-30.9624	25.5793	-1.9272	.0214	30.9625	25.6518
26.00	6.2424	.0428	.0341	-31.1202	25.6931	-1.9358	.0215	31.1202	25.7659
27.00	6.2711	.0430	.0342	-31.2634	25.8113	-1.9447	.0216	31.2634	25.8845
28.00	6.3009	.0432	.0344	-31.4121	25.9340	-1.9539	.0217	31.4121	26.0076
29.00	6.3318	.0434	.0346	-31.5663	26.0614	-1.9635	.0218	31.5663	26.1353
30.00	6.3639	.0436	.0347	-31.7262	26.1934	-1.9735	.0219	31.7263	26.2677
31.00	6.3971	.0438	.0349	-31.8919	26.3302	-1.9838	.0220	31.8919	26.4048
32.00	6.4315	.0441	.0351	-32.0634	26.4718	-1.9944	.0222	32.0634	26.5468
33.00	6.4671	.0443	.0353	-32.2408	26.6183	-2.0055	.0223	32.2409	26.6937
34.00	6.5040	.0446	.0355	-32.4244	26.7698	-2.0169	.0224	32.4244	26.8457
35.00	6.5420	.0448	.0357	-32.6141	26.9264	-2.0287	.0225	32.6141	27.0028
36.00	6.5813	.0451	.0359	-32.8100	27.0882	-2.0409	.0227	32.8101	27.1650
37.00	6.6219	.0454	.0362	-33.0124	27.2553	-2.0535	.0228	33.0124	27.3325
38.00	6.6638	.0457	.0364	-33.2212	27.4277	-2.0665	.0230	33.2213	27.5054
39.00	6.7070	.0460	.0366	-33.4367	27.6056	-2.0799	.0231	33.4367	27.6838
40.00	6.7516	.0463	.0369	-33.6589	27.7891	-2.0937	.0233	33.6589	27.8678
41.00	6.7975	.0466	.0371	-33.8880	27.9782	-2.1079	.0234	33.8881	28.0575
42.00	6.8449	.0469	.0374	-34.1241	28.1732	-2.1226	.0236	34.1242	28.2530
43.00	6.8937	.0472	.0376	-34.3674	28.3740	-2.1378	.0238	34.3675	28.4544
44.00	6.9440	.0476	.0379	-34.6180	28.5809	-2.1533	.0239	34.6180	28.6619

ORIGINAL PAGE IS  
OF POOR QUALITY

Table 25 (contd)

Time, days	$a_{AD}$ , $10^{11} \text{ km/s}^2$	$F_{ADx}$ , $10^6 \text{ N}$	$F_{ADy}$ , $10^6 \text{ N}$	$F_{ADz}$ , $10^6 \text{ N}$	$M_{ADx}^{(C)}$ , $10^6 \text{ N}\cdot\text{m}$	$M_{ADy}^{(C)}$ , $10^6 \text{ N}\cdot\text{m}$	$M_{ADz}^{(C)}$ , $10^6 \text{ N}\cdot\text{m}$	$ F_{AD} $ , $10^6 \text{ N}$	$ M_{AD}^{(C)} $ , $10^6 \text{ N}\cdot\text{m}$
45.00	6.9957	.0479	.0382	-34.8760	28.7939	-2.1694	.0241	34.8760	28.8755
46.00	7.0490	.0483	.0385	-35.1415	29.0131	-2.1859	.0243	35.1416	29.0954
47.00	7.1038	.0487	.0388	-35.4148	29.2388	-2.2029	.0245	35.4149	29.3217
48.00	7.1602	.0491	.0391	-35.6960	29.4709	-2.2204	.0247	35.6960	29.5544
49.00	7.2182	.0495	.0394	-35.9852	29.7097	-2.2384	.0249	35.9853	29.7939
50.00	7.2779	.0499	.0397	-36.2827	29.9553	-2.2569	.0251	36.2827	30.0402
51.00	7.3392	.0503	.0401	-36.5885	30.2077	-2.2759	.0253	36.5885	30.2934
52.00	7.4023	.0507	.0404	-36.8928	30.4673	-2.2955	.0255	36.9029	30.5536
53.00	7.4671	.0512	.0408	-37.2258	30.7340	-2.3156	.0257	37.2259	30.8211
54.00	7.5336	.0516	.0411	-37.5577	31.0080	-2.3362	.0260	37.5578	31.0959
55.00	7.6020	.0521	.0415	-37.8987	31.2895	-2.3574	.0262	37.8987	31.3782
56.00	7.6723	.0526	.0419	-38.2489	31.5786	-2.3792	.0264	38.2489	31.6681
57.00	7.7444	.0531	.0423	-38.6084	31.8754	-2.4016	.0267	38.6085	31.9658
58.00	7.8185	.0536	.0427	-38.9776	32.1802	-2.4245	.0269	38.9777	32.2714
59.00	7.8945	.0541	.0431	-39.3565	32.4930	-2.4481	.0272	39.3565	32.5851
60.00	7.9724	.0546	.0435	-39.7453	32.8140	-2.4723	.0275	39.7453	32.9070
61.00	8.0525	.0552	.0440	-40.1442	33.1434	-2.4971	.0277	40.1443	33.2373
62.00	8.1345	.0557	.0444	-40.5534	33.4812	-2.5226	.0280	40.5535	33.5761
63.00	8.2187	.0563	.0449	-40.9731	33.8277	-2.5487	.0283	40.9731	33.9236
64.00	8.3050	.0569	.0453	-41.4033	34.1829	-2.5754	.0286	41.4034	34.2798
65.00	8.3935	.0575	.0458	-41.8444	34.5471	-2.6029	.0289	41.8445	34.6450
66.00	8.4842	.0581	.0463	-42.2966	34.9204	-2.6310	.0292	42.2966	35.0194
67.00	8.5771	.0588	.0468	-42.7598	35.3028	-2.6698	.0296	42.7598	35.4029
68.00	8.6723	.0594	.0474	-43.2343	35.6946	-2.6893	.0299	43.2343	35.7957
69.00	8.7698	.0601	.0479	-43.7202	36.0958	-2.7195	.0302	43.7203	36.1981
70.00	8.8696	.0608	.0484	-44.2177	36.5065	-2.7505	.0306	44.2178	36.6100
71.00	8.9717	.0615	.0490	-44.7269	36.9269	-2.7822	.0309	44.7270	37.0316
72.00	9.0762	.0622	.0496	-45.2479	37.3570	-2.8146	.0313	45.2480	37.4629
73.00	9.1831	.0629	.0501	-45.7809	37.7971	-2.8477	.0316	45.7809	37.9042
74.00	9.2924	.0637	.0507	-46.3258	38.2470	-2.8816	.0320	46.3259	38.3554
75.00	9.4041	.0644	.0514	-46.8827	38.7068	-2.9163	.0324	46.8828	38.8165
76.00	9.5183	.0652	.0520	-47.4519	39.1766	-2.9517	.0328	47.4519	39.2877
77.00	9.6349	.0660	.0526	-48.0331	39.6565	-2.9878	.0332	48.0332	39.7689
78.00	9.7539	.0668	.0533	-48.6265	40.1464	-3.0247	.0336	48.6266	40.2602
79.00	9.8754	.0677	.0539	-49.2320	40.6463	-3.0624	.0340	49.2320	40.7615
80.00	9.9992	.0685	.0546	-49.8495	41.1562	-3.1008	.0345	49.8496	41.2728
81.00	10.1255	.0694	.0553	-50.4790	41.6759	-3.1400	.0349	50.4791	41.7940
82.00	10.2541	.0703	.0560	-51.1202	42.2052	-3.1798	.0353	51.1203	42.3249
83.00	10.3851	.0712	.0567	-51.7731	42.7443	-3.2205	.0358	51.7732	42.8655
84.00	10.5184	.0721	.0574	-52.4375	43.2928	-3.2618	.0362	52.4376	43.4155
85.00	10.6539	.0730	.0582	-53.1130	43.8505	-3.3038	.0367	53.1131	43.9748
86.00	10.7915	.0740	.0589	-53.7993	44.4172	-3.3465	.0372	53.7994	44.5431
87.00	10.9313	.0749	.0597	-54.4962	44.9925	-3.3898	.0377	54.4962	45.1200
88.00	11.0731	.0759	.0605	-55.2030	45.5760	-3.4338	.0382	55.2031	45.7052
89.00	11.2168	.0769	.0612	-55.9194	46.1675	-3.4784	.0386	55.9194	46.2983
90.00	11.3623	.0779	.0620	-56.6447	46.7663	-3.5235	.0392	56.6448	46.8989
91.00	11.5094	.0789	.0628	-57.3781	47.3719	-3.5691	.0397	57.3782	47.5061
92.00	11.6581	.0799	.0637	-58.1193	47.9838	-3.6152	.0402	58.1194	48.1198

ORIGINAL PAGE IS  
OF POOR QUALITY

Table 25 (contd)

Time, days	$a_{AD}$ , $10^{11} \text{ km/s}^2$	$F_{ADx}$ , $10^6 \text{ N}$	$F_{ADy}$ , $10^6 \text{ N}$	$F_{ADz}$ , $10^6 \text{ N}$	$M_{ADx}^{(C)}$ , $10^6 \text{ N}\cdot\text{m}$	$M_{ADy}^{(C)}$ , $10^6 \text{ N}\cdot\text{m}$	$M_{ADz}^{(C)}$ , $10^6 \text{ N}\cdot\text{m}$	$ \bar{F}_{AD} $ , $10^6 \text{ N}$	$ \bar{M}_{AD}^{(C)} $ , $10^6 \text{ N}\cdot\text{m}$
92.00	11.5855	.0794	.0633	-57.7576	47.6852	-3.5927	.0399	57.7577	47.8203
93.00	11.7309	.0804	.0641	-58.4823	48.2835	-3.6378	.0404	58.4824	48.4203
94.00	11.8425	.0814	.0649	-59.2381	48.9075	-3.6848	.0409	59.2382	49.0461
95.00	12.0406	.0825	.0657	-60.0263	49.5582	-3.7338	.0415	60.0264	49.6987
96.00	12.2054	.0836	.0666	-60.8478	50.2365	-3.7849	.0421	60.8479	50.3789
97.00	12.3771	.0848	.0676	-61.7038	50.9432	-3.8382	.0426	61.7039	51.0876
98.00	12.5559	.0860	.0686	-62.5954	51.6793	-3.8936	.0433	62.5955	51.8258
99.00	12.7421	.0873	.0696	-63.5237	52.4457	-3.9514	.0439	63.5238	52.5944
100.00	12.9360	.0886	.0706	-64.4901	53.2435	-4.0115	.0446	64.4902	53.3945
101.00	13.1376	.0900	.0717	-65.4955	54.0736	-4.0740	.0453	65.4956	54.2269
102.00	13.3474	.0915	.0729	-66.5412	54.9370	-4.1391	.0460	66.5413	55.0927
103.00	13.5655	.0930	.0741	-67.6287	55.8348	-4.2067	.0467	67.6288	55.9930
104.00	13.7922	.0945	.0753	-68.7589	56.7679	-4.2770	.0475	68.7590	56.9288
105.00	14.0278	.0961	.0766	-69.9334	57.7375	-4.3501	.0483	69.9335	57.9012
106.00	14.2725	.0978	.0779	-71.1530	58.7445	-4.4259	.0492	71.1532	58.9110
107.00	14.5264	.0995	.0793	-72.4192	59.7898	-4.5047	.0501	72.4193	59.9593
108.00	14.7900	.1014	.0808	-73.7331	60.8746	-4.5864	.0510	73.7332	61.0472
109.00	15.0633	.1032	.0823	-75.0953	61.9993	-4.6712	.0519	75.0954	62.1750
110.00	15.3465	.1052	.0838	-76.5075	63.1652	-4.7590	.0529	76.5076	63.3442
111.00	15.6398	.1072	.0854	-77.9698	64.3725	-4.8500	.0539	77.9699	64.5549
112.00	15.9435	.1093	.0871	-79.4834	65.6222	-4.9441	.0549	79.4835	65.8082
113.00	16.2575	.1114	.0888	-81.0488	66.9146	-5.0415	.0560	81.0489	67.1042
114.00	16.5819	.1136	.0905	-82.6663	68.2499	-5.1421	.0571	82.6664	68.4434
115.00	16.9167	.1159	.0924	-84.3355	69.6281	-5.2459	.0583	84.3357	69.8255
116.00	17.2620	.1183	.0943	-86.0569	71.0492	-5.3530	.0595	86.0570	71.2506
117.00	17.6176	.1207	.0962	-87.8295	72.5127	-5.4633	.0607	87.8296	72.7183
118.00	17.9832	.1232	.0982	-89.6524	74.0177	-5.5767	.0620	89.6525	74.2275
119.00	18.3587	.1258	.1002	-91.5241	75.5631	-5.6931	.0633	91.5243	75.7772
120.00	18.7435	.1284	.1023	-93.4428	77.1471	-5.8124	.0646	93.4429	77.3658
121.00	19.1372	.1311	.1045	-95.4054	78.7675	-5.9345	.0659	95.4055	78.9907
122.00	19.5392	.1339	.1067	-97.4093	80.4219	-6.0592	.0673	97.4094	80.6499
123.00	19.9486	.1367	.1089	-99.4503	82.1069	-6.1861	.0687	99.4504	82.3397
124.00	20.3644	.1396	.1112	-101.5235	83.8186	-6.3151	.0702	101.5236	84.0562
125.00	20.7856	.1424	.1135	-103.6233	85.5522	-6.4457	.0716	103.6234	85.7947
126.00	21.2108	.1454	.1158	-105.7430	87.3023	-6.5776	.0731	105.7432	87.5498
127.00	21.6385	.1483	.1182	-107.8751	89.0626	-6.7102	.0746	107.8753	89.3150
128.00	22.0668	.1512	.1205	-110.0106	90.8256	-6.8430	.0760	110.0107	91.0831
129.00	22.4940	.1541	.1228	-112.1402	92.5838	-6.9755	.0775	112.1403	92.8463
130.00	22.9178	.1571	.1251	-114.2528	94.3281	-7.1069	.0790	114.2530	94.5954
131.00	23.3358	.1599	.1274	-116.3367	96.0485	-7.2365	.0804	116.3369	96.3208
132.00	23.7454	.1627	.1297	-118.3789	97.7346	-7.3635	.0818	118.3791	98.0116
133.00	24.1440	.1655	.1318	-120.3657	99.3749	-7.4871	.0832	120.3659	99.6566
134.00	24.5285	.1681	.1339	-122.2825	100.9574	-7.6064	.0845	122.2827	101.2436
135.00	24.8959	.1706	.1359	-124.1142	102.4697	-7.7203	.0858	124.1144	102.7601
136.00	25.2431	.1730	.1378	-125.8452	103.8988	-7.8280	.0870	125.8454	104.1933

Table 26. Total force and torque on Mariner Venus/Mercury spacecraft

Time, days	$a_R$ , $10^{11} \text{ km/s}^2$	$F_{Rx}$ , $10^6 \text{ N}$	$F_{Ry}$ , $10^6 \text{ N}$	$F_{Rz}$ , $10^6 \text{ N}$	$M_{Rx}^{(C)}$ , $10^6 \text{ N}\cdot\text{m}$	$M_{Ry}^{(C)}$ , $10^6 \text{ N}\cdot\text{m}$	$M_{Rz}^{(C)}$ , $10^6 \text{ N}\cdot\text{m}$	$ \bar{F}_R $ , $10^6 \text{ N}$	$ \bar{M}_R^{(C)} $ , $10^6 \text{ N}\cdot\text{m}$
.00	12.4707	.0400	.0950	-62.1705	21.9922	-1.8108	.0201	62.1706	22.0667
1.00	12.4798	.0400	.0950	-62.2161	22.0083	-1.8121	.0201	62.2161	22.0827
2.00	12.4908	.0401	.0951	-62.2708	22.0275	-1.8137	.0202	62.2709	22.1021
3.00	12.5036	.0401	.0952	-62.3346	22.0500	-1.8155	.0202	62.3347	22.1246
4.00	12.5183	.0402	.0954	-62.4077	22.0757	-1.8176	.0202	62.4078	22.1504
5.00	12.5415	.0402	.0977	-62.5235	22.0286	-1.8200	.0202	62.5236	22.1037
6.00	12.5698	.0403	.1010	-62.6644	21.9489	-1.8227	.0203	62.6645	22.0244
7.00	12.6003	.0403	.1045	-62.8165	21.8681	-1.8256	.0203	62.8166	21.9442
8.00	12.6330	.0404	.1081	-62.9799	21.7862	-1.8288	.0203	62.9800	21.8628
9.00	12.6681	.0405	.1118	-63.1547	21.7030	-1.8323	.0204	63.1548	21.7803
10.00	12.7055	.0406	.1156	-63.3410	21.6186	-1.8360	.0204	63.3411	21.6965
11.00	12.7452	.0407	.1196	-63.5389	21.5328	-1.8400	.0204	63.5391	21.6113
12.00	12.7973	.0408	.1236	-63.7487	21.4455	-1.8443	.0205	63.7489	21.5246
13.00	12.8318	.0409	.1278	-63.9705	21.3564	-1.8489	.0205	63.9707	21.4363
14.00	12.8787	.0410	.1322	-64.2445	21.2654	-1.8538	.0206	64.2047	21.3461
15.00	12.9281	.0411	.1366	-64.4509	21.1724	-1.8590	.0207	64.4511	21.2539
16.00	12.9801	.0412	.1412	-64.7099	21.0772	-1.8644	.0207	64.7101	21.1595
17.00	13.0346	.0413	.1460	-64.9818	20.9794	-1.8702	.0208	64.9819	21.0627
18.00	13.0918	.0415	.1509	-65.2667	20.8791	-1.8762	.0208	65.2669	20.9632
19.00	13.1516	.0416	.1559	-65.5649	20.7758	-1.8826	.0209	65.5651	20.8609
20.00	13.2141	.0417	.1611	-65.8767	20.6694	-1.8892	.0210	65.8769	20.7555
21.00	13.2795	.0419	.1664	-66.2024	20.5596	-1.8962	.0211	66.2027	20.6469
22.00	13.3476	.0421	.1719	-66.5423	20.4462	-1.9035	.0212	66.5425	20.5346
23.00	13.4187	.0422	.1775	-66.8966	20.3290	-1.9111	.0212	66.8969	20.4186
24.00	13.4928	.0424	.1833	-67.2658	20.2076	-1.9190	.0213	67.2660	20.2985
25.00	13.5698	.0426	.1893	-67.6500	20.0818	-1.9272	.0214	67.6503	20.1741
26.00	13.6500	.0428	.1954	-68.0497	19.9515	-1.9358	.0215	68.0500	20.0452
27.00	13.7334	.0430	.2017	-68.4652	19.8162	-1.9447	.0216	68.4655	19.9114
28.00	13.8200	.0432	.2082	-68.8969	19.6758	-1.9539	.0217	68.8972	19.7726
29.00	13.9099	.0434	.2149	-69.3451	19.5300	-1.9635	.0218	69.3454	19.6285
30.00	14.0032	.0436	.2217	-69.8102	19.3786	-1.9735	.0219	69.8106	19.4789
31.00	14.0999	.0438	.2286	-70.2926	19.2215	-1.9838	.0220	70.2930	19.3236
32.00	14.2003	.0441	.2358	-70.7927	19.0584	-1.9944	.0222	70.7931	19.1625
33.00	14.3042	.0443	.2430	-71.3108	18.8892	-2.0055	.0223	71.3112	18.9954
34.00	14.4119	.0446	.2505	-71.8476	18.7136	-2.0169	.0224	71.8480	18.8220
35.00	14.5232	.0448	.2580	-72.4027	18.5323	-2.0287	.0225	72.4032	18.6430
36.00	14.6384	.0451	.2656	-72.9769	18.3450	-2.0409	.0227	72.9774	18.4582
37.00	14.7574	.0454	.2734	-73.5702	18.1522	-2.0535	.0228	73.5707	18.2680
38.00	14.8803	.0457	.2811	-74.1827	17.9544	-2.0665	.0230	74.1833	18.0730
39.00	15.0070	.0460	.2889	-74.8142	17.7529	-2.0799	.0231	74.8148	17.8743
40.00	15.1373	.0463	.2965	-75.4639	17.5496	-2.0937	.0233	75.4645	17.6741
41.00	15.2713	.0466	.3040	-76.1319	17.3453	-2.1079	.0234	76.1325	17.4730
42.00	15.4090	.0469	.3112	-76.8183	17.1402	-2.1226	.0236	76.8189	17.2712
43.00	15.5504	.0472	.3183	-77.5234	16.9347	-2.1378	.0238	77.5241	17.0691
44.00	15.6957	.0476	.3250	-78.2475	16.7290	-2.1533	.0239	78.2482	16.8671

Table 26 (contd)

Time, days	$a_R$ , $10^{11} \text{ km/s}^2$	$F_{Rx}$ , $10^6 \text{ N}$	$F_{Ry}$ , $10^6 \text{ N}$	$F_{Rz}$ , $10^6 \text{ N}$	$M_{Rx'}^{(C)}$ , $10^6 \text{ N.m}$	$M_{Ry'}^{(C)}$ , $10^6 \text{ N.m}$	$M_{Rz'}^{(C)}$ , $10^6 \text{ N.m}$	$ F_R $ , $10^6 \text{ N}$	$\left M_R^{(C)}\right $ , $10^6 \text{ N.m}$
45.00	15.8448	.0479	.3314	-78.9908	16.5237	-2.1694	.0241	78.9915	16.6655
46.00	15.9977	.0483	.3373	-79.7533	16.3192	-2.1859	.0243	79.7541	16.4649
47.00	16.1546	.0487	.3429	-80.5354	16.1160	-2.2029	.0245	80.5362	16.2658
48.00	16.3154	.0491	.3480	-81.3369	15.9150	-2.2204	.0247	81.3377	16.0691
49.00	16.4802	.0495	.3525	-82.1585	15.7162	-2.2384	.0249	82.1593	15.8748
50.00	16.6490	.0499	.3564	-83.0000	15.5207	-2.2569	.0251	83.0008	15.6839
51.00	16.8218	.0503	.3598	-83.8615	15.3292	-2.2759	.0253	83.8623	15.4973
52.00	16.9966	.0507	.3624	-84.7431	15.1426	-2.2955	.0255	84.7438	15.3156
53.00	17.1795	.0512	.3642	-85.6447	14.9617	-2.3156	.0257	85.6455	15.1399
54.00	17.3644	.0516	.3654	-86.5665	14.7875	-2.3362	.0260	86.5672	14.9709
55.00	17.5533	.0521	.3657	-87.5083	14.6209	-2.3574	.0262	87.5091	14.8098
56.00	17.7463	.0526	.3651	-88.4704	14.4626	-2.3792	.0264	88.4711	14.6570
57.00	17.9432	.0531	.3637	-89.4523	14.3144	-2.4016	.0267	89.4530	14.5145
58.00	18.1442	.0536	.3614	-90.4544	14.1766	-2.4245	.0269	90.4552	14.3825
59.00	18.3492	.0541	.3583	-91.4762	14.0508	-2.4481	.0272	91.4769	14.2625
60.00	18.5581	.0546	.3543	-92.5177	13.9378	-2.4723	.0275	92.5184	14.1554
61.00	18.7709	.0552	.3495	-93.5789	13.8387	-2.4971	.0277	93.5796	14.0622
62.00	18.9877	.0557	.3440	-94.6596	13.7546	-2.5226	.0280	94.6602	13.9840
63.00	19.2084	.0563	.3379	-95.7597	13.6864	-2.5487	.0283	95.7603	13.9217
64.00	19.4326	.0569	.3312	-96.8787	13.6352	-2.5754	.0286	96.8793	13.8764
65.00	19.6612	.0575	.3241	-98.0172	13.6017	-2.6029	.0289	98.0177	13.8486
66.00	19.8933	.0581	.3168	-99.1745	13.5869	-2.6310	.0292	99.1750	13.8393
67.00	20.1292	.0588	.3096	-100.3504	13.5913	-2.6598	.0296	100.3509	13.8492
68.00	16.5661	.0594	-5.0361	-82.4340	13.6156	-2.6893	.0299	82.5877	13.8787
69.00	16.7659	.0601	-5.1052	-83.4275	13.6603	-2.7195	.0302	83.5835	13.9284
70.00	16.9682	.0608	-5.1748	-84.4337	13.7256	-2.7505	.0306	84.5922	13.9985
71.00	17.1730	.0615	-5.2445	-85.4526	13.8117	-2.7822	.0309	85.6134	14.0892
72.00	17.3803	.0622	-5.3140	-86.4837	13.9191	-2.8146	.0313	86.6469	14.2008
73.00	17.5900	.0629	-5.3830	-87.5270	14.0477	-2.8477	.0316	87.6924	14.3335
74.00	17.8021	.0637	-5.4511	-88.5320	14.1982	-2.8816	.0320	88.7496	14.4877
75.00	18.0164	.0644	-5.5182	-89.6483	14.3709	-2.9163	.0324	89.8180	14.6638
76.00	18.2330	.0652	-5.5843	-90.7259	14.5666	-2.9517	.0328	90.8976	14.8627
77.00	18.4517	.0660	-5.6495	-91.8144	14.7864	-2.9878	.0332	91.9881	15.0853
78.00	18.6726	.0668	-5.7138	-92.9135	15.0313	-3.0247	.0336	93.0890	15.3326
79.00	18.8954	.0677	-5.7777	-94.0228	15.3025	-3.0624	.0340	94.2001	15.6059
80.00	19.1203	.0685	-5.8414	-95.1418	15.6013	-3.1008	.0345	95.3210	15.9065
81.00	19.3470	.0694	-5.9051	-96.2703	15.9289	-3.1400	.0349	96.4512	16.2355
82.00	19.5754	.0703	-5.9693	-97.4074	16.2862	-3.1798	.0353	97.5901	16.5939
83.00	19.8056	.0712	-6.0341	-98.5529	16.6746	-3.2205	.0358	98.7375	16.9828
84.00	20.0373	.0721	-6.0999	-99.7061	17.0949	-3.2618	.0362	99.8925	17.4034
85.00	20.2704	.0730	-6.1668	-100.8063	17.5479	-3.3038	.0367	101.0546	17.8562
86.00	20.5047	.0740	-6.2352	-102.0327	18.0343	-3.3465	.0372	102.2230	18.3422
87.00	20.7402	.0749	-6.3050	-103.2044	18.5548	-3.3898	.0377	103.3968	18.8620
88.00	20.9765	.0759	-6.3765	-104.3804	19.1099	-3.4338	.0382	104.5750	19.4160
89.00	21.2135	.0769	-6.4499	-105.5597	19.7001	-3.4784	.0386	105.7566	20.0049
90.00	21.4510	.0779	-6.5252	-106.7410	20.3258	-3.5235	.0392	106.9403	20.6290
91.00	21.6865	.0789	-6.6024	-107.9229	20.9869	-3.5691	.0397	108.1247	21.2863
92.00	21.94890	.0799	-6.4413	-97.0579	21.6842	-3.6152	.0402	97.1595	21.9836

**ORIGINAL PAGE IS  
OF POOR QUALITY**

Table 26 (contd)

Time, days	$a_R$ , $10^{11} \text{ km/s}^2$	$F_{Rx}$ , $10^6 \text{ N}$	$F_{Ry}$ , $10^6 \text{ N}$	$F_{Rz}$ , $10^6 \text{ N}$	$M_{Rx}^{(C)}$ , $10^6 \text{ N}\cdot\text{m}$	$M_{Ry}^{(C)}$ , $10^6 \text{ N}\cdot\text{m}$	$M_{Rz}^{(C)}$ , $10^6 \text{ N}\cdot\text{m}$	$ F_R $ , $10^6 \text{ N}$	$ M_R^{(C)} $ , $10^6 \text{ N}\cdot\text{m}$
92.00	19.4324	.0794	-4.4271	-96.7758	20.9194	-3.5927	.0399	96.8770	21.2257
93.00	19.6504	.0804	-4.4782	-97.8616	21.4361	-3.6378	.0404	97.9640	21.7426
94.00	19.8771	.0814	-4.5321	-98.9902	21.9840	-3.6848	.0409	99.0939	22.2907
95.00	20.1126	.0825	-4.5889	-100.1630	22.5652	-3.7338	.0415	100.2681	22.8720
96.00	20.3573	.0836	-4.6488	-101.3813	23.1810	-3.7849	.0421	101.4878	23.4880
97.00	20.6113	.0848	-4.7119	-102.6461	23.8333	-3.8382	.0426	102.7543	24.1404
98.00	20.8749	.0860	-4.7785	-103.9589	24.5240	-3.8936	.0433	104.0687	24.8312
99.00	21.1485	.0873	-4.8486	-105.3207	25.2552	-3.9514	.0439	105.4323	25.5624
100.00	21.4321	.0886	-4.9226	-106.7330	26.0291	-4.0115	.0446	106.8465	26.3364
101.00	21.7262	.0900	-5.0005	-108.1967	26.8476	-4.0740	.0453	108.3123	27.1550
102.00	22.0308	.0915	-5.0826	-109.7132	27.7136	-4.1391	.0460	109.8309	28.0210
103.00	22.3462	.0930	-5.1690	-111.2836	28.6296	-4.2067	.0467	111.4036	28.9370
104.00	22.6727	.0945	-5.2601	-112.9088	29.5983	-4.2770	.0475	113.0313	29.9057
105.00	23.0105	.0961	-5.3560	-114.5900	30.6229	-4.3501	.0483	114.7152	30.9304
106.00	23.3597	.0978	-5.4570	-116.3280	31.7062	-4.4259	.0492	116.4559	32.0137
107.00	23.7204	.0995	-5.5632	-118.1233	32.8516	-4.5047	.0501	118.2543	33.1590
108.00	24.0928	.1014	-5.6750	-119.9768	34.0628	-4.5864	.0510	120.1110	34.3703
109.00	24.4770	.1032	-5.7927	-121.8884	35.3428	-4.6712	.0519	122.0260	35.6501
110.00	24.8729	.1052	-5.9164	-123.8588	36.6961	-4.7590	.0529	124.0001	37.0035
111.00	22.8473	.1072	-3.0811	-113.8599	38.1259	-4.8500	.0539	113.9017	38.4332
112.00	23.2185	.1093	-3.1562	-115.7092	39.6370	-4.9441	.0549	115.7523	39.9442
113.00	23.5996	.1114	-3.2360	-117.6074	41.2332	-5.0415	.0560	117.6520	41.5403
114.00	23.9902	.1136	-3.3206	-119.5531	42.9191	-5.1421	.0571	119.5993	43.2260
115.00	24.3900	.1159	-3.4102	-121.5445	44.6983	-5.2459	.0583	121.5924	45.0051
116.00	24.7969	.1183	-3.5050	-123.5811	46.5731	-5.3530	.0595	123.6309	46.8798
117.00	25.2172	.1207	-3.6048	-125.6646	48.5391	-5.4633	.0607	125.7163	48.8457
118.00	25.6449	.1232	-3.7096	-127.7946	50.5946	-5.5767	.0620	127.8485	50.9010
119.00	26.0816	.1258	-3.8194	-129.9695	52.7380	-5.6931	.0633	130.0257	53.0444
120.00	26.5269	.1284	-3.9343	-132.1870	54.9677	-5.8124	.0646	132.2456	55.2742
121.00	26.9800	.1311	-4.0541	-134.4435	57.2811	-5.9345	.0659	134.5047	57.5877
122.00	27.4403	.1339	-4.1789	-136.7355	59.6761	-6.0592	.0673	136.7994	59.9829
123.00	27.9067	.1367	-4.3085	-139.0577	62.1483	-6.1861	.0687	139.1245	62.4555
124.00	28.3780	.1396	-4.4427	-141.4043	64.6930	-6.3151	.0702	141.4741	65.0005
125.00	28.8529	.1424	-4.5814	-143.7683	67.3037	-6.4457	.0716	143.8414	67.6117
126.00	29.3297	.1454	-4.7241	-146.1419	69.9727	-6.5776	.0731	146.2183	70.2813
127.00	29.8066	.1483	-4.8704	-148.5162	72.6909	-6.7102	.0746	148.5961	73.0000
128.00	30.2817	.1512	-5.0197	-150.8810	75.4466	-6.8430	.0760	150.9645	75.7563
129.00	30.7527	.1541	-5.1714	-153.2256	78.2280	-6.9755	.0775	153.3129	78.6384
130.00	30.1872	.1571	-4.0531	-150.4388	81.0201	-7.1069	.0790	150.4934	81.3312
131.00	30.6235	.1599	-4.1818	-152.6112	83.8063	-7.2365	.0804	152.6686	84.1182
132.00	31.0483	.1627	-4.3106	-154.7261	86.5685	-7.3635	.0818	154.7862	86.8811
133.00	31.4587	.1655	-4.4384	-156.7693	89.2866	-7.4871	.0832	156.8322	89.6000
134.00	31.8518	.1681	-4.5641	-158.7261	91.9392	-7.6064	.0845	158.7918	92.2533
135.00	32.2959	.1706	-4.6542	-160.9385	93.6968	-7.7203	.0858	161.0058	94.0143
136.00	32.7470	.1730	-4.7254	-163.1862	95.0025	-7.8280	.0870	163.2547	95.3245

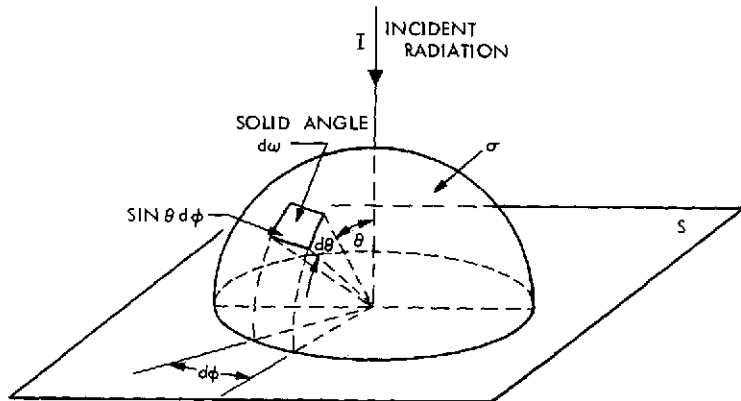


Fig. 1. Radiation reflected from an elementary surface area

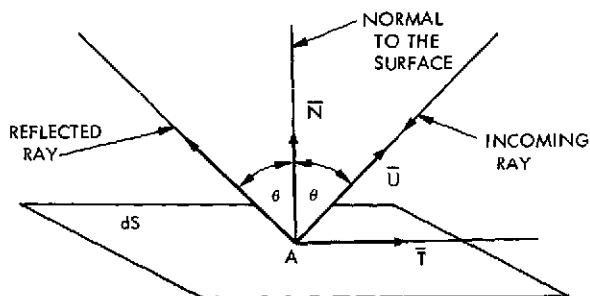


Fig. 2. Orientation of unit vectors along the tangent and normal to the reflecting surface

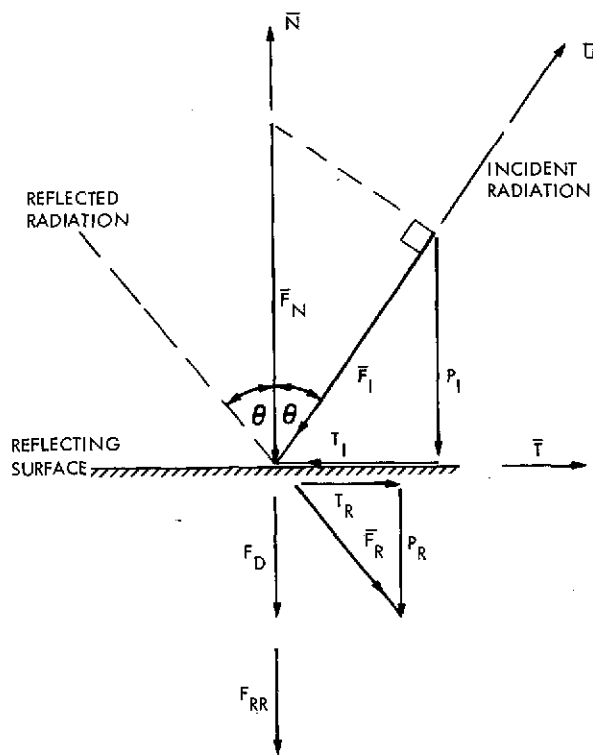


Fig. 3. Force diagram

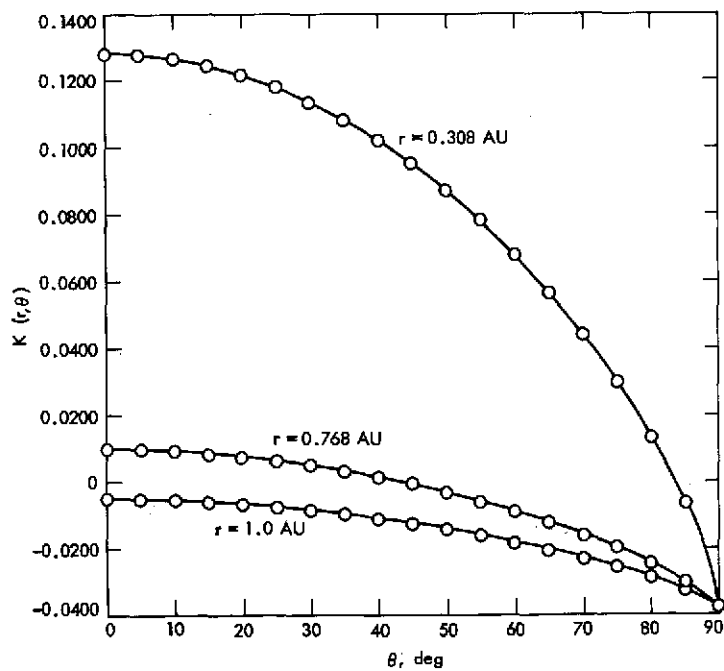


Fig. 4. Function  $K(r, \theta)$  versus the angle of incidence for the Mariner Venus/Mercury spacecraft solar panels

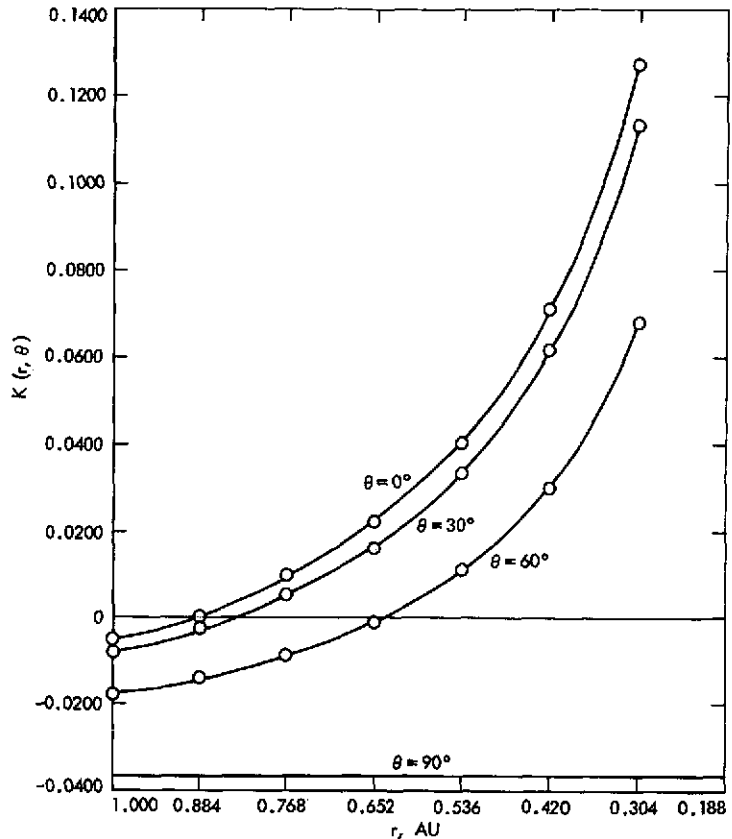


Fig. 5. Function  $K(r, \theta)$  versus the heliocentric distance for the Mariner Venus/Mercury spacecraft solar panels

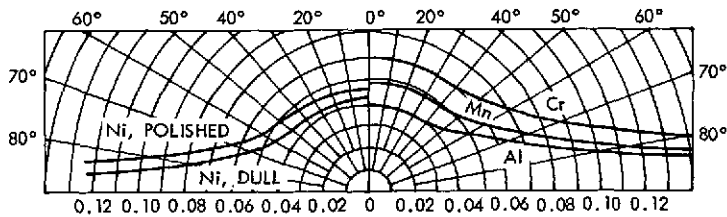


Fig. 6. Directional emissivity of solid materials. The temperature of the radiating metal surfaces was around 420 K (300°F), that of the nonmetallic surfaces between 273 and 366 K (32 and 200°F) [from E. Schmidt and E. Eckert, Forsch. Gebiete Ingenieurw., Vol. 6, pp. 175-183, 1935]

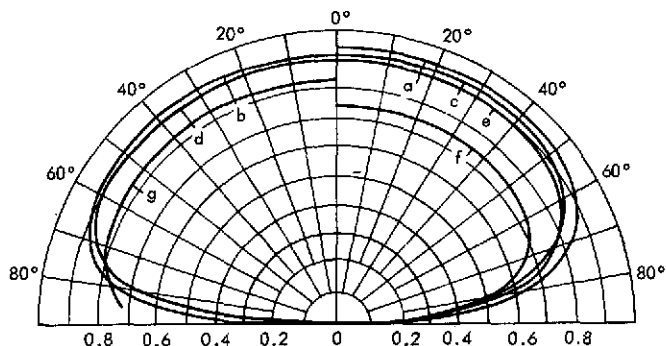


Fig. 7. Emissivity of materials in different directions: (a) wet ice, (b) wood, (c) glass, (d) paper, (e) clay, (f) copper oxide, (g) aluminum oxide. The temperature of the radiating metal surfaces was around 420 K (300°F), that of the nonmetallic surfaces between 273 and 366 K (32 and 200°F) [from E. Schmidt and E. Eckert, Forsch. Gebiete Ingenieurw., Vol. 6, pp. 175-183, 1935]

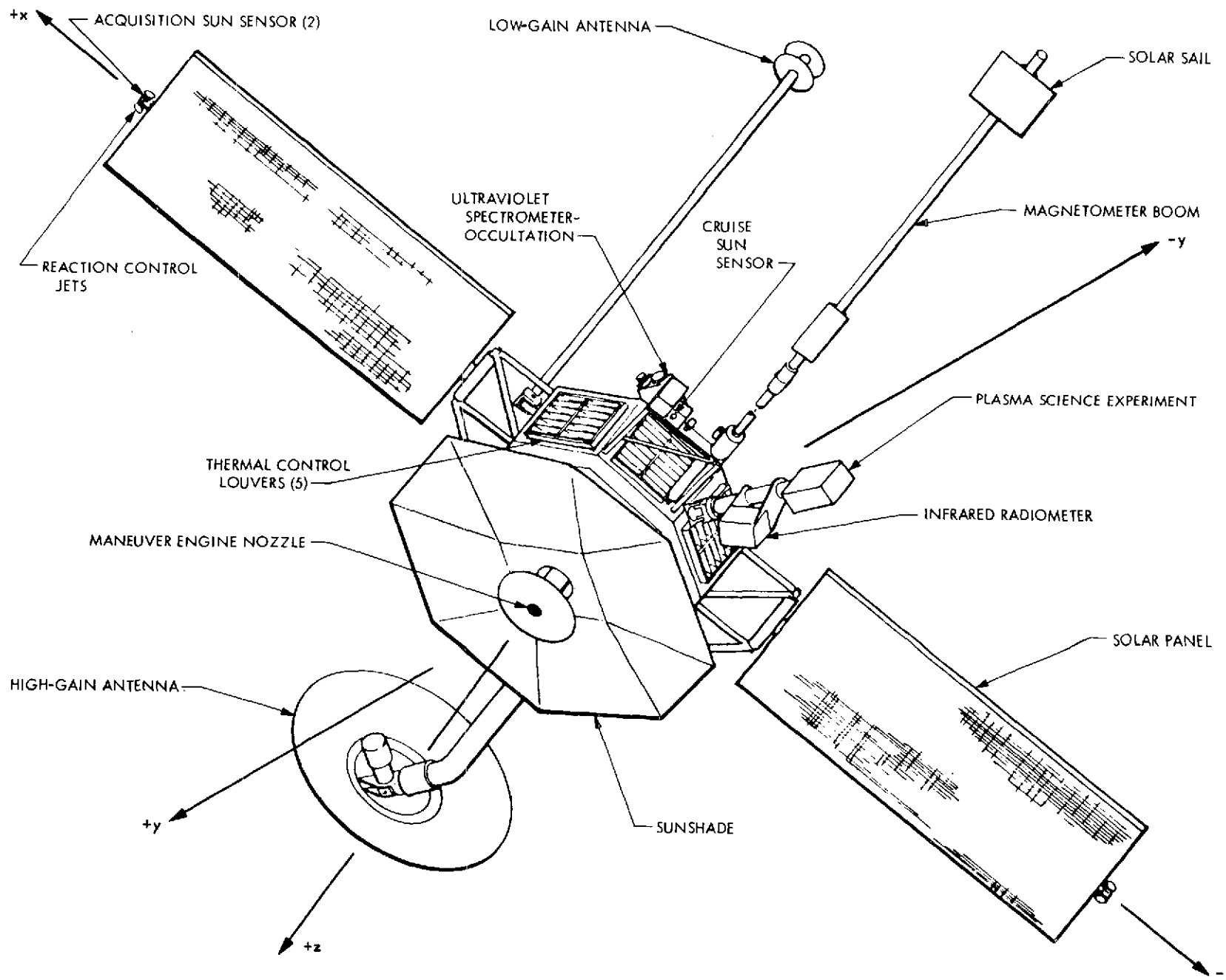


Fig. 8. Mariner Venus/Mercury 1973 spacecraft (Sun side)

ORIGINAL PAGE IS  
OF POOR QUALITY

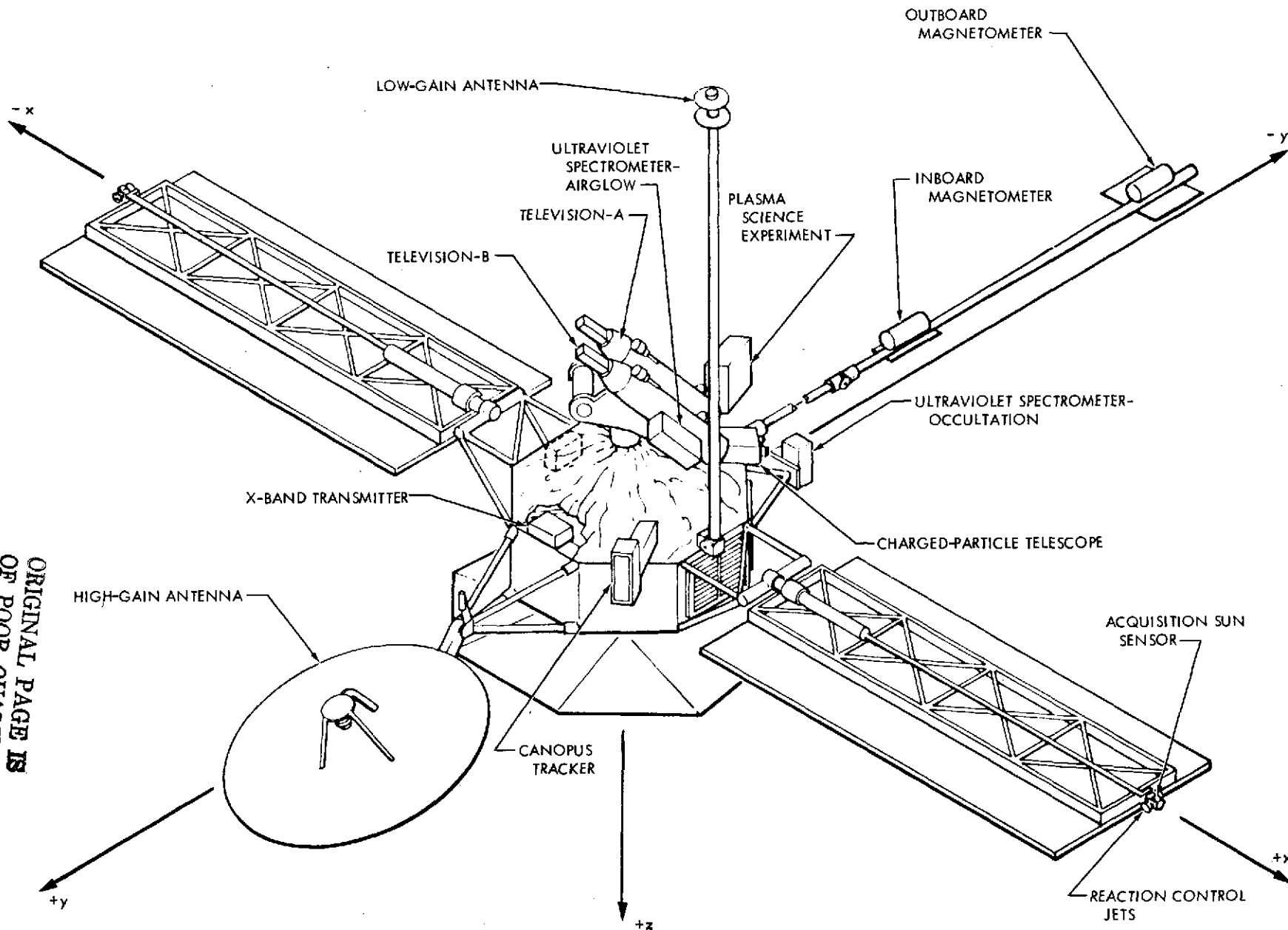


Fig. 9. Mariner Venus/Mercury 1973 spacecraft (shaded side)

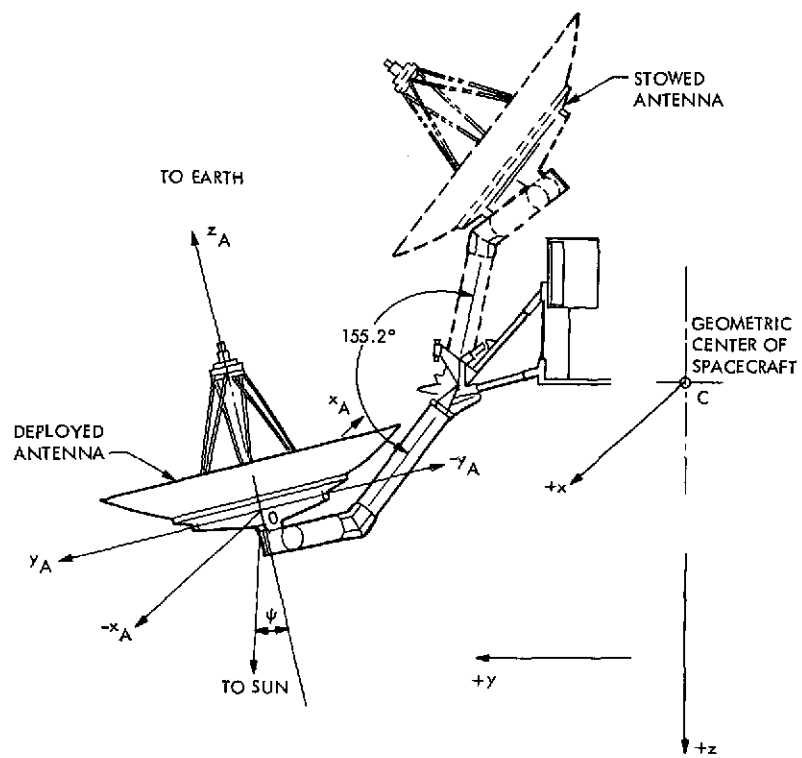


Fig. 10. High-gain antenna geometry

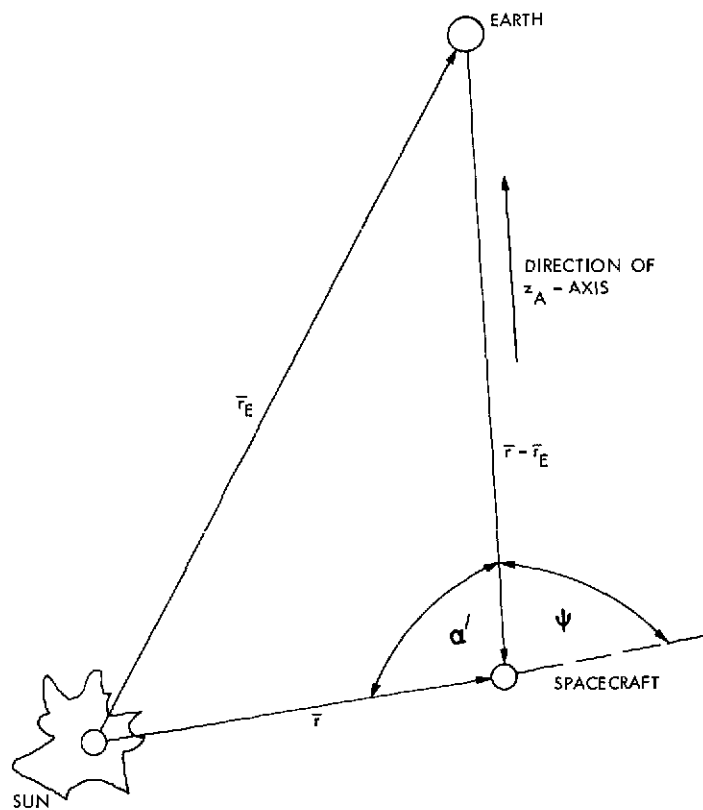


Fig. 11. Sun-Earth-spacecraft geometry

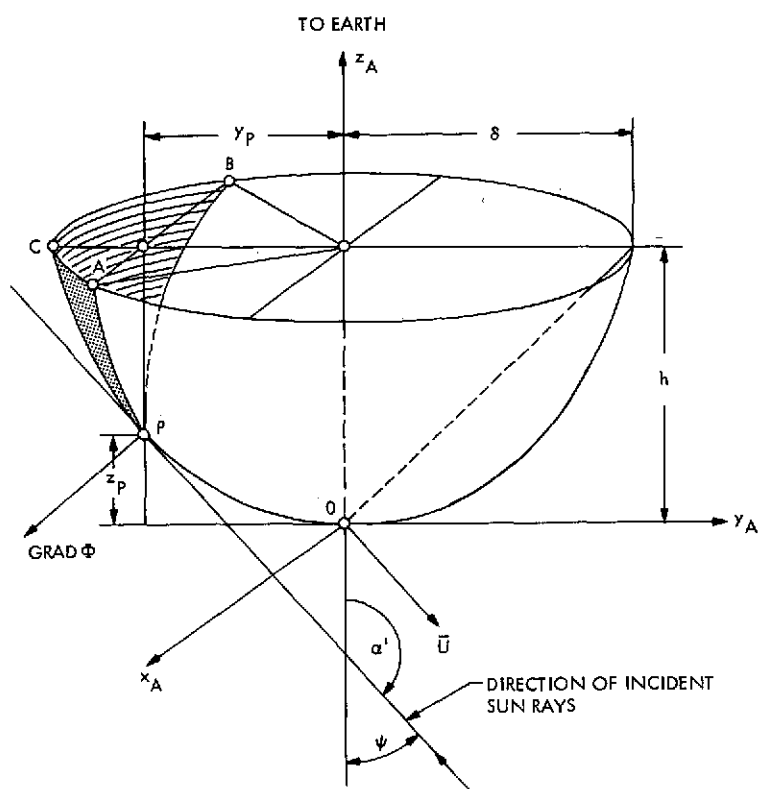


Fig. 12. Solar radiation on the convex side  
of the reflector

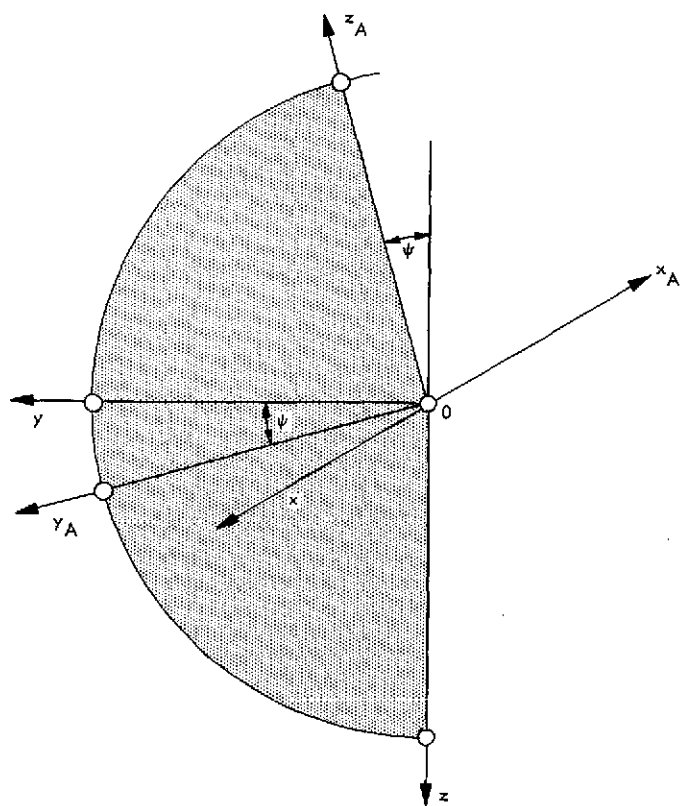


Fig. 13. Relationship between the antenna system and the geometric spacecraft system

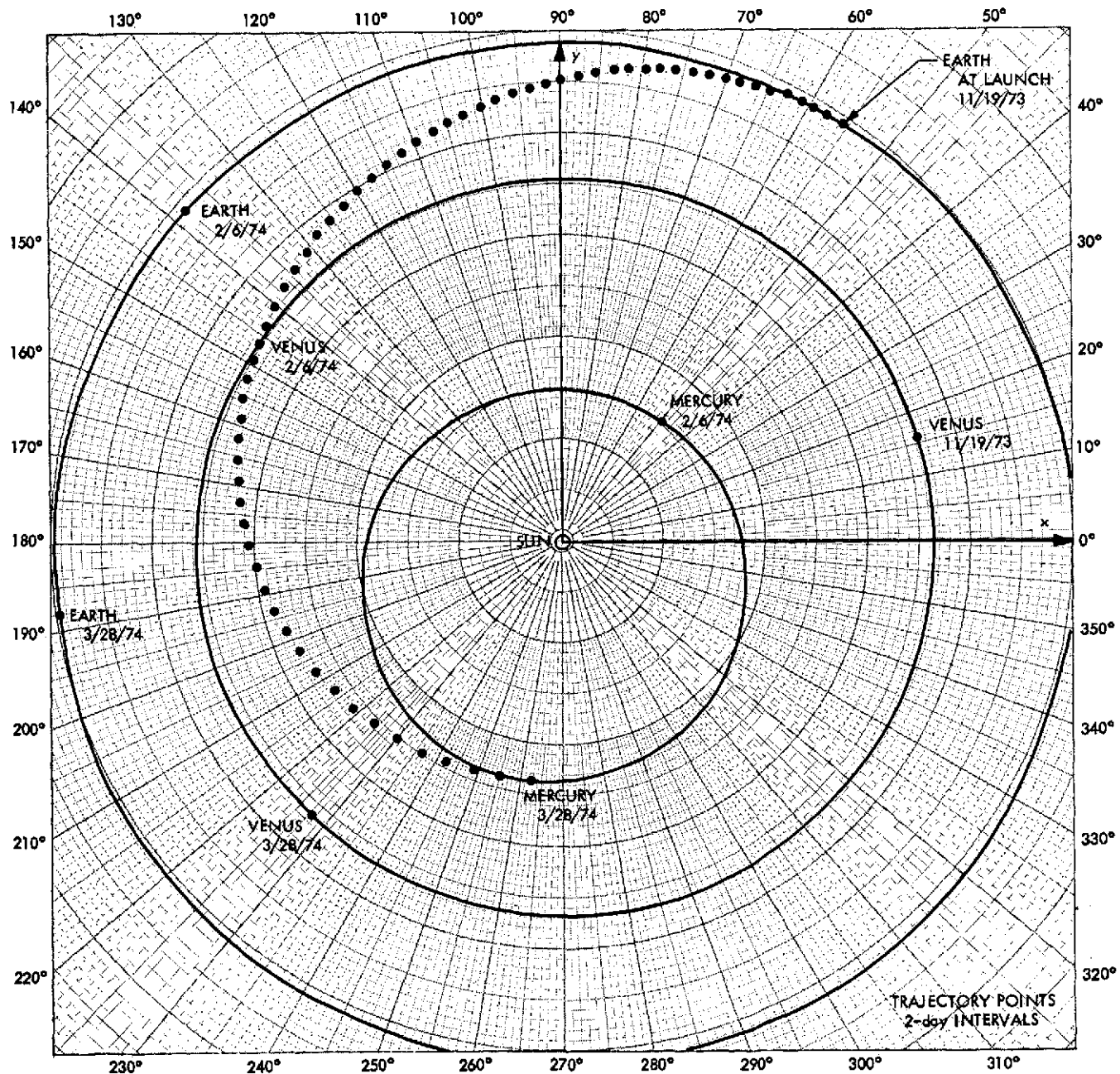


Fig. 14. Projections of heliocentric trajectory in ecliptic plane: launch November 19; Venus arrival February 6; Mercury arrival March 28

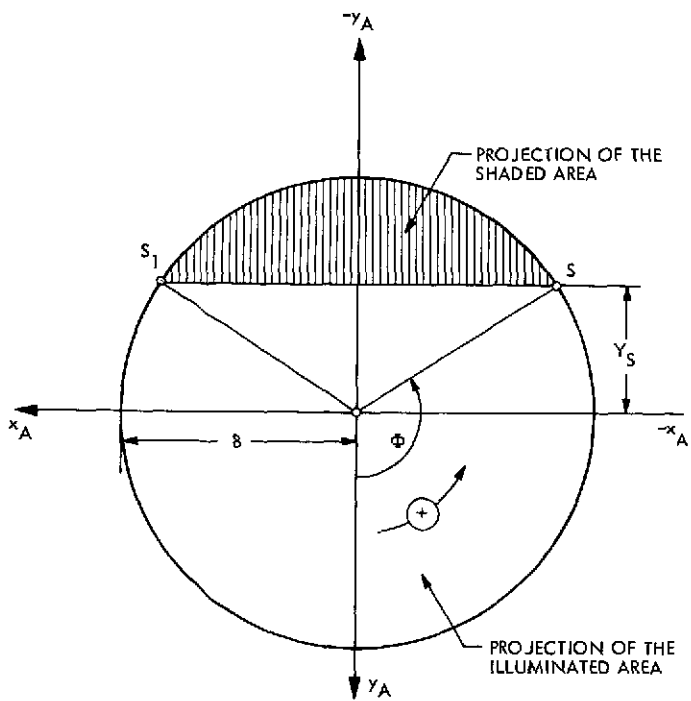


Fig. 15. Projection of the illuminated outside area of the reflector on the  $xy$ -plane of reference

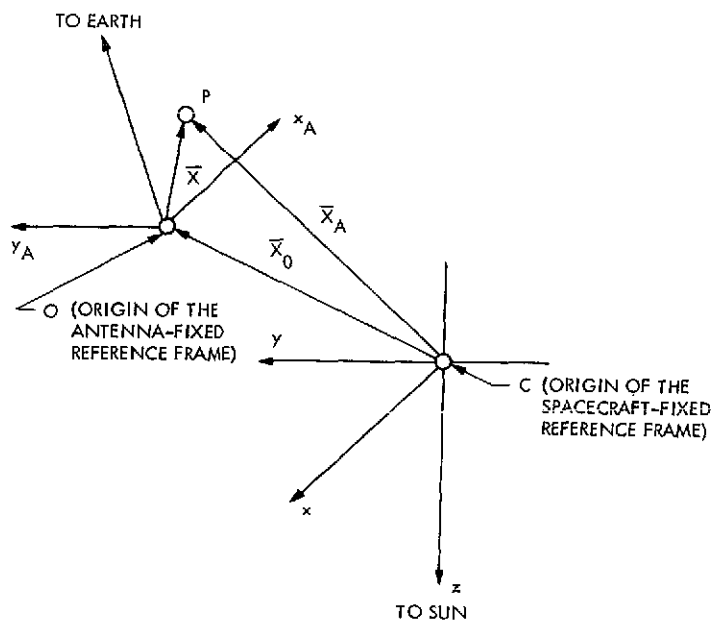


Fig. 16. Relative positions of the two reference frames

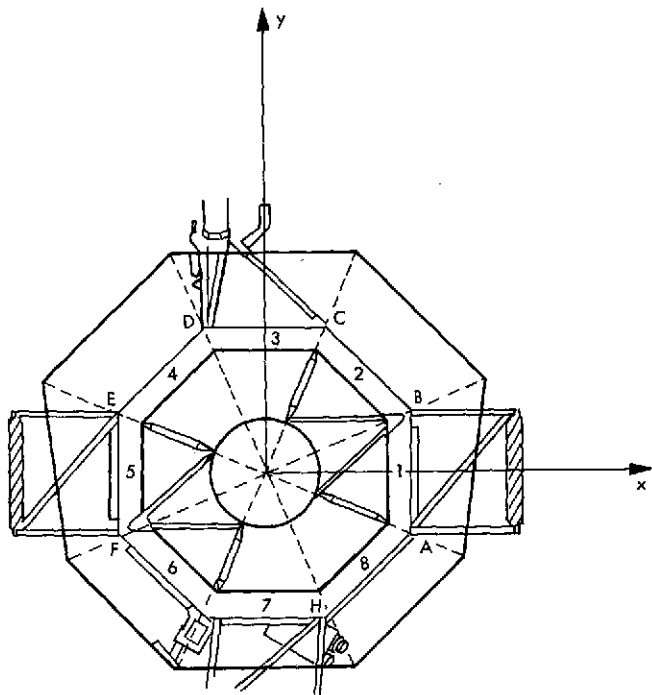


Fig. 17. Octagonal sunshade

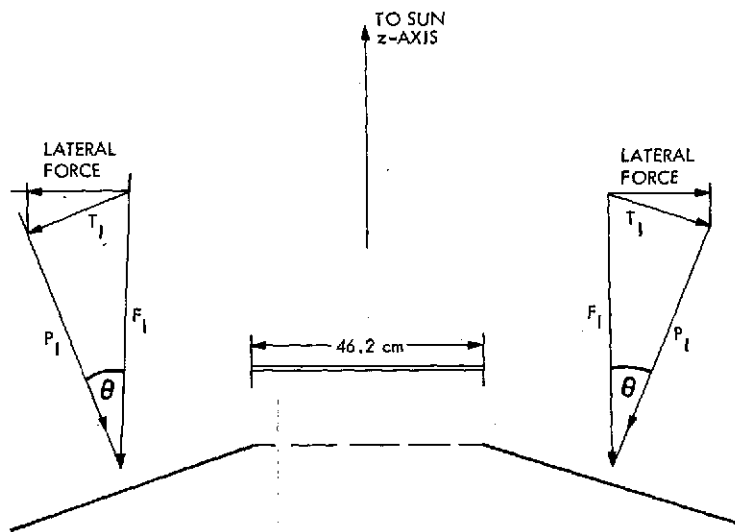


Fig. 18. Cross section of the octagonal sunshade and force diagram

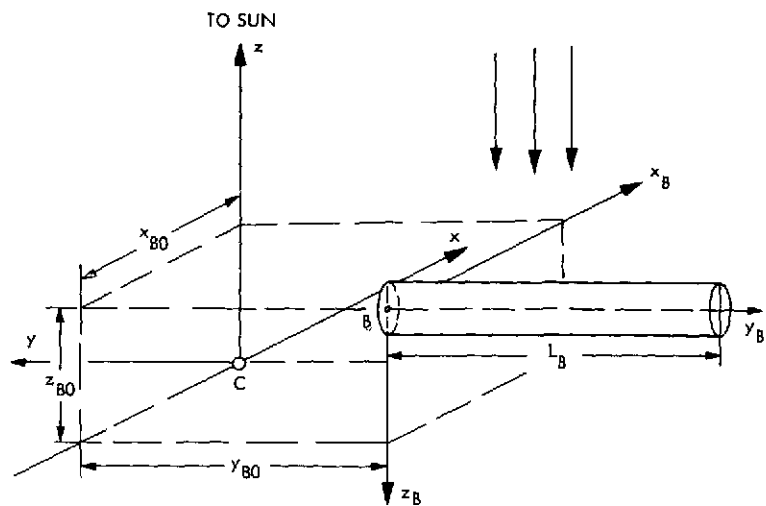


Fig. 19. Solar radiation on the cylindrical surface of the magnetometer boom

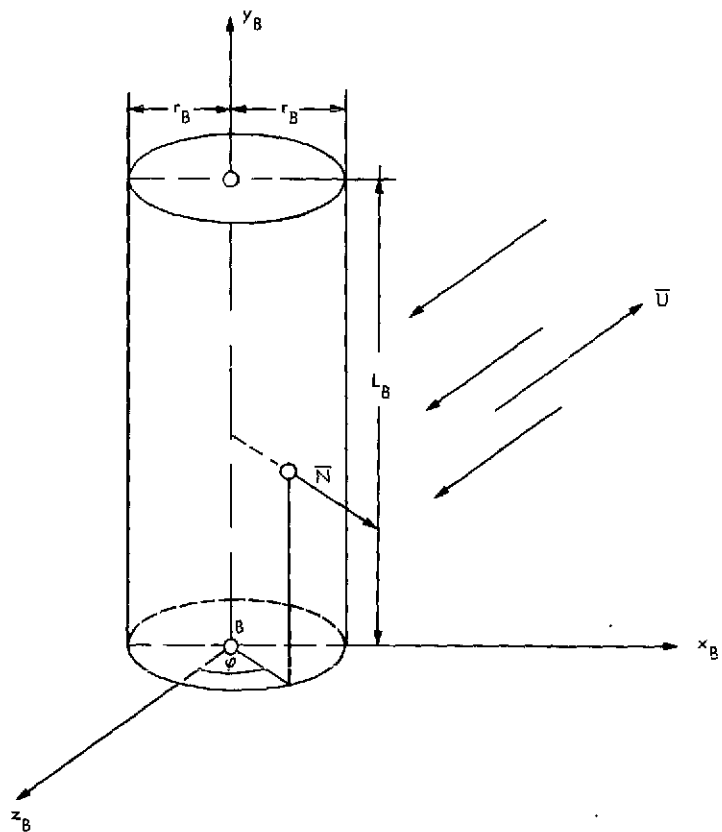


Fig. 20. Solar radiation force on the cylindrical surface of the magnetometer boom in the boom-fixed reference frame

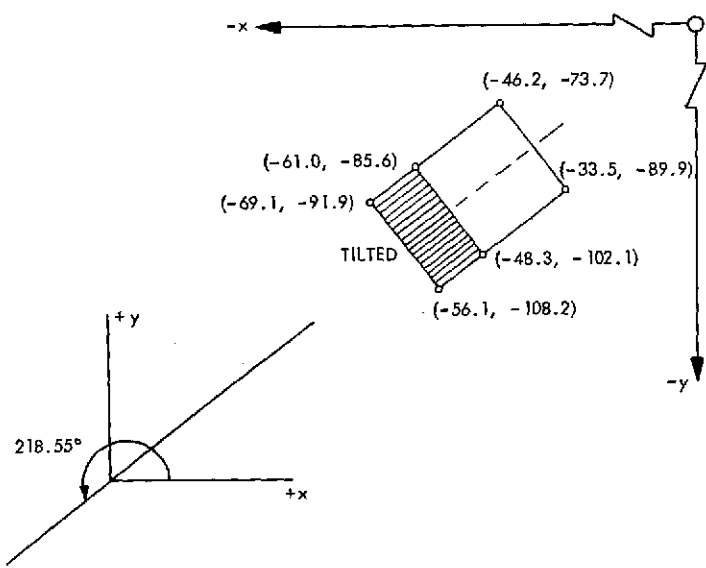


Fig. 21. Position of two IRR sunshades

ORIGINAL PAGE IS  
OF POOR QUALITY

## APPENDIX

### PROGRAM FOR COMPUTATION OF THE COMPONENTS OF THE SOLAR RADIATION FORCE AND THE MOMENT OF THE SOLAR RADIATION FORCE

-FOR,IS SOLE,SOLE

C\*\*\*\*\*  
C THIS PROGRAM COMPUTES THE COMPONENTS OF THE SOLAR PRESSURE FORCE AND  
C THE MOMENT OF THE SOLAR PRESSURE FORCE ON THE REFLECTOR OF THE HIGH GAIN  
C ANTENNA AND SOLAR PANELS OF THE MARINER VENUS/MERCURY 1973 SPACECRAFT.  
C  
C FOR THE CONVEX SURFACE OF THE HIGH GAIN ANTENNA REFLECTOR  
C THE THERMAL RE-RADIATION PART IS OBTAINED BY A DOUBLE INTEGRATION (DOUBLE  
C GAUSSIAN QUADRATURE) IN POLAR COORDINATES WITH BOTH CONSTANT AND VARIABLE  
C INTEGRATION LIMITS. SINCE THE ILLUMINATED AREA IS SYMMETRIC WITH RESPECT  
C TO THE YA-AXIS OF THE ANTENNA SYSTEM OF REFERENCE, THE COMPONENTS FX,  
C MY, AND MZ ARE PRESET TO BE ZERO. THE SURFACE OF THE HIGH GAIN ANTENNA  
C REFLECTOR IS A PARABOLOID OF REVOLUTION.  
C  
C NOMENCLATURE  
C  
C EPSF = EMISSIVITY OF THE ILLUMINATED SURFACE OF THE ANTENNA  
C (CONVEX)  
C EPSB = EMISSIVITY OF THE CONCAVE SURFACE OF THE ANTENNA  
C REFLECTOR  
C GAMMA = REFLECTIVITY COEFFICIENT OF THE ILLUMINATED SURFACE  
C BETA = SPECULAR REFLECTIVITY PARAMETER OF THE HIGH GAIN ANTENNA  
C REFLECTOR (CONVEX SIDE)  
C SIGMA = STEFAN-S CONSTANT (5.6697E-08 KG/SEC\*\*3\*DEGK\*\*4)  
C SOLAR = SOLAR CONSTANT (1.353E+03 KG/SEC\*\*3)  
C COND = THERMAL CONDUCTIVITY OF THE ANTENNA REFLECTOR  
C (1.2921 KG.M/SEC\*\*3\*DEGK)  
C DEPTH = THICKNESS OF THE ANTENNA (0.0191 M)  
C DELTA = RADIUS OF THE APERTURE OF THE ANTENNA REFLECTOR  
C (0.686 M)  
C ZETA = DEPTH OF THE ANTENNA REFLECTOR (0.216 M)  
C PSI = SUPPLEMENT OF THE SUN-SPACECRAFT-EARTH ANGLE  
C EL = DISTANCE OF THE PROJECTION OF THE SHADOW-LINE FROM THE  
C X-AXIS  
C FI = INTEGRATION LIMIT FOR PHI IN CASE OF A SHADOW  
C CRT = CRITICAL VALUE OF THE ANGLE PSI WHEN THE SHADOW APPEARS  
C RAT = LAMBDA (IN THE REFERENCE), CONSTANT OF THE REFLECTOR  
C CTT = JAWORSKI-S CONSTANT ((EPSF-EPSB)/(EPSF+EPSB))  
C P,Q = COEFFICIENTS IN THE EXPANSION OF THE EXPRESSION FOR  
C THE THERMAL RE-RADIATION  
C  
C AX = THE SEMI-MAJOR AXIS OF THE SPACECRAFT-S ELLIPTIC  
C ORBIT (KM)  
C AXE = THE SEMI-MAJOR AXIS OF THE ELLIPTIC ORBIT OF THE EARTH (KM)  
C ECC = THE ORBITAL ECCENTRICITY OF THE SPACECRAFT  
C ECCE = ECCENTRICITY OF THE EARTH-S ORBIT

C INCL = THE INCLINATION OF THE SPACECRAFT-S ORBITAL PLANE TO  
C THE FUNDAMENTAL REFERENCE PLANE (EQUATORIAL PLANE  
C OF THE EARTH FOR 1950.0)  
C EPSLN = OBLIQUITY OF THE ECLIPTIC  
C NODE = THE RIGHT ASCENSION OF THE ASCENDING NODE OF THE  
C SPACECRAFT-S ORBIT  
C OMEGA = ARGUMENT OF THE PERIAPSIS OF THE SPACECRAFT-S ORBIT  
C EOMEGA = ARGUMENT OF THE EARTH-S PERIAPSIS  
C THETA = TRUE ANOMALY OF THE SPACECRAFT  
C ETHETA = TRUE ANOMALY OF THE EARTH  
C M = MEAN ANOMALY OF THE SPACECRAFT  
C ME = MEAN ANOMALY OF THE EARTH  
C E = ECCENTRIC ANOMALY OF THE SPACECRAFT  
C EE = ECCENTRIC ANOMALY OF THE EARTH  
C MSTART = MEAN ANOMALY OF THE SPACECRAFT AT THE TIME OF  
C INITIALIZATION T = TSTART  
C MESTRT = MEAN ANOMALY OF THE EARTH AT THE TIME OF INITIALIZATION  
C TSTART = BEGINNING OF THE CRUISE PHASE  
C GM = GRAVITATIONAL CONSTANT OF THE SUN  
C MEAN = MEAN ORBITAL MOTION OF THE SPACECRAFT  
C MEANE = MEAN ORBITAL MOTION OF THE EARTH  
C PER = ORBITAL PERIOD OF THE SPACECRAFT  
C NPTS = NUMBER OF POINTS ON THE TRAJECTORY  
C TSTEP = TIME STEP  
C RHO = HELIOCENTRIC POSITION VECTOR OF THE SPACECRAFT IN  
C ASTRONOMICAL UNITS (AU)  
C RHOE = HELIOCENTRIC POSITION VECTOR OF THE EARTH IN  
C ASTRONOMICAL UNITS (AU)

C EPOCH = TSTART = 1973, NOVEMBER 09, 19 HRS, 27 MIN, 58 SEC -  
C JULIAN DAY NUMBER  
C TJDO = 2441996.31108586520

C X,Y,Z ARE COORDINATES OF THE SPACECRAFT IN THE EARTH EQUATORIAL PLANE  
C XE,YE,ZE ARE EQUATORIAL COORDINATES OF THE EARTH

C POLAR COORDINATES IN THE PROGRAM ARE XA = -R\*SIN(PHI), YA = R\*COS(PHI)

C THEORETICAL FORMULATION FOR THE THERMAL RE-RADIATION

C 1. EQUATION-

C EPSF\*TFRONT\*\*4 + ETA\*EPSB\*TBACK\*\*4 =  
C (SOLAR/SIGMA)\*((AU/R)\*\*2)\*(1.-GAMMA)\*COS(THETA)  
C (ENERGY BALANCE, GAUSS- THEOREM)

C 2. EQUATION-

C TFRONT = TBACK + (D\*SIGMA\*EPSB/COND)\*TBACK\*\*4  
C (BOUNDARY CONDITIONS, LAPLACE-S EQUATION)

C REFERENCES-

- C 1. R.M.GEORGEVIC, TECHNICAL MEMORANDUM 33-494, OCTOBER 1, 1971  
C 2. R.M.GEORGEVIC, TECHNICAL MEMORANDUM 391-429, MARCH 30, 1973

C \*\*\*\*\*

C SPECIFICATIONS-

ORIGINAL PAGE IS  
OF POOR QUALITY.

```

C
      REAL INTGRL(6,3)
      REAL KONST(100),KNUM(100)
      REAL M(100),ME(100)
      REAL NODE,INCL,MSTART,MESTRT,MEAN,MEANE,MASS
      REAL MU(100)
      INTEGER TLT1,TLT2
      DIMENSION S(10),W(10),PSI(100),ALFA(100),RHO(100),ENTGRL(100,6)
      DIMENSION THETA(100),ETHETA(100),X(100),Y(100),Z(100),XE(100),
1     YE(100),ZE(100)
      DIMENSION RHOE(100)
      DIMENSION E(100),EE(100),DTHETA(100),DETHTA(100)
      DIMENSION XORB(100),YORB(100),XORBE(100),YORBE(100),R(100),RE(100)
      DIMENSION DOT(100),UX(100),UY(100),UZ(100),URSQ(100),UR(100)
      DIMENSION FORCE(100),TORQUE(100),TIME(100)
      DIMENSION DTLT(100)
      =DIMENSION XFOR(100),YFOR(100),ZFOR(100),XTOR(100),YTOR(100),
1     ZTOR(100),FOR(100),TOR(100)
      DIMENSION FLUX(100),FUNK(100),FNU(100),GFACT(100)
      DIMENSION TFRONT(100),TBACK(100)
      DIMENSION DFI(100)
      DIMENSION DPSI(100)
      DIMENSION DM(100),DME(100),DE(100),DEE(100)
      DIMENSION ACC(100),SPACC(100)
      DIMENSION XFORCE(100),YFORCE(100),ZFORCE(100),FTOTAL(100)
      DIMENSION FADX(100),FADY(100),FADZ(100),FAD(100)
      DIMENSION TADX(100),TADY(100),TADZ(100),TAD(100)
      DIMENSION ADACC(100)
      DIMENSION XTORG(100),YTORG(100),ZTORG(100)
      UIMENSION TOTFX(100),TOTFY(100),TOTFZ(100),TOTF(100),TOTACC(100)
      DIMENSION TOTMX(100),TOTMY(100),TOTMZ(100),TOTMOM(100)
      COMMON DELTA,S,W,FI,EL,P,Q,CTT,RAT,PSI,NPTS,GAMMA,ZETA,ELES
      DATA ACY/2.073/,ACZ/-0.562/
      DATA PI/3.141592654/
      DATA DAY/86400.0/
      DATA SPEED/2.997925E+08/

```

```

C
      NAMELIST/INPUT/DELTA, EPSF,EPSB,GAMMA,SIGMA,SOLAR,COND,DEPTH,W,S,
1     ECC,ECCE,TSTART,TSTEP,AX,AXE,INCL,OMEGA,EOMEGA,EPSLN,NODE,
2     GM,MASS,AU,MSTART,MESTRT,ZETA,EPSF1,EPSB1,GAMMA1,DEPTH1,NCASE,
3     MORE,N,TLT1,TLT2,T0,T1,T2,SPEC,AREA
      RAD = 180.0/PI
7000 READ(5,INPUT)
      WRITE(6,3000)
3000 FORMAT(1H1,4X///)
      WRITE(6,INPUT)
      KASE = NCASE-MORE
      MEAN = SQRT(GM/AX**3)
      MEANE = SQRT(GM/AXE**3)
      DMEAN = MEAN*DAY*RAD
      DMEANE = MEANE*DAY*RAD
      PER = 2.0*PI/(MEAN*DAY)
      PERE = 2.0*PI/(MEANE*DAY)
      ETA = SQRT((1.0+ECC)/(1.0-ECC))
      ETAE = SQRT((1.0+ECCE)/(1.0-ECCE))
      ENODE = 0.0
      GO TO (2001,2002),KASE
2001 WRITE(6,1001)

```

```

1001 FORMAT(1H1,35X,'EARTH-VENUS CRUISE PHASE')//)
GO TO 2003
2002 WRITE(6,1002)
1002 FORMAT(1H1,35X,'VENUS-MERCURY CRUISE PHASE')//)
2003 WRITE(6,2)
   WRITE(6,3)AX,ECC,INCL,NODE,EOMEGA,MSTART,DMEAN
   WRITE(6,4)
   WRITE(6,3)AX,ECC,EPSLN,ENODE,EOMEGA,MESTRT,DMEANE
2 FORMAT(36X,'HELIOPCENTRIC ECLIPTIC ORBITAL PARAMETERS OF THE ',
1  'SPACECRAFT')
4 FORMAT( /36X,'HELIOPCENTRIC ECLIPTIC ORBITAL PARAMETERS OF THE ',
1  'EARTH')
3 FORMAT(38X,'AX =',E16.8,1X,'KM',//,37X,'ECC =',F16.11//,36X,'INCL =',
1  F16.11,1X,'DEG',//,36X,'NODE =',F16.11,1X,'DEG',//,35X,'OMEGA =',
2  F16.11,1X,'DEG',//,34X,'MSTART =',F16.11,1X,'DEG',//,36X,'MEAN =',
3  F16.11,1X,'DEG/DAY')
   INCL = INCL/RAD
   OMEGA = OMEGA/RAD
   EOMEGA = EOMEGA/RAD
   EPSLN = EPSLN/RAD
   NODE = NODE/RAD
   MSTART = MSTART/RAD
   MESTRT = MESTRT/RAD
   EPS = EPSF+EPSB
   EPS1 = EPSF1+EPSB1
   EPSRAT = EPSF1/EPSB1
   ELES = -1000000.0*SOLAR/SPEED
   C = SIGMA*DEPTH*EPSB/COND
   TEMP = SOLAR*(1.0-GAMMA)/(SIGMA*EPS)
   TSTAR = TEMP**0.25
   A = C*TSTAR**3
   B = 3.0*A*EPSF/EPS
   CTT = (EPSF-EPSB)/EPS
   CT1 = (EPSF1-EPSB1)/EPS1
   D = DEPTH1
   AFAC = SIGMA*D*EPSB1/COND
   P = 8.0*A*EPSF*EPSB/EPS**2
   EF = -(11.0*EPSF-3.0*EPSB)/(2.0*EPS)
   Q = EF*A*P
   CRT = ATAN(DELTA/(2.0*ZETA))
   DCRT = CRT*RAD
   RAT = ZETA/DELTA**2
C
C COMPUTATION OF UNPERTURBED POSITIONS OF THE SPACECRAFT AND THE EARTH
C
   CI = COS(INCL)
   SI = SIN(INCL)
   CN = COS(NODE)
   SN = SIN(NODE)
   CO = COS(OMEGA)
   SO = SIN(OMEGA)
   CIE = COS(EPSLN)
   SIE = SIN(EPSLN)
   CNE = COS(ENODE)
   SNE = SIN(ENODE)
   COE = COS(EOMEGA)
   SOE = SIN(EOMEGA)
   PX = CN*CO - SN*SO*CI
   PY = SN*CO + CN*SO*CI
   PZ = SO*SI

```

ORIGINAL PAGE IS  
OF POOR QUALITY

```

QX = -CN*SO - SN*CO*CI
QY = -SN*SO + CN*CO*CI
QZ = CO*SI
RX = SN*SI
RY = -CN*SI
RZ = CI
PXEQ = PX
PYEQ = PY*CIE - PZ*SIE
PZEQ = PY*SIE + PZ*CIE
QXEQ = QX
QYEQ = QY*CIE - QZ*SIE
QZEQ = QY*SIE + QZ*CIE
RXEQ = RX
RYEQ = RY*CIE - RZ*SIE
RZEQ = RY*SIE + RZ*CIE
PXE = CNE*COE - SNE*SOE*CIE
PYE = SNE*COE + CNE*SOE*CIE
PZE = SOE*SIE
QXE = -CNE*SOE - SNE*COE*CIE
QYE = -SNE*SOE + CNE*COE*CIE
QZE = COE*SIE
RXE = SNE*SIE
RYE = -CNE*SIE
RZE = CIE
DO 5 I=1,5
K = 6-I
W(I+5) = W(K)
S(I+5) = -S(K)
5 CONTINUE
TEST1 = PX**2 + PY**2 + PZ**2 -1.0
TEST2 = QX**2 + QY**2 + QZ**2 -1.0
TEST3 = RX**2 + RY**2 + RZ**2 -1.0
TEST4 = PX**2 + QX**2 + RX**2 -1.0
TEST5 = PY**2 + QY**2 + RY**2 -1.0
TEST6 = PZ**2 + QZ**2 + RZ**2 -1.0
TEST7 = PX*QX + PY*QY + PZ*QZ
TEST8 = PX*RX + PY*RY + PZ*RZ
TEST9 = QX*RX + QY*RY + QZ*RZ
TEST10 = PX*PY + QX*QY + RX*RY
TEST11 = PX*PZ + QX*QZ + RX*RZ
TEST12 = PY*PZ + QY*QZ + RY*RZ
CHECK1 = PXEQ**2 + PYEQ**2 + PZEQ**2 - 1.0
CHECK2 = QXEQ**2 + QYEQ**2 + QZEQ**2 - 1.0
CHECK3 = RXEQ**2 + RYEQ**2 + RZEQ**2 - 1.0
CHECK4 = PXEQ**2 + QXEQ**2 + RXEQ**2 - 1.0
CHECK5 = PYEQ**2 + QYEQ**2 + RYEQ**2 - 1.0
CHECK6 = PZEQ**2 + QZEQ**2 + RZEQ**2 - 1.0
CHECK7 = PXEQ*QXEQ + PYEQ*QYEQ + PZEQ*QZEQ
CHECK8 = PXEQ*RXEQ + PYEQ*RYEQ + PZEQ*RZEQ
CHECK9 = QXEQ*RXEQ + QYEQ*RYEQ + QZEQ*RZEQ
CHECK10 = PXEQ*PYEQ + QXEQ*QYEQ + RXEQ*RYEQ
CHECK11 = PXEQ*PZEQ + QXEQ*QZEQ + RXEQ*RZEQ
CHECK12 = PYEQ*PZEQ + QYEQ*QZEQ + RYEQ*RZEQ
TST1 = PXE**2 + PYE**2 + PZE**2 - 1.0
TST2 = QXE**2 + QYE**2 + QZE**2 - 1.0
TST3 = RXE**2 + RYE**2 + RZE**2 - 1.0
TST4 = PXE**2 + QXE**2 + RXE**2 - 1.0
TST5 = PYE**2 + QYE**2 + RYE**2 - 1.0
TST6 = PZE**2 + QZE**2 + RZE**2 - 1.0

```

```

TST7 = PXE*QXE + PYE*QYE + PZE*QZE
TST8 = PXE*RXE + PYE*RYE + PZE*RZE
TST9 = QXE*RXE + QYE*RYE + QZE*RZE
TST10 = PXE*PYE + QXE*QYE + RXE*RYE
TST11 = PXE*PZE + QXE*QZE + RXE*RZE
TST12 = PYE*PZE + QYE*QZE + RYE*RZE
WRITE(6,8)
WRITE(6,909)PX,PXEQ,PY,PYEQ,PZ,PZEQ,QX,QXEQ,QY,QYEQ,QZ,QZEQ,
1 RX,RXEQ,RY,RYEQ,RZ,RZEQ
WRITE(6,11)
WRITE(6,8012)TEST1,CHECK1,TEST2,CHECK2,TEST3,CHECK3,TEST4,CHECK4,
1 TEST5,CHECK5,TEST6,CHECK6,TEST7,CHECK7,TEST8,CHECK8,TEST9,
2 CHECK9,TEST10,CHEK10,TEST11,CHEK11,TEST12,CHEK12
WRITE(6,111)
WRITE(6,13)
WRITE(6,9)PXE,PYE,PZE,QXE,QYE,QZE,RXE,RYE,RZE
WRITE(6,14)
WRITE(6,12)TST1,TST2,TST3,TST4,TST5,TST6,TST7,TST8,TST9,TST10,
1 TST11,TST12
WRITE(6,121)
WRITE(6,8022)
WRITE(6,17)
WRITE(6,18)
8 FORMAT(//36X,'VECTORS P,Q,R OF THE SPACECRAFT',//,36X,'ECLIPTIC',
1 42X,'EQUATORIAL')
909 FORMAT(2(36X,'PX =',F10.6)/,2(36X,'PY =',F10.6)/,
1 2136X,'PZ =',F10.6)/,2(36X,'QX =',F10.6)/,
2 2(36X,'QY =',F10.6)/,2(36X,'QZ =',F10.6)/,
3 2(36X,'RX =',F10.6)/,2(36X,'RY =',F10.6)/,
4 2(36X,'RZ =',F10.6)/)
11 FORMAT(//36X,'ORTHOGONALITY TESTS')
8012 FORMAT(/(36X,F10.6,36X,F10.6))
111 FORMAT(1H1,5X)
13 FORMAT(//36X,'EQUATORIAL VECTORS P,Q,R OF THE EARTH')
9 FORMAT(36X,'PX =',F10.6/,36X,'PY =',F10.6/,36X,'PZ =',F10.6/,
1 36X,'QX =',F10.6/,36X,'QY =',F10.6/,36X,'QZ =',F10.6/,36X,'RX =',
2 F10.6/,36X,'RY =',F10.6/,36X,'RZ =',F10.6/)
14 FORMAT(//36X,'ORTHOGONALITY TESTS')
12 FORMAT(/(36X,F10.6))
121 FORMAT(//10X,'EPOCH (TSTART) = NOVEMBER 9, 1973')
8022 FORMAT(10X,'TRAJECTORY SWITCH ON FEBRUARY 9, 1974')
17 FORMAT(1H1,35X,'HELIOCENTRIC EQUATORIAL COORDINATES OF '
1 'SPACECRAFT AND EARTH')
18 FORMAT(2X,'TIME',8X,'X(KM)',9X,'Y(KM)',9X,'Z(KM)',7X,'RHO(AU)',
1 7X,'XE(KM)',8X,'YE(KM)',8X,'ZE(KM)',8X,'RHOE',8X,'PSI',
2 1X,'(DAYS)',103X,'(AU)',7X,'(DEG)')
DO 16 NPTS = 1,N
M(NPTS) = MSTART + (NPTS-1)*MEAN*TSTEP
ME(NPTS) = MESTRT + (NPTS-1)*MEANE*TSTEP
E(NPTS) = ANOM(ECC,M(NPTS))
EE(NPTS) = ANOM(ECCE,ME(NPTS))
R(NPTS) = AX*(1.0-ECC*COS(E(NPTS)))
RE(NPTS) = AXE*(1.0-ECCE*COS(EE(NPTS)))
RHO(NPTS) = R(NPTS)/AU
RHOE(NPTS) = RE(NPTS)/AU
THETA(NPTS) = 2.0*ATAN(ETA*TAN(E(NPTS)/2.0))
ETHETA(NPTS) = 2.0*ATAN(ETAE*TAN(EE(NPTS)/2.0))
IF(E(NPTS).GE.2.0*PI)E(NPTS)=E(NPTS)-2.0*PI
IF(EE(NPTS).GE.2.0*PI)EE(NPTS)=EE(NPTS)-2.0*PI

```

```

IF(M(NPTS).GE.2.0*PI)M(NPTS)=M(NPTS)-2.0*PI
IF(ME(NPTS).GE.2.0*PI)ME(NPTS)=ME(NPTS)-2.0*PI
XORB(NPTS) = R(NPTS)*COS(THETA(NPTS))
YORB(NPTS) = R(NPTS)*SIN(THETA(NPTS))
XORBE(NPTS) = RE(NPTS)*COS(ETHETA(NPTS))
YORBE(NPTS) = RE(NPTS)*SIN(ETHETA(NPTS))
XE(NPTS) = PXE*XORBE(NPTS) + QXE*YORBE(NPTS)
X(NPTS) = PXEQ*XORB(NPTS) + QXEQ*YORB(NPTS)
Y(NPTS) = PYEQ*XORB(NPTS) + QYEQ*YORB(NPTS)
Z(NPTS) = PZEQ*XORB(NPTS) + QZEQ*YORB(NPTS)
YE(NPTS) = PYE*XORBE(NPTS) + QYE*YORBE(NPTS)
ZE(NPTS) = PZE*XORBE(NPTS) + QZE*YORBE(NPTS)
TIME(NPTS) = TSTART + ((NPTS-1)*TSTEP)/DAY
UX(NPTS) = X(NPTS)-XE(NPTS)
UY(NPTS) = Y(NPTS)-YE(NPTS)
UZ(NPTS) = Z(NPTS)-ZE(NPTS)
URSQ(NPTS) = UX(NPTS)**2 + UY(NPTS)**2 + UZ(NPTS)**2
UR(NPTS) = SQRT(URSQ(NPTS))
DOT(NPTS) = -UX(NPTS)*X(NPTS)-UY(NPTS)*Y(NPTS)-UZ(NPTS)*Z(NPTS)
PSI(NPTS) = ACOS(DOT(NPTS)/(UR(NPTS)*R(NPTS)))
DPSI(NPTS) = PSI(NPTS)*RAD
IF(PSI(NPTS).GT.PI/2.0)PSI(NPTS)=PI/2.0
IF(PSI(NPTS).LT.0.0)PSI(NPTS)=PSI(NPTS)+PI
ALFA(NPTS) = PSI(NPTS)*RAD
IF(ALFA(NPTS).GT.90.0)ALFA(NPTS)=90.0
IF(NPTS.EQ.51)WRITE(6,180)
IF(NPTS.EQ.141)WRITE(6,180)
180 FORMAT(1H1,1X,
1      'TIME',8X,'X(KM)',9X,'Y(KM)',9X,'Z(KM)',7X,'RHO(AU)',,
2      7X,'XE(KM)',8X,'YE(KM)',8X,'ZE(KM)',8X,'RHOE',8X,'PSI',/,
3      1X,'(DAYS)',103X,'(AU)',7X,'(DEG)',)
      WRITE(6,19)TIME(NPTS),
1      X(NPTS),Y(NPTS),Z(NPTS),RHO(NPTS),XE(NPTS),YE(NPTS),
2      ZE(NPTS),RHOE(NPTS),DPSI(NPTS)
19 FORMAT(1X,F6.2,3E14.6,F12.6,3E14.6,F12.6,F11.2)
16 CONTINUE
      WRITE(6,181)
181 FORMAT(1H1,29X,'TIME',5X,'THETA',6X,'E',8X,'M',5X,'THETAE',5X,
1      'EE',7X,'ME' /29X,'(DAYS)',6(4X,'(DEG)'),)
      DO 33 NPTS=1,N
      DTHETA(NPTS) = THETA(NPTS)*RAD
      DETHTA(NPTS) = ETHETA(NPTS)*RAD
      IF(DTHETA(NPTS).LT.0.0)DTHETA(NPTS)=DTHETA(NPTS)+360.0
      IF(DETHHTA(NPTS).LT.0.0)DETHHTA(NPTS)=DETHHTA(NPTS)+360.0
      DM(NPTS) = M(NPTS)*RAD
      DME(NPTS) = ME(NPTS)*RAD
      DE(NPTS) = E(NPTS)*RAD
      DEE(NPTS) = EE(NPTS)*RAD
      IF(DM(NPTS).LT.0.0)DM(NPTS)=DM(NPTS)+360.0
      IF(DME(NPTS).LT.0.0)DME(NPTS)=DME(NPTS)+360.0
      IF(DE(NPTS).LT.0.0)DE(NPTS)=DE(NPTS)+360.0
      IF(DEE(NPTS).LT.0.0)DEE(NPTS)=DEE(NPTS)+360.0
      IF(DE(NPTS).GE.360.0)DE(NPTS)=DE(NPTS)-360.0
      IF(DEE(NPTS).GE.360.0)DEE(NPTS)=DEE(NPTS)-360.0
      IF(DM(NPTS).GE.360.0)DM(NPTS)=DM(NPTS)-360.0
      IF(DME(NPTS).GE.360.0)DME(NPTS)=DME(NPTS)-360.0
      IF(NPTS.EQ.51)WRITE(6,182)
      IF(NPTS.EQ.151)WRITE(6,182)
182 FORMAT(1H1,29X,'TIME',5X,'THETA',6X,'E',8X,'M',5X,'THETAE',5X,
1      'EE',7X,'ME' /29X,'(DAYS)',6(4X,'(DEG)'),)

```

```

      WRITE(6,190)TIME(NPTS),DTHETA(NPTS),DE(NPTS),DM(NPTS),
1      DETHTA(NPTS),DEE(NPTS),DME(NPTS)
190 FORMAT(29X,F6.2,6F9.2)
33 CONTINUE
C
C COMPUTATION OF COMPONENTS OF THE SOLAR RADIATION FORCE AND ITS MOMENT
C ON THE HIGH-GAIN ANTENNA REFLECTOR
C
      WRITE(6,22)
      WRITE(6,15)
      WRITE(6,35)
22 FORMAT(1H1,5X)
15 FORMAT(25X,'COMPONENTS OF THE SOLAR PRESSURE FORCE AND TORQUE '
1      'ON THE HIGH GAIN ANTENNA REFLECTOR',//,25X,'OF THE MARINER '
2      'VENUS/MERCURY SPACECRAFT, ALONG THE AXES OF THE ANTENNA-FIXED'
3      '//,25X,'REFERENCE SYSTEM IN E+06 NEWTONS AND E+06 NEWTON-'
4      'METERS',//,25X,'RESPECTIVELY. THE ACCELERATION IS GIVEN IN '
5      'E+11 KM/SEC**2//')
35 FORMAT(//,2X,'TIME',6X,'PSI',8X,'ACC',     6X,'XFORCE',5X,'YFORCE',
1      5X,'ZFORCE',4X,'XTORQUE',4X,'YTORQUE',4X,'ZTORQUE',6X,'FORCE',
2      5X,'TORQUE',8X,'FI',//,
3      1X,'(DAYS)',4X,'(DEG)',105X,'(DEG)//')
DO 30 NPTS=1,N
IF(PSI(NPTS),NE.PI/2.0)GO TO 6
FI = PI/2.0
PSI(NPTS) = FI
ALFA(NPTS) = FI*RAD
EL = 0.0
GO TO 7
6 UPS = 2.0*RAT*TAN(PSI(NPTS))
IF(PSI(NPTS),EQ.0.0)UPS = 0.99999999/DELTA
YPS = -1.0/UPS
EL = YPS
DEN = -UPS*DELTA
IF(ABS(DEN),LE.1.0)FI=PI
IF(ABS(DEN),GT.1.0)FI=ACOS(1.0/DEN)
7 DO 20 J=1,6
DO 10 L=1,3
IF(PSI(NPTS),LE.CRT)INTGRL(J,L)=CRPHI(J,L)
IF(PSI(NPTS),GT.CRT)INTGRL(J,L)=CRPHI(J,L)+VRPHI(J,L)
MU(NPTS) = 1.0/RHO(NPTS)
TERMA = (MU(NPTS))**2
TERMB = (MU(NPTS))**3.5
TERMC = (MU(NPTS))**5
ENTGRL(NPTS,J) = TERMA*INTGRL(J,1) + TERMB*INTGRL(J,2) +
1      TERMC*INTGRL(J,3)
XFORCE(NPTS) = -ENTGRL(NPTS,1)
YFORCE(NPTS) = ENTGRL(NPTS,2)*COS(PSI(NPTS)) +
1      ENTGRL(NPTS,3)*SIN(PSI(NPTS))
ZFORCE(NPTS) = ENTGRL(NPTS,2)*SIN(PSI(NPTS)) -
1      ENTGRL(NPTS,3)*COS(PSI(NPTS))
FTOTAL(NPTS) = SQRT(XFORCE(NPTS)**2 + YFORCE(NPTS)**2 +
1      ZFORCE(NPTS)**2)
FORCE(NPTS) = SQRT(ENTGRL(NPTS,2)**2 + ENTGRL(NPTS,3)**2)
TORQUE(NPTS) = ABS(ENTGRL(NPTS,4))
ACC(NPTS) = 100.0*FORCE(NPTS)/MASS
XTORQ(NPTS) = -ENTGRL(NPTS,4)+ACY*ZFORCE(NPTS)-ACZ*YFORCE(NPTS)
YTORQ(NPTS) = 0.0
ZTORQ(NPTS) = 0.0
10 CONTINUE

```

ORIGINAL PAGE IS  
OF POOR QUALITY

```

20 CONTINUE
DFI(NPTS) = FI*RAD
IF(NPTS.EQ.46)WRITE(6,183)
IF(NPTS.EQ.141)WRITE(6,183)
183 FORMAT(1H1,1X,
1      'TIME',6X,'PSI',8X,'ACC',   6X,'XFORCE',5X,'YFORCE',
2      5X,'ZFORCE',4X,'XTORQUE',4X,'YTORQUE',4X,'ZTORQUE',6X,'FORCE',
3      5X,'TORQUE',8X,'FI',//,
4      1X,'(DAYS)',4X,'(DEG)',105X,'(DEG)//')
      WRITE(6,36)TIME(NPTS),ALFA(NPTS),ACC(NPTS),(ENTGRL(NPTS,J),
1      J=1,6),FORCE(NPTS),TORQUE(NPTS),DFI(NPTS)
36 FORMAT(1X,F6.2,3X,F6.2,F11.4,8F11.4,F11.2)
30 CONTINUE
C
C COMPUTATION OF THE COMPONENTS OF THE SOLAR RADIATION FORCE AND ITS
C MOMENT ON TWO SOLAR PANELS
C
      WRITE(6,1)
      WRITE(6,351)
1 FORMAT(1H1,24X,'COMPONENTS OF THE SOLAR PRESSURE FORCE AND TORQUE',
1      'ON THE SOLAR PANELS',//,25X,'OF THE MARINER VENUS/MERCURY 1973',
2      'SPACECRAFT, ALONG THE AXES OF THE SPACECRAFT-FIXED',
3      //,25X,'REFERENCE SYSTEM IN E+06 NEWTONS AND E+06 NEWTON-',
4      'METERS',//,25X,'RESPECTIVELY. THE ACCELERATION IS GIVEN IN ',
5      'E+11 KM/SEC**2//')
351 FORMAT(//,2X,'TIME',6X,'TILT',7X,'ACC',   6X,'XFORCE',5X,'YFORCE',
1      5X,'ZFORCE',4X,'XTORQUE',4X,'YTORQUE',4X,'ZTORQUE',6X,'FORCE',
2      5X,'TORQUE',//,
3      1X,'(DAYS)',4X,'(DEG)//')
DO 300 NPTS=1,N
IF(NPTS.LT.TLT1)TLT=T0/RAD
IF(NPTS.GE.TLT1.AND.NPTS.LT.TLT2)TLT=T1/RAD
IF(NPTS.GE.TLT2)TLT=T2/RAD
RECIP = (MU(NPTS))**2
PNX = 0.0
PNY = SIN(TILT)
PNZ = COS(TILT)
FLUX(NPTS) = (SOLAR/SIGMA)*(1.0-GAMMA1)*RECIP*COS(TILT)
EX = 450.0
CALL NEWTON(EX,XKSI,      EPSF1,EPSB1,AFACT,FLUX(NPTS))
TBACK(NPTS) = XKSI
TFRONT(NPTS) = TBACK(NPTS)*(1.0+AFACT*TBACK(NPTS)**3)
KNUM(NPTS) = EPSF1*TFRONT(NPTS)**4 - EPSB1*TBACK(NPTS)**4
KONST(NPTS) = KNUM(NPTS)/FLUX(NPTS)
XFOR(NPTS) = 0.0
PART1 = 2.0*GAMMA1*SPEC*(COS(TILT))**2
BOFEF = 2.0/3.0
FUNK(NPTS) = BOFEF*(GAMMA1*(1.0-SPEC)+(1.0-GAMMA1)*KONST(NPTS))
FNU(NPTS) = PART1 + FUNK(NPTS)*COS(TILT)
XTOR(NPTS) = 0.0
YTOR(NPTS) = 0.0
ZTOR(NPTS) = 0.0
GFACT(NPTS) = ELES*AREA*MU(NPTS)**2
YFOR(NPTS) = GFACT(NPTS)*PNY*FNU(NPTS)
ZFOR(NPTS) = GFACT(NPTS)*(PNZ*FNU(NPTS)+(1.0-GAMMA1*SPEC)*
1      COS(TILT))
FOR(NPTS) = SQRT(YFOR(NPTS)**2 + ZFOR(NPTS)**2)

```

```

TOR(NPTS) = ABS(XTOR(NPTS))
SPACC(NPTS) = 100.0*FOR(NPTS)/MASS
DTLT(NPTS) = TILT*RAD
IF(NPTS.EQ.46)WRITE(6,184)
IF(NPTS.EQ.141)WRITE(6,184)
184 FORMAT(1H1,1X,
1      'TIME',6X,'TILT',7X,'ACC', 6X,'XFORCE',5X,'YFORCE',
2      5X,'ZFORCE',4X,'XTORQUE',4X,'YTORQUE',4X,'ZTORQUE',6X,'FORCE',
3      5X,'TORQUE',//,
4          1X,'(DAYS)',4X,'(DEG)//')
      WRITE(6,7001)TIME(NPTS),DTLT(NPTS),SPACC(NPTS),XFOR(NPTS),
1      YFOR(NPTS),ZFOR(NPTS),XTOR(NPTS),YTOR(NPTS),ZTOR(NPTS),
2      FOR(NPTS),TOR(NPTS)
7001 FORMAT(1X,F6.2,3X,F6.2,9F11.4)
300 CONTINUE
      WRITE(6,352)
352 FORMAT(1H1,29X,'TIME',6X,'TILT',7X,'RHO(AU)',10X,'MU',8X,
1      'TFRONT',7X,'TBACK',14X,'K',//,29X,'(DAYS)',4X,'(DEG)//')
DO 350 NPTS=1,N
IF(NPTS.EQ.51)WRITE(6,185)
IF(NPTS.EQ.151)WRITE(6,185)
185 FORMAT(1H1,29X,'TIME',6X,'TILT',7X,'RHO(AU)',10X,'MU',8X,
1      'TFRONT',7X,'TBACK',14X,'K',//,29X,'(DAYS)',4X,'(DEG)//')
      WRITE(6,7002)TIME(NPTS),DTLT(NPTS),RHO(NPTS),MU(NPTS),
1      TFRONT(NPTS),TBACK(NPTS),KONST(NPTS)
7002 FORMAT(29X,F6.2,3X,F6.2,6F14.6)
350 CONTINUE
      WRITE(6,1100)
      WRITE(6,1101)
1100 FORMAT(1H1,9X,'COMPONENTS OF THE SOLAR PRESSURE FORCE IN THE ',
1      'SPACECRAFT-FIXED',//,10X,'REFERENCE FRAME IN E+06 NEWTONS//')
1101 FORMAT(11X,'TIME',3X,'RHO(AU)',4X,'PSI',7X,'XFORCE',6X,
1      'YFORCE',6X,'ZFORCE',7X,'FORCE',//,10X,'(DAYS)',12X,'(DEG)//')
DO 1014 NPTS=1,N
IF(NPTS.EQ.46)WRITE(6,186)
IF(NPTS.EQ.141)WRITE(6,186)
186 FORMAT(1H1,10X,
1      'TIME',3X,'RHO(AU)',4X,'PSI',7X,'XFORCE',6X,
2      'YFORCE',6X,'ZFORCE',7X,'FORCE',//,10X,'(DAYS)',12X,'(DEG)//')
      WRITE(6,1015)TIME(NPTS),RHO(NPTS),ALFA(NPTS),XFORCE(NPTS),
1      YFORCE(NPTS),ZFORCE(NPTS),FTOTAL(NPTS)
1015 FORMAT(10X,F6.2,F9.6,F9.3,4F12.6)
1014 CONTINUE
C
C COMPUTATION OF SOLAR RADIATION FORCES AND TORQUES ON ADIABATIC
C SURFACES OF THE MARINER VENUS/MERCURY SPACECRAFT.
C
      CFORX = -0.008711
      CFORY = -0.006941
      CFORZ = 6.337135
      CMOMX = -5.23199
      CMOMY = 0.39419
      CMOMZ = -0.00438
C
      WRITE(6,7003)
      WRITE(6,7004)
7003 FORMAT(1H1,24X,'COMPONENTS OF THE SOLAR RADIATION FORCE '

```

ORIGINAL PAGE IS  
OF POOR QUALITY

```

1      'AND TORQUE ON ADIABATIC SURFACES',//,25X,'IN E+06 NEWTONS'
2      ' AND E+06 NEWTON-METERS RESPECTIVELY',//,25X,'ACCELERATION '
3      'IN E+11 KM/SEC**2')
7004 FORMAT(/2X, 'TIME',17X,           'ACC',   6X,'XFORCE',5X,'YFORCE',
1      5X,'ZFORCE',4X,'XTORQUE',4X,'YTORQUE',4X,'ZTORQUE',6X,'FORCE',
2      5X,'TORQUE',//,
3      1X,'(DAYS)//)
DO 1102 NPTS=1,N
ELMU = ELES*MU(NPTS)**2
FADX(NPTS) = CFORX*ELMU
FADY(NPTS) = CFORY*ELMU
FADZ(NPTS) = CFORZ*ELMU
TADX(NPTS) = CMOMX*ELMU
TADY(NPTS) = CMOMY*ELMU
TADZ(NPTS) = CMOMZ*ELMU
FAD(NPTS) = SQRT(FADX(NPTS)**2+FADY(NPTS)**2+FADZ(NPTS)**2)
TAD(NPTS) = SQRT(TADX(NPTS)**2+TADY(NPTS)**2+TADZ(NPTS)**2)
ADACC(NPTS) = 100.0*FAD(NPTS)/MASS
IF(NPTS.EQ.46)WRITE(6,187)
IF(NPTS.EQ.141)WRITE(6,187)
187 FORMAT(1H1,1X,
1      'TIME',17X,           'ACC',   6X,'XFORCE',5X,'YFORCE',
2      5X,'ZFORCE',4X,'XTORQUE',4X,'YTORQUE',4X,'ZTORQUE',6X,'FORCE',
3      5X,'TORQUE',//,
4      1X,'(DAYS)//)
WRITE(6,7010)TIME(NPTS),ADACC(NPTS),FADX(NPTS),FADY(NPTS),
1     FADZ(NPTS),TADX(NPTS),TADY(NPTS),TADZ(NPTS),FAD(NPTS),
2     TAD(NPTS)
7010 FORMAT(1X,F6.2,9X,9F11.4)
1102 CONTINUE
WRITE(6,7005)
WRITE(6,7006)
7005 FORMAT(1H1,24X,'TOTAL FORCE AND TORQUE ON MVM-73 SPACECRAFT '
1      'IN E+06 NEWTONS AND',//,25X,'E+06 NEWTON-METERS RESPECTIVELY.'
2      'ACCELERATION',//,25X,'IN E+11 KM/SEC**2')
7006 FORMAT(/2X, 'TIME',17X,           'ACC',   6X,'XFORCE',5X,'YFORCE',
1      5X,'ZFORCE',4X,'XTORQUE',4X,'YTORQUE',4X,'ZTORQUE',6X,'FORCE',
2      5X,'TORQUE',//,
3      1X,'(DAYS)//)
DO 9000 NPTS=1,N
TOTFX(NPTS) = XFORCE(NPTS)+XFOR(NPTS)+FADX(NPTS)
TOTFY(NPTS) = YFORCE(NPTS)+YFOR(NPTS)+FADY(NPTS)
TOTFZ(NPTS) = ZFORCE(NPTS)+ZFOR(NPTS)+FADZ(NPTS)
TOTMX(NPTS) = XTORG(NPTS)+TADX(NPTS)
TOTMY(NPTS) = TADY(NPTS)
TOTMZ(NPTS) = TADZ(NPTS)
TOTF(NPTS) = SQRT(TOTFX(NPTS)**2+TOTFY(NPTS)**2+TOTFZ(NPTS)**2)
TOTMOM(NPTS) = SQRT(TOTMX(NPTS)**2+TOTMY(NPTS)**2+TOTMZ(NPTS)**2)
TOTACC(NPTS) = 100.0*TOTF(NPTS)/MASS
IF(NPTS.EQ.46)WRITE(6,9010)
IF(NPTS.EQ.141)WRITE(6,9010)
9010 FORMAT(1H1,1X,
1      'TIME',17X,           'ACC',   6X,'XFORCE',5X,'YFORCE',
2      5X,'ZFORCE',4X,'XTORQUE',4X,'YTORQUE',4X,'ZTORQUE',6X,'FORCE',
3      5X,'TORQUE',//,
4      1X,'(DAYS)//)
WRITE(6,9020)TIME(NPTS),TOTACC(NPTS),TOTFX(NPTS),TOTFY(NPTS),

```

```
1 TOTFZ(NPTS),TOTMX(NPTS),TOTMY(NPTS),TOTMZ(NPTS),TOTF(NPTS),
2 TOTMOM(NPTS)
9020 FORMAT(1X,F6.2,9X,9F11.4)
9000 CONTINUE
      WRITE(6,1010)
      WRITE(6,101)P,Q
      WRITE(6,105)A,B,TSTAR
      WRITE(6,1011)DCRT
      WRITE(6,1013)ELES
      WRITE(6,1012)PER,PERE
1010 FORMAT(1H1,24X,'AUXILIARY CONSTANTS')
101 FORMAT(//,25X,'P =',F20.8/,25X,'Q =',F20.8//)
105 FORMAT(25X,'A =',F20.8/,25X,'B =',F20.8/,75X,'TSTAR =',F20.8,2X,
1     'DEGK'/////)
1011 FORMAT(25X,'CRITICAL ANGLE =',F10.3,2X,'DEGREES')
1013 FORMAT(/25X,'ELES =',F20.8)
1012 FORMAT(//20X,'ORBITAL PERIOD OF SPACECRAFT =',F16.8,2X,'DAYS',//,
1     21X,'ORBITAL PERIOD OF THE EARTH =',F16.8,2X,'DAYS')
      IF(MORE.NE.0)GO TO 7000
      CALL EXIT
      END
```

```
-FOR,IS ANOM,ANOM
      FUNCTION ANOM(ECC,M)
C
C THIS FUNCTION SUBROUTINE SOLVES THE KEPLER-S EQUATION BY ITERATIONS
C
      REAL M
      DATA EPS/.000005/
      ANOM = M
      2 ANOM = M + ECC*SIN(ANOM)
      TEST = ANOM - M - ECC*SIN(ANOM)
      IF(ABS(TEST).GT.EPS)GO TO 2
      IF(ABS(TEST).LE.EPS)RETURN
      END
```

```
-FOR,IS CRPHI,CRPHI
      FUNCTION CRPHI(J,L)
C
C THIS FUNCTION SUBROUTINE PERFORMS THE DOUBLE INTEGRATION IN POLAR
C COORDINATES WITH CONSTANT INTEGRATION LIMITS.
C INTEGRATION LIMITS ARE R = 0,DELTA, PHI = 0,FI. CRPHI IS THE DOUBLE
C VALUE OF THE INTEGRAL.
C
DIMENSION S(10),W(10)
DIMENSION PSI(100)
COMMON DELTA,S,W,FI,EL,P,Q,CTT,RAT,PSI,NPTS,GAMMA,ZETA,ELES
CRPHI = 0.0
DO 20 I=1,10
SUM = 0.0
RI = DELTA*(S(I)+1.0)/2.0
DO 10 K=1,10
PHII = FI*(S(K)+1.0)/2.0
IF(IJ.LE.3)SUM=SUM+W(K)*F(RI,PHII,J,L)
IF(J.GT.3)SUM=SUM+W(K)*T(RI,PHII,J,L)
10 CONTINUE
CRPHI = CRPHI + W(I)*SUM
20 CONTINUE
CRPHI = DELTA*CRPHI*FI/2.
RETURN
END
```

ORIGINAL PAGE IS  
OF POOR QUALITY

```

-FOR,IS VRPHI,VRPHI
      FUNCTION VRPHI(J,L)
C
C THIS FUNCTION SUBROUTINE PERFORMS THE DOUBLE INTEGRATION IN POLAR
C COORDINATES WITH A VARIABLE UPPER INTEGRATION LIMIT FOR R. INTEGRATION
C LIMITS ARE R = 0,R(PHI), WHERE R(PHI) = EL/COS(PHI), PHI = 0,FI.
C VRPHI IS THE DOUBLE VALUE OF THE INTEGRAL.
C
C RI IS THE VARIABLE UPPER LIMIT FOR R. R = R(PHI)
C
      DIMENSION S(10),W(10)
      DIMENSION PSI(100)
      COMMON DELTA,S,W,FI,EL,P,Q,CTT,RAT,PSI,NPTS,GAMMA,ZETA,ELES
      DATA PI/3.141592654/
      IF(PI-FI.EQ.0.0)RETURN
      VRPHI = 0.0
      DO 20 I=1,10
      PHII = ((PI-FI)*S(I)+PI+FI)/2.0
      RI = EL/COS(PHII)
      SUM = 0.0
      DO 10 K=1,10
      RIJ = RI*(S(K)+1.0)/2.0
      IF(IJ.LE.3)SUM=SUM+W(K)*F(RIJ,PHII,J,L)
      IF(IJ.GT.3)SUM=SUM+W(K)*T(RIJ,PHII,J,L)
10    CONTINUE
      VRPHI = VRPHI + W(I)*RI*SUM
20    CONTINUE
      VRPHI = VRPHI*(PI-FI)/2.0
      RETURN
      END

```

```
-FOR,IS NEWTON,NEWTON
      SUBROUTINE NEWTON(EX,XKSI,EPSF,EPSB,A,FLUX)
C ****
C *      NEWTON-S METHOD FOR APPROXIMATE ROOTS          *
C *      V( ) = 0  IS THE EQUATION                      *
C *      G IS THE FIRST DERIVATIVE OF THE FUNCTION V    *
C ****
C
      DATA EPS/.00001/
      X = EX
      5 Y = V(X,EPSF,EPSB,A,FLUX)
      Z = G(X,EPSF,EPSB,A)
      DX = -(Y/Z)
      X = X + DX
      IF(ABS(DX).GT.EPS)GO TO 5
      XKSI = X
      RETURN
      END
```

```
-FOR,IS V,V
  FUNCTION V(X,EPSF,EPSB,A,FLUX)
  TERM = 1. + A*(X**3)
  V = (X**4)*(EPSF*(TERM**4)+    EPSB) - FLUX
  RETURN
  END
```

```
-FOR,IS G,G
FUNCTION G(X,EPSF,EPSB,A)
TERM = 1. + A*(X**3)
TERM1 = 1. + 4.*A*(X**3)
G = 4.*(X**3)*(EPSF*TERM1*(TERM**3) + EPSB)
RETURN
END
```

```

-FOR,IS F,F
    FUNCTION F(R,PHI,J,L)
C   FUNCTION F IS THE INTEGRAND FUNCTION FOR THE SOLAR FORCE EXPRESSION
C
    REAL NX,NY,NZ
    DIMENSION S(10),W(10)
    DIMENSION PSI(100)
    COMMON DELTA,S,W,FI,EL,P,Q,CTT,RAT,PSI,NPTS,GAMMA,ZETA,ELES
    BOFEF = 2.0/3.0
    FACTOR = (GAMMA+(1.0-GAMMA)*CTT)*BOFEF
    XA = -R*SIN(PHI)
    YA = R*COS(PHI)
    ZA = RAT*(R**2)
    WRT = SQRT(1.0+4.0*RAT*ZA)
    UY = SIN(PSI(NPTS))
    UZ = -COS(PSI(NPTS))
    NX = 2.0*RAT*XA/WRT
    NY = 2.0*RAT*YA/WRT
    NZ = -1.0/WRT
    CTHETA = NY*UY+NZ*UZ
    COEF = CTHETA*R*WRT
    AP = P*COEF*(CTHETA**0.75)*(1.0-GAMMA)*ELES*BOFEF
    AQ = Q*COEF*(CTHETA**1.5)*(1.0-GAMMA)*ELES*BOFEF
    K = (J-1)*3+L
    GO TO (1,2,3,4,5,6,7,8,9),K
1  F = 0.0
    RETURN
2  F = 0.0
    RETURN
3  F = 0.0
    RETURN
4  F = (FACTOR*NY+UY)*COEF*ELES
    RETURN
5  F = AP*NY
    RETURN
6  F = AQ*NY
    RETURN
7  F = (FACTOR*NZ+UZ)*COEF*ELES
    RETURN
8  F = AP*NZ
    RETURN
9  F = AQ*NZ
    RETURN
END

```

```

-FOR,IS T,T
    FUNCTION T(R,PHI,J,L)
C   FUNCTION T IS THE INTEGRAND FUNCTION FOR THE SOLAR TORQUE EXPRESSION
C
REAL NX,NY,NZ
DIMENSION S(10),W(10)
DIMENSION PSI(100)
COMMON DELTA,S,W,FI,EL,P,Q,CTT,RAT,PSI,NPTS,GAMMA,ZETA,ELES
BOFEF = 2.0/3.0
FACTOR = (GAMMA+(1.0-GAMMA)*CTT)*BOFEF
XA = -R*SIN(PHI)
YA = R*COS(PHI)
ZA = RAT*(R**2)
WRT = SQRT(1.0+4.0*RAT*ZA)
UY = SIN(PSI(NPTS))
UZ = -COS(PSI(NPTS))
NX = 2.0*RAT*XA/WRT
NY = 2.0*RAT*YA/WRT
NZ = -1.0/WRT
CTHETA = NY*UY+NZ*UZ
COEF = CTHETA*R*WRT
AP = P*COEF*(CTHETA**0.75)*(1.0-GAMMA)*ELES*BOFEF
AQ = Q*COEF*(CTHETA**1.5)*(1.0-GAMMA)*ELES*BOFEF
XN = YA*NZ-ZA*NY
XU = YA*UZ-ZA*UY
G = 0.0
K = (J-1)*3+L-9
GO TO 1,2,3,4,5,6,7,8,9,K
1 T = (FACTOR*XN+XU)*COEF*ELES
RETURN
2 T = AP*XN
RETURN
3 T = AQ*XN
RETURN
4 T = 4.0*G
RETURN
5 T = 5.0*G
RETURN
6 T = 6.0*G
RETURN
7 T = 7.0*G
RETURN
8 T = 8.0*G
RETURN
9 T = 9.0*G
RETURN
END
C ****
C ****
C ****
C ****

```

```
$INPUT
DELTA = 0.686
EPSF = 0.89
EPSB = 0.90
GAMMA = 0.10
SIGMA = 5.6697E-08
SOLAR = 1.353E+03
COND = 1.2921
DEPTH = 0.0191
W =          .29552422,.26926672,.21908636,.14945135,.06667134
S =          -.14887434,-.43339539,-.67940957,-.86506337,-.97390653
ECC = 0.23924529
ECCE = .01675011416266
TSTART = 0.0
TSTEP = 86400.
AX = 0.11974322E+9
AXE = .1495990706E+9
INCL = 3.2591328
EPSLN = 23.44268327
OMEGA = 181.42842
EOMEGA = 102.4908625
NODE = 40.188362
GM = .132712499E+12
MASS = 498.534
AU = .1495978930E+9
MSTART = 186.2238661
MESTRT = 305.4690256
ZETA = .216
EPSF1 = 0.79
EPSB1 = 0.85
GAMMA1 = 0.22
DEPTH1 = 0.0127
NCASE = 2
N = 93
TLT1 = 69
TLT2 = 93
T0 = 0.0
T1 = 45.0
T2 = 58.0
SPEC = 0.75
AREA = 5.8312
MORE = 1
$END
```

```
$INPUT
ECC = 0.25930279
TSTART = 92.0
AX = 0.93117523E+8
INCL = 4.3515604
EPSLN = 23.44268327
OMEGA = 271.456334
EOMEGA = 102.4908625
NODE = 10.168681
MSTART = 252.61864
MESTRT = 36.143130
N = 82
TLT1 = 20
TLT2 = 39
T0 = 58.0
T1 = 68.0
T2 = 71.0
MORE =
$END
-FIN
```